THE HONG KONG POLYTECHNIC UNIVERSITY
INSTITUTE OF TEXTILES AND CLOTHING

FABRIC STRAIN SENSOR INTEGRATED WITH CNPECS FOR REPEATED LARGE DEFORMATION

Weijing YI

A thesis submitted in partial fulfillment of the requirements
for the degree of Doctor of Philosophy

May 2012

CERTIFICATE OF ORIGINALITY

I hereby declare that this thesis is my own work and that, to the best of my knowledge and belief, it reproduces no material previously published or written, nor material that has been accepted for the award of any other degree or diploma, except where due acknowledgment has been made in the text.

_____ (Signed)

YI WEI JING (Name of student)

ABSTRACT

Wearable strain sensors have wide applications in rehabilitation, detection of human posture and gesture, and personal protection in sports and workplaces. They should be flexible, soft and able to measure large strain with good fatigue resistance. Conventional strain gauges like metallic foil are accurate, but they are too rigid to be wearable and the working range is limited to only several percent, which cannot satisfy the requirement of repeated large strain measurement in smart textiles. Carbon nanoparticle (CNP) filled elastomer composites (CNPECs) are of great interest due to their flexibility and sensing behavior at large deformation. On the other hand, knitted fabrics made from elastic fibers have good repeatability under cyclic extension without fracture at large deformation. Hence, the objective of this thesis is to investigate the fabric strain sensors integrated with CNPECs for repeated large deformation.

Conductive CNPECs were fabricated and studied. High porous but low structured CNPs and room temperature vulcanized (RTV) silicone elastomer (SE) as well as silicone oil (SO) were selected as materials for the conductive composites based on a literature review. The mechanical and electrical properties of the composites were studied. The results show that the introduction of SO decreases modulus of the composites to less than 1 MPa without affecting their deformability. After volatilization of the excessive SO with a heat treatment, the composites showed good stability, which was confirmed by thermal gravimetric analysis. The electrical resistivity of the composites was dependent on CNP concentration. With the increase of CNP concentration, percolation appeared. The ranges of insulating, percolation and post-percolation were divided at the CNP concentration of 0.5 wt% and 2.5 wt%, respectively. The conductivity of the composites was explained by

an equivalent circuit consisting of resistors and capacitors. I-V curves and impedance spectra confirmed the domination of electron hopping conductive mechanism of the composites with CNP loading in the percolation range, where the strain sensitivity of the composite was high, but the workable strain range is narrow and electromechanical behavior is obvious nonlinear with a large capacitive effect. They limited strain sensing applications in smart textiles where a large strain range is essential. In the post-percolation range, the sensitivity of the composites decreases. However, the workable strain sensing range increased and linearity improved simultaneously without increasing the modulus of the composite. The composite with 9 wt% CNPs could be extended up to 100% strain with good repeatability in strain measurement up to 50%. The composite also showed marginal strain rate dependence from 0.0017-0.17 /s and small humidity effect of 0.63%. The temperature had a significant effect on the strain sensitivity of the CNPECs. In addition, the fatigue resistance of the CNPECs was not sufficient for repeated applications in smart textiles.

Electrically conductive fabrics were fabricated by coating CNPECs on knitted fabrics via screen printing process. The influences of processing parameters, such as printing times, CNP concentrations, on the variation of electrical resistance were systematically studied. The electromechanical behavior of the conductive fabrics was studied for both DC and AC conditions. When subject to direct current, the conductive fabrics possessed linear I-V curves when the applied voltage is in the range of -1 V/mm and 1 V/mm, the slope varied with the strain applied from 0 to 60%. The impedance spectra of the CNPEC coated fabrics demonstrated that the CNPEC fabric with higher CNP concentration was less dependent on frequency. The capacitive behavior could be neglected up to 10^3 Hz even with strain of 60% for the sample of 9.0CNP. Compared to the CNPECs, the strain

sensitivity of the conductive fabric increased by about 100%. A mechanical pretreatment has been examined, and the results showed that the pretreatment increased significantly the strain sensing stability of the conductive fabric. The resistance change of the conductive fabric was found to be dependent on strain rate in the range of 0.02-4 /s. The effects of temperature and humidity were also studied experimentally at constant temperatures and relative humidity. The electrical resistance had a variation of 5% when temperature changed from 0 to 60 ^{0}C. The resistance varied only approximate 2% when the relative humidity changed from 20 to 90%.

The strain distribution of knitted fabric under uniaxial tensile strain was analyzed using digital image correlation analysis (DIC) method, which demonstrated gradient distribution with the highest strain between two neighboring stitches and the lowest at the center of yarn. After coated on the knitted fabrics, the CNPECs also show gradient distribution under extension due to the good adhesion between composites and fabrics. The combination of nonlinear resistance-strain behavior of the CNPECs and non-even distribution of strain of the coated fabrics was attributed to the higher strain sensitivity of the coated fabrics compared to that of CNPECs.

Extended on the studies of CNPECs and the coated conductive fabrics, a fabric strain sensor was designed and fabricated. The performance of the fabric strain sensor was evaluated experimentally. The Young's modulus of the packaged fabric strain sensor was less than 1 MPa; the strain gauge factor was 4.76 within the strain range of 0-40% and the hysteresis was 5.5%; the resistance relaxation was 5.56% with a constant strain of 40%; the fatigue life of the sensor was more than 100,000 cycles.

PUBLICATIONS

Referred Journal Publications

1. **W.J. Yi**, Y.Y. Wang, G.F. Wang, X.M. Tao, *Investigation of carbon black/silicone elastomer/ dimethyl silicone oil composites for flexible strain sensors*. Polymer Testing, 2012. 31(5):P. 677-684.

2. Y.Y. Wang, T. Hua, B. Zhu, Q. Li, **W.J. Yi**, X.M. Tao, *Novel fabric pressure sensors: design, fabrication, and characterization.* Smart Materials & Structures, 2011. 20(6): 065015

3. **W.J. Yi**, X.M. Tao, G.F. Wang, Y.Y. Wang, *Performance specifications and evaluation methods for fabric strain sensors*. Journal of Xi'an Polytechnic University, 2009. 23(2): P. 75-80.

4. **W.J. Yi**, Y.Y. Wang, G.F. Wang, X.M. Tao, *Fabric strain sensor based on CNP/SE/SO composites for repeated large strain measurement*, to be submitted.

Conference papers

1. **W.J. Yi**, Y.Y. Wang, G.F. Wang, X.M. Tao, *A Novel Fabric Strain Sensor Based on CB/SR Composites for Large Strain Measurement*, Conference of the International Journal of Arts and Sciences, Nov 28-Dec 3, 2010. Gottenheim, Germany (Abstract)

2. **W.J.** Yi, Y.Y. Wang, G.F. Wang, X.M. Tao, *Flexible Carbon Black/ Silicone Elastomer/ Silicone Oil Composites for Pressure Measurement*, The Fiber Society Spring 2011 Conference, May, 23-25, 2011. Hong Kong, China.

ACKNOWLEDGEMENTS

First and foremost, I would like to express my sincere gratitude and appreciation to my chief supervisor, Professor X.M.Tao, for her invaluable academic advice and professional guidance throughout the research. Special thanks should be given for her patience in training me in the ways of conducting research critically, systematically and logically, which will benefit me to solve problems in both research and life.

I would like to acknowledge with gratitude the financial support of The Hong Kong Polytechnic University for a postgraduate scholarship. Research facilities and technical support from the Institute of Textiles and Clothing are gratefully acknowledged.

I would also to express my special thanks to Prof. T.X. Yu, Dr. Y.Y. Wang, Dr. G. F. Wang, Dr. T. Hua, Dr. B. Zhu, Dr. L. Shu, Mr. S. Chen for their valuable advices and discussions.

Finally, I would like to give my most particular thanks to my wife C. Sun for her love, encouragement and support, to my parents and parents-in-law for their constant encouragement, understanding and love. Without their support, I could not complete my PhD study successfully.

TABLE OF CONTENTS

LIST OF FIGURES

LIST OF TABLES

NOTATIONS

CF	carbon fiber
CNP	carbon nanoparticle
CNPECs	Carbon nanoparticle filled elastomer composites
CTAB	cetyltrimethyl ammonium bromide
DBP	dibutylphthalate
DIC	digital image correlation analysis
EO	ethylene-octene
EVA	ethylene-vinyl acetate
EVO	evoprene
EPDM	ethylene propylenediene M-class rubber
FESEM	field emission scanning electron microscope
GF	gauge factor
GP	graphite powder
ICP	intrinsically conductive polymers
I-V	current-voltage
NBR	acrylonitrile butadiene rubber
NR	natural rubber
NTC	negative coefficient of temperature
PAN	polyacrylonitrile
PANI	polyaniline
PDMS	poly(dimethylsiloxane)
PET	polyester
PMMA	polymethyl methacrylate

PPy	polypyrrole
PTs	polythiophenes
PU	polyurethane
RTV	room temperature vulcanized
SE	silicone elastomer
SO	silicone oil
SWCNT	single-walled carbon nanotubes
TEM	transmission electron microscopy
TGA	thermal-gravimetric analysis
TPE	thermoplastic elastomer

CHAPTER 1

INTRODUCTION

1.1 Background

In recent years, considerable developments have been made in smart textiles due to the advances of textile materials, structures and the combination of them with other technologies (such as biotechnology, information technology, microelectronics, computing science, nanotechnology and micro-electromechanical machines). Smart textiles is defined as the textile materials and structures that can sense and react to environmental conditions or stimuli, such as those from mechanical, thermal, chemical, electrical, magnetic or other sources [1]. Three components may be present in smart textiles: sensors, actuators and controlling units, in which sensors play a role as nerve system to detect signals; actuators act upon the detected electrical signals either directly or from a central control unit, and convert them into physical phenomena; controlling units work like the brain with cognition, reasoning and activating capacities. On the initial stage of studying, smart textiles were fabricated for wearing by attaching existing electronic components on clothing using conventional technology [2]. However, the shape of textiles can be changed for a large extent when force is exerted, whereas most of the existing electronic components are rigid. When integrated together, the original physical properties of textile materials will be affected, resulting stress concentration at the boundary of soft and solid materials. So the development of flexible and soft electronic elements is necessary, in which the sensing devices especially strain sensors are more essential for the important status in smart textiles and their wide application

potential.

A sensor is a device that receives a stimulus and responds with an electrical signal [3, 4]. The strain sensors not only can be used to measure the numerical value changes of deformation or displacement but also can be transferred to pressure sensors or on/off switches just with a simple structure changes. Various strain sensors have been developed and commercially used in different fields based on metal alloys with good accuracy. However, they cannot fulfill the requirements of the accurate wearable sensing applications such as posture or gesture simulation and detection [5-7] and online respiration monitoring, etc., where measurement of cyclic movement and relatively large deformation of human body is needed. There are additional requirements of strain sensors in smart textiles besides the basic ones (i.e., suitable sensitivity, low hysteresis, high accuracy, quick responding time, predictable temperature and humidity effect, long-term environmental and chemical stability, insignificant or predictable strain rate effect, etc.), which are listed:

- Low Young's modulus that compatible to human skin and textile materials (lower than 1 MPa)
- Large working range of more than 20%
- Good electromechanical repeatability under cyclic measurement and fatigue resistance more than 100,000 cycles
- Reliable connection with substrate textile materials and outside data acquisition circuit

Based on the conversion phenomena of inductance [8], capacitance [9], optical [10] and

resistance [11], attempts have been made to use flexible or soft materials as sensing unit. However, up to date, most of them are still restricted in research labs due to the limitations of price, reliability and performances. In order to develop a strain sensor with low price and satisfy performances, the sensing materials, sensor structures, treatment methods and sensing mechanisms need to be systematically studied.

1.2 Objectives

Flexible and soft strain sensors are promising sensing elements in smart textiles and numerous prototypes have been fabricated in recent years. However, there are still many challenges for commercial ones that can fulfill the requirements of weariable applications. The objective of the present study is to develop flexible and soft strain sensors that can meet the requirements of wearable applications with characteristics of low modulus, large strain measuring range, good fatigue life, suitable sensitivity and good reliability using optimized fabrication process and treatment parameters. The thesis presents a comprehensive study of the carbon nano-particle/silicone elastomers /silicone oil (CNP/SE/SO) composites based fabric strain sensors with the following objectives:

1. To select suitable sensing materials, fabrication methods and treatment parameters, fabricating conductive CNP/SE/SO composites by considering the performances for wearable sensing application.

2. To study the electrical, mechanical, and thermal properties of the conductive composites and to examine the factors that influences the sensing performance of the composites.

3. To design and develop the conductive fabric based on CNP/SE/SO composites and knitted fabric, and investigate the processing parameters which affect the performance of the conductive fabric.

4. To characterize the conductive fabric for wearable applications.

5. To design and fabric flexible and soft strain sensors, evaluate the performance, investigate the sensing mechanism and to develop an applicable model to forecast the sensing behavior of the sensor.

1.3 Methodology

The research methodology adopted in this study includes the following details:

1. Fabrication and characterization of CNP/SE/SO composites

In this project, solution aided mixing method is adopted to fabricate CNP/SE/SO composites. The vulcanized conductive composites is characterized with field emission scanning electron microscope (FESEM), thermo-gravimetric analysis instruments (TGA), etc. The resistance of the composites is measured with digital multi-meter using 2-wire method and insulation resistance measurement instrument. Extension and force is recorded by Universal Material Tester (Instron 5566). I-V and impedance analysis are characterized by photomultiplier detection system and electrochemical interface combined with frequency response analyzer, respectively. The effect of temperature and humidity is controlled in an environmental chamber (Votsch T/C 600) and electrical resistance is recorded by multi-meter. The conductive mechanism of composites is

studied based on an equivalent circuit consisting of resistors and capacitors.

2. Fabrication and characterization of conductive fabrics

The conductive composites are coated on knitted fabric using screen printing method. Parameters affecting the sensing performances of the conductive fabric are explored by considering the composites and fabric characteristics. The resistance of the conductive fabric is measured with E-fabric Tester, which was developed in our laboratory with reference to ASTM D4496-04. Other performances of the conductive fabric are evaluated using the same methods as for conductive composites.

3. Design, fabrication and characterization of flexible strain sensors

The conductive fabric is connected with silver coated yarns using stitching and coating method. The non-sensing part of the sensor is combined with woven fabric using thermoplastic polyurethane film. The sensor is packaged with silicone rubber. The electromechanical properties of the sensors at room temperature are measured with Instron combined with digital multi-meter. The resistance under various temperature and humidity are controlled by climate chamber.

4. Sensing mechanism of fabric strain sensor

The deformation behavior of knitted fabric and conductive fabric with speckle is recorded by optical microscope, and the tensile strain is analyzed using digital image correlation method. The sensing mechanism of the fabric strain sensor is studied combing the strain field of knitted fabric and the nonlinear sensing behavior of CNP/SE/SO composites.

1.4 Project Significance

Despite the blooming of smart textiles in recent years, there are fewer reliable devices that can be used for sensing, actuating and controlling in wearable applications. The work is a great effort to develop a market acceptable sensing devices that can be used in smart textiles. The study on the flexible CNP/SE/SO based fabric strain sensor for repeated large strain measurement represents a great challenge and significant contribution to the advancement of our knowledge on sensor technology as well as textile industry. It is expected that this project will inspire the developments of flexible and soft devices, accelerate the cross-fertilization of the different disciplines like textiles, electronic and measuring. Study on conducting and sensing mechanism of conductive composite and fabric strain sensor will support deeply performance improvement of the sensor. The combination of strain sensor technology with textile industry will bring out more highly value-added products, which will benefit the textile, apparel and other industry world-wide.

1.5 Structure of the Thesis

The thesis comprises of six chapters, its structure is outline in Figure 1.1.

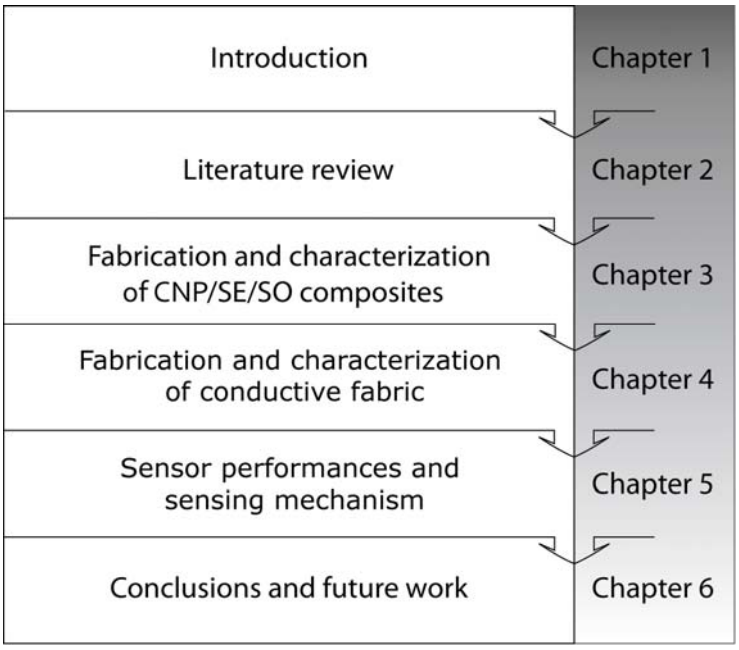

Figure 1.1 Structure of the thesis

Chapter 1 briefly introduces the background information of the smart textiles and the necessary of flexible strain sensors. The statement of problems existed in them put forth the objective of developing strain sensors with good sensing performances and low modulus, high working range, high fatigue resistance in repeated large deformation and reliable connection with substrate and circuit. Finally, research methodology adopted in the thesis is summarized.

Chapter 2 provides a comprehensive literature review regarding to the materials, fabrication methods, structures and performances of different kinds of flexible strain sensors. The proposed materials and fabrication methods for the novel fabric strain sensors with elevated performances are also included in this part.

Chapter 3 presents the detailed investigation of CNP/SE/SO composites. The electrical, mechanical and thermal properties of them are studied and optimized by considering the sensing behavior for wearing applications. The conductive mechanism of the conductive

composites is also discussed based on an equivalent circuit consisting of resistors and capacitors.

On the basis of the results obtained from chapter 3, conductive fabrics by coating three-phase CNP/SE/SO composites on knitted fabrics are described in chapter 4. The investigation on the compositions of conductive composite, sensor structures, processing methods is conducted with respect to their performances.

Chapter 5 designs and evaluates the performances of the packaged strain sensors. The mechanism that contributes to the strain sensing behavior of fabric strain sensor is examined based on the deformation behavior of knitted fabric and the non-linear sensing behavior of conductive composites.

Finally, this thesis is closed with a summarization of the main findings of the study in Chapter 6. Some suggestions on possible future work are also discussed.

References

1. Tao, X.M., *Smart fibres, fabrics and clothing*2001, Cambridge: Woodhead Pub Co.
2. Gandhi, M.V. and B.D. Thompson, *Smart Materials and Structures*1992: Springer.
3. Fraden, J., *Handbook of Modern Sensors - Physics, Designs and Applications*. Third ed2003, New York: Springer.
4. Cho, G., *Smart clothing: technology and applications*2010, Boca Raton: CRC Press.
5. Lorussi, F., W. Rocchia, E.P. Scilingo, A. Tognetti, and D. De Rossi, *Wearable, redundant fabric-based sensor arrays for reconstruction of body segment posture.* Ieee Sensors Journal, 2004. **4**(6): p. 807-818.
6. Cochrane, C., V. Koncar, M. Lewandowski, and C. Dufour, *Design and development of a flexible strain sensor for textile structures based on a conductive polymer composite.* Sensors, 2007. **7**(4): p. 473-492.
7. Mattmann, C., F. Clemens, and G. Troster, *Sensor for measuring strain in textile.*

Sensors, 2008. **8**(6): p. 3719-3732.
8. Wijesiriwardana, R., *Inductive fiber-meshed strain and displacement transducers for respiratory measuring systems and motion capturing systems.* Ieee Sensors Journal, 2006. **6**(3): p. 571-579.
9. Matsuzaki, R. and A. Todoroki, *Wireless strain monitoring of tires using electrical capacitance changes with an oscillating circuit.* Sensors and Actuators a-Physical, 2005. **119**(2): p. 323-331.
10. Babchenko, A. and J. Maryles, *Graded-index plastic optical fiber for deformation sensing.* Optics and Lasers in Engineering, 2007. **45**(7): p. 757-760.
11. Cochrane, C., M. Lewandowski, and V. Koncar, *A Flexible Strain Sensor Based on a Conductive Polymer Composite for in situ Measurement of Parachute Canopy Deformation.* Sensors, 2010. **10**(9): p. 8291-8303.

CHAPTER 2

LITERATURE REVIEW

2.1 Introduction

As mentioned in the previous chapter, the strain sensors that can be used in smart textiles are essentially necessary and reserve many researchers' attention. To compatible with the soft objectives and achieved the accurate data, the strain sensors should have additional characteristics of low modulus (lower than 1 MPa), high strain working range (beyond 20%) and high fatigue resistance (higher than 100,000 times) as well as reliable integration with substrate materials and circuit besides good sensing performances.

In this chapter, the flexible and soft strain sensors are systematically reviewed and evaluated according to different sensing mechanism. The group of sensors in which the desired performances are available to achieve is highlighted and reviewed in detail by considering the materials, structures, fabrication methods and performances.

2.2 Inductive Flexible Strain Sensors

The sensing mechanism of inductive strain sensors is based on the variation of mutual inductance resulted from the dimensional change of paired inductive coils. The coils can be fabricated by arranging the electro-conductive fibers (polymeric and metallic) with different conductivity levels in helical paths by flat bed-knitting technology [1], as shown in Figure 2.1. This kind of sensors (transducers) is flexible and soft due to the knitted structure adopted and be able to measure large displacement even angular displacement

approximately. However, the accuracy and reliability of the sensor at repeated measurement is not good, the applications are limited due to the circular configuration of the sensor.

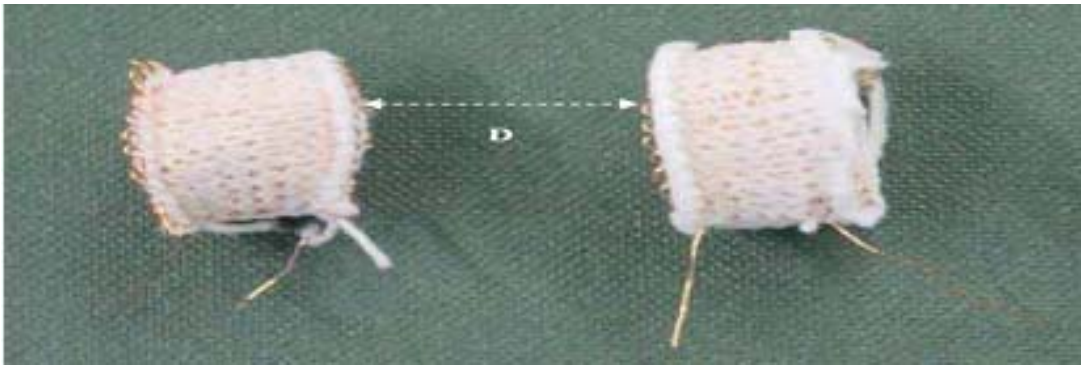

Figure 2.1 Inductive coil for linear displacement measurement [1]

2.3 Capacitive Flexible Strain Sensors

Through capacitive changing, flexible strain sensor was designed by inserting dielectric material into a couple of electrodes to form an electrical condenser [2], as shown in Figure 2.2, the rubber and steel wires were used as dielectric material and electrodes, respectively. The tensile strain is determined by the capacitance change of the electrical condenser, resulting from spacing change between the steel wires. The benefit of the capacitive strain sensor lies in that they can be made to small sizes to form sensing matrix. However, to measure the strain of objectives, i.e., changes in capacitance, a complicated oscillating circuit should be designed to measure oscillating frequency. Furthermore, the maximum strain that can be measured by this kind of sensor is still less than one percent, which cannot meet the requirement of wearable applications with strain range more than 20%.

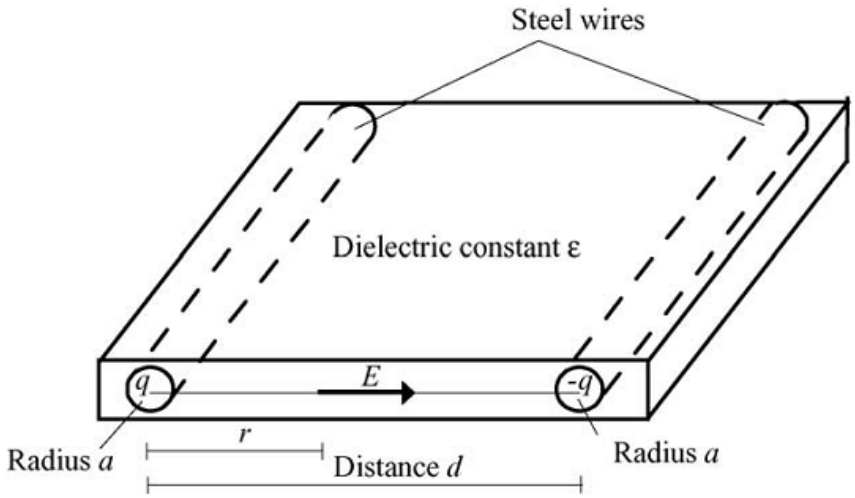

Figure 2.2 Electrical condenser based on steel wire and rubber for strain measurement [2]

2.4 Polymer Optical Fiber Strain Sensors

Polymer optical fiber sensors using Bragg grating, intensity and interferometric principles are usually employed for internal strain measurement due to their high accuracy, stability, lightweight and small size, which are suitable to embed in small sized structures to measure the strain and/or strain distributions. The most significant advantages of the sensors are that they are immune to the influence of electromagnetic interference whereas other electrical based sensors will be invalid [3-10], while the disadvantages of the sensors are that they cover not only the complex measuring procedure and expensive accessorial equipment, but also relatively smaller strain measuring range and higher rigidity [11].

2.5 Resistive Flexible Strain Sensors

Measure the change in resistance value caused by deformation is a main stream to fabricate strain sensors with good sensing performances. The strain gauges can further be used as pressure sensors due to the resistance change can further relate to applied force

that contributed to the deformation. The resistive effect can be demonstrated by the sensitivity of the strain sensor, which can be represented by gauge factor (GF), which is defined as the fraction of the electrical resistance increment, $\Delta R / R_0$, per unit strain, that is,

$$GF = \frac{\Delta R / R_0}{\varepsilon} \tag{2-1}$$

where R_0 is initial resistance of the strain gauge, ΔR is the resistance change due to deformation, ε is the applied strain. The materials and characteristics of some traditional resistive strain gauges are shown in Table 2.1.

Table 2.1 Characteristics of Some Resistive Strain Gauges

Material	Gauge factor (GF)	Temperature coefficient of resistance ($^0C^{-1}\times10^{-6}$)
57%Cu-43%Ni	2.0	10.8
Platinum alloys	4.0-6.0	2,160
Silicon	-100 to +150	90,000

Source: Ref [12].

Although advantages of relatively low resistance, high sensitivity and stable response are usually demonstrated by the traditional strain gauges made of metal foils, the rigidity and lower elongation ratio (in the range of 0.1% - 0.5%) are the most significant factors hindering their integrate applications in the field of smart textiles.

To facilitate resistive type strain sensor with performances suitable for wearable application, one route is to endow inelastic electrical conductive fibers/yarns or inherent conductive polymers with elastic structures through knitting, coating or pasting method, the sensing behavior is mainly contributed to the change of contact resistance. The other

route is to use elastic piezo-resistive composites prepared by filling conductive particles into an elastic matrix.

2.5.1 Intrinsically Conductive Polymer/Filament/Yarn Based Flexible Strain Sensor

In the past few years, intrinsically conductive polymers (ICP) such as polypyrrole (PPy), polyaniline (PANI), polythiophenes (PTs) etc. have been extensively studied in many applications like chemical and biosensors, actuators, photovoltaics, rechargeable batteries, separation films, etc. The good conductivity of them can be ascribed to the polymer chains containing long conjugated double bonds [13]. Among the reported ICPs, PPy received more attention as potential sensor materials due to its easy fabrication, high conductivity and non-toxicity [14]. However, the brittleness and small inherent elasticity of the material limited its direct applications in wearable strain sensors with flexibility and large deformation.

Since the flexibility and easy deformability of textile materials in all directions, especially their capability of support large deformations like tensile, shear, bending, and compression without deteriorating their initial physical properties, they can be made into conductive fibers or fabrics with high conductivity by coating PPy on its surface with the methods of electro-chemical polymerization, in situ polymerization or chemical deposition, etc. [15-23]. Based on these studies, the strain sensing behavior of PPy coated Lycra fabric was investigated by De Rossi etc. [24] in 1997 for sensorized fabric glove and sock. The electrical resistance of the fabric decreased about 20% with tensile strain of 1%, which corresponding to a gauge factor of about -13.25, as strains beyond 1%, the resistance change saturates and no further sensing behavior can be observed. Under cyclic measurement, the conductive fabric showed relatively good repeatability. However, the

obvious temperature sensitivity (resistance decreased about 60% when temperature increased from 20 ^{0}C to 60 ^{0}C), and the low working range limited their real wearing applications.

The strain sensing element fabricated by coating PPy onto textile materials has good potential for measuring and controlling of human movements and activities and have been studied by many researchers [14, 21, 25-29]. Oh et al. [30] and Kim et al. [31] reported that the electrical resistance increased monotonically with elongation up to 50% with a gauge factor of about 0.5 and 3 for PPy coated elastic Nylon/Spandex and polyester (PET)/Spandex fabric, respectively. The gauge factor was increased to 12 and 13 reported in [32] and [33] respectively. However, their strain measuring range is limited to 1%. By using screen printing method with chemical vapor deposition under low temperature, the gauge factor of the PPy coated knitted fabric was significantly increased to 210 at maximum strain of 50% [34]. The working range further increased to 70% with solution phase chemical polymerization method [35], which demonstrating the feasibility of PPy coated fabrics as flexible strain sensors for large strain measurement.

Besides textile materials, rubbers were also been studied as supporting substrates of PPy [36] to fabricate strain sensors in assisting the air muscle control. Butyl rubber was selected as substrate for the similarity in the mechanical behavior compared to air muscle while the PPy coating layer denote the rubber with sensing ability. The gauge factor of the sensor achieved is about 0.65 at strain range of 10%.

For the huge difference in elasticity between the conductive PPy and textiles/rubbers, there must be some micro-cracks appeared in the conductive PPy layer if the tensile strain

beyond a limit, resulting to the unsynchronized deforming ability of PPy coated sensors at the first and successive extensions. The unsynchronized electromechanical behavior can be stabilized by pre-treating the sensor with a strain beyond its working range [34]. The opening/closing of the cracks at loading/unloading cycles contributed to the high strain sensitivity of PPy coated sensors and was deemed as the sensing mechanism [36, 37], which have been demonstrated by the SEM morphology in Figure 2.3. After the pretreatment, the sensors exhibit high sensitivity and large working range. Unfortunately, the environmental stability of PPy is poor, which is a major problem that hinders the industrial application of this kind of sensors. Considerable efforts have been made to increase the stability of PPy based strain sensors by chemicals aided process or make it denser to avoid attack of oxygen [29, 38, 39]. However, the efforts of stabilization treatment are partially counteracted by the cracks on the coating layer arising from pretreatment of the sensor.

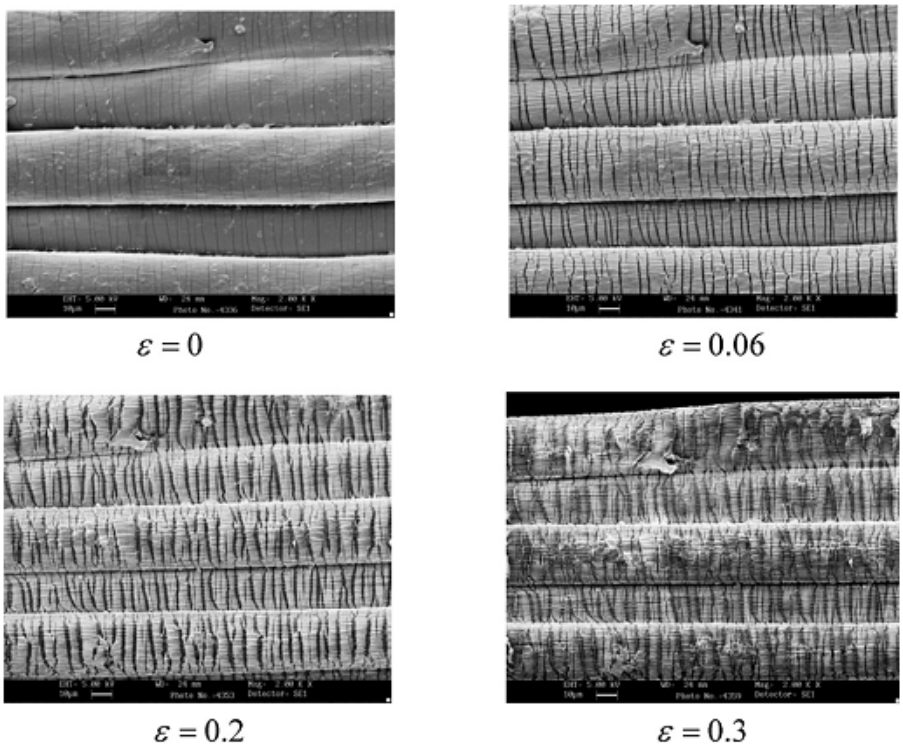

Figure 2.3 SEM microphotographs of PPy-coated polyurethane (PU) fibers at different strain levels. [37]

Besides PPy, PANI is also a good inherently conductive polymer. The potential applications of PANI based strain sensors were also studied by coated on PET yarns through absorption of yarns in PANI solution [40], the similar unsolved problems exist as those for PPy, which limited their industrial applications.

In 1999, Philips Research Laboratories developed a jacket incorporated with flexible strain sensors for measuring upper limb and body movement at the joint positions [41]. The sensor was fabricated by knitting conductive carbon fibers into fabric using plating structure. The electrical resistance of the sensor changed under extension and the electrical signal can be transmitted from the sensor to measuring devices by knitted track tape containing conductive wires (Figure 2.4). Gibbs et al. [42] designed and fabricated a wearable strain sensing device for continuous monitoring of joint movements (Figure 2.5). The strain sensing device is actually a textile based potential divider that using inelastic conductive fiber as sliding track and elastic cord as deformation undertaker. The corresponding resistance change under deformation can be measured by a coupled resistance measuring device.

(a) (b)

Figure 2.4 (a) Strain sensor based on carbon fiber knitted fabric and knitted conductive tracking (b) sensing jackets [41, 43, 44]

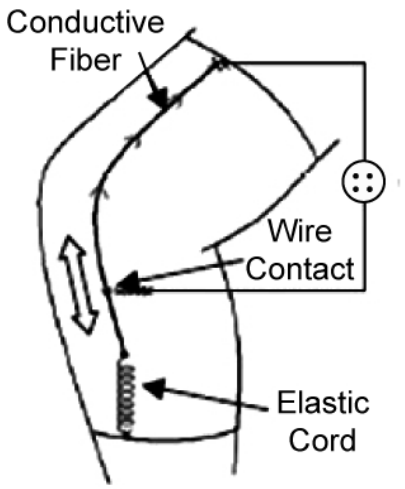

Figure 2.5 Schematic of strain sensing device designed by Gibbs et al. [42]

The feasibility of conductive fabric knitted with stainless steel multi-filament yarn [45-47] and polyacrylonitrile (PAN) oxidized carbon fiber [47, 48] was investigated respectively for the desired sensing performances, where the contact resistance of the overlapped conductive yarns due to variation of fabric structure was considered as the reason of resistance changes of the materials, which was shown in Figure 2.6. The sensitivity of the strain sensing fabrics achieved is about 5 expressed by gauge factor when maximum strain was set to 20% for the stainless steel one and gauge factor more than 3.0 with maximum strain of 30% for the carbon fiber one. Both of them can work at high temperature and the sensitivity can be adjusted by changing of fabric structures. Due to the knitted structure adopted, relatively good flexible properties and large strain measuring ranges were demonstrated. However, The repeatability of them are not good enough, the weight penalties as well as rigidity of the stainless steel and high crisp properties of carbon fiber undermined their comfort and stability under long term application. Furthermore, the introducing of rigid stainless steel or carbon fibers into textile materials may alter the strain field of textiles significantly [49], which will affect the accuracy of measured results. The unstable initial status of the sensors due to coarse

needle gauge and worse reliability also hinders their further industrial applications.

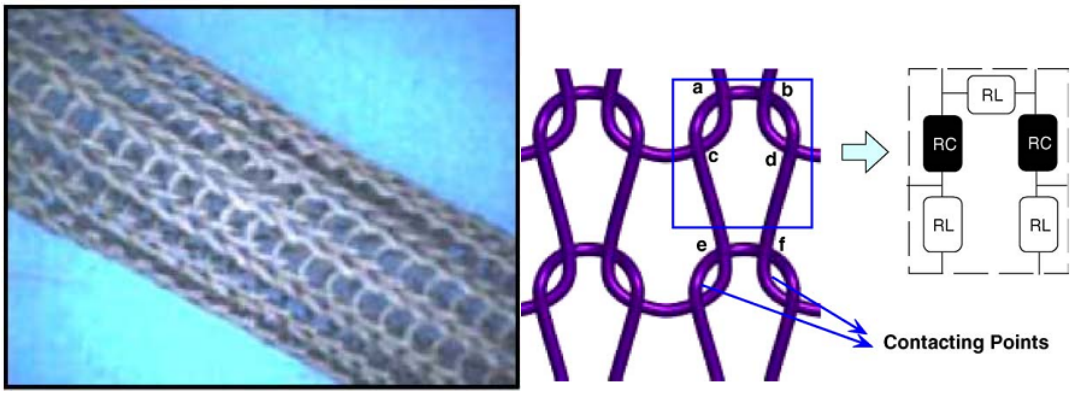

Figure 2.6 Tubular stainless steel knitted fabric sensor and its simulated circuit [47]

With yarns consisting of elastic fibers and polyester as core, a yarn based flexible strain sensor was fabricated by wrapping conductive carbon-coated fibers outside [50, 51]. The sensitivity of the sensor can be adjusted from 3 to 9 with strain range of about 25% when the conductive yarns and their twist levels changed accordingly. Based on the sensor, elastic belt, band and even garment can be fabricated for monitoring respiration signal. The schematic of the sensor and respiration monitoring band is shown in Figure 2.7. The configuration of the yarn based sensor is 1 dimensional and its size is relatively small, which is a benefit for the application in smart textiles. The repeatability of the sensor is also good. The disadvantage of the sensor lies in the worse reliability of conductive connection, for which the sensor is suit for respiration monitoring, but not for accurate strain measurement.

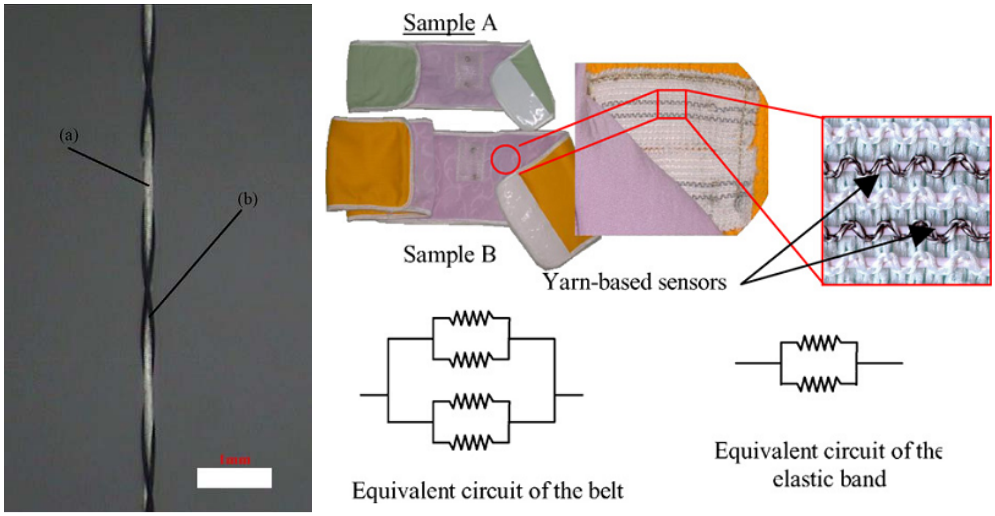

Figure 2.7 Yarn based sensor, elastic belt and band for respiration monitoring and the equivalent circuit. [50]

Carbon nanotubes (CNTs) exhibit excellent mechanical, electrical and thermal properties. Pure CNT fibers or yarns show piezo-resistive property, by aligning and transferring them onto a polymer substrate [52], a strain sensor with gauge factor of about 11.5 can be achieved, as shown in Figure 2.8. However, the strain working range of the sensor is less than 1% for the rigidity of the polymer, furthermore, the safety of the CNT based materials also should be carefully considered when they were used near human skin, for the needle like CNT is easy to penetrate into human skin. These disadvantages hindered the direct application of the sensor in smart textiles [53].

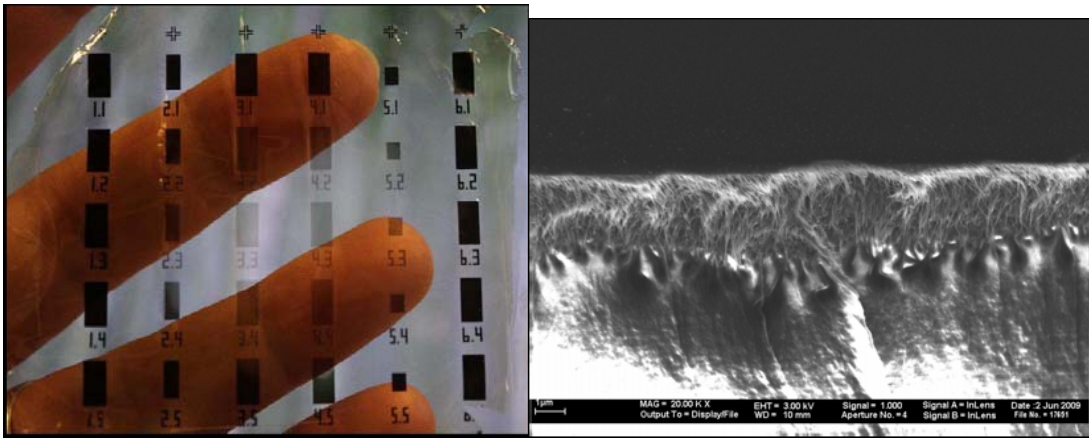

Figure 2.8 CNT based strain gauge and SEM picture after transferred the strain gauge on

a polymer. [52]

To increase the working range of the CNT based sensor, CNT was aligned to a thin layer perpendicular to the strain axis and then adhered to elastic poly(dimethylsiloxane) (PDMS) substrate by strong van der Walls forces. The fabrication process is shown in Figure 2.9. The strain sensor fabricated by this method demonstrating a very high working range up to 200% due to opening and closing of gaps between CNTs. It also shows a monotonic resistivity-strain relationship which can be characterized by two linear regions with gauge factor of 0.82 (0 to ~40% strain) and 0.06 (~60 to 200%) respectively [54]. The final strain sensor after package showed a better linearity compared the un-packaged one, good repeatability up to 10,000 cycles in strain range of 150% and low resistance creep as well as short response time, which can be used for human motion detection, several prototypes about the application of the sensors in wearable devices and the achieved signals were shown in Figure 2.10. Though very good performances have been achieved for the CNT based sensor, the complicated fabrication process for aligning and transferring the nanotubes and the corresponding high cost limited their wide industrial application.

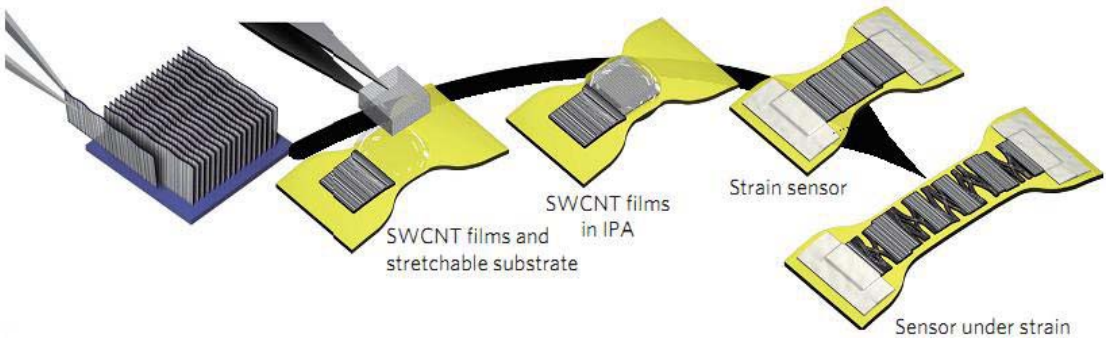

Figure 2.9 Fabrication process of SWCNT strain sensor [54]

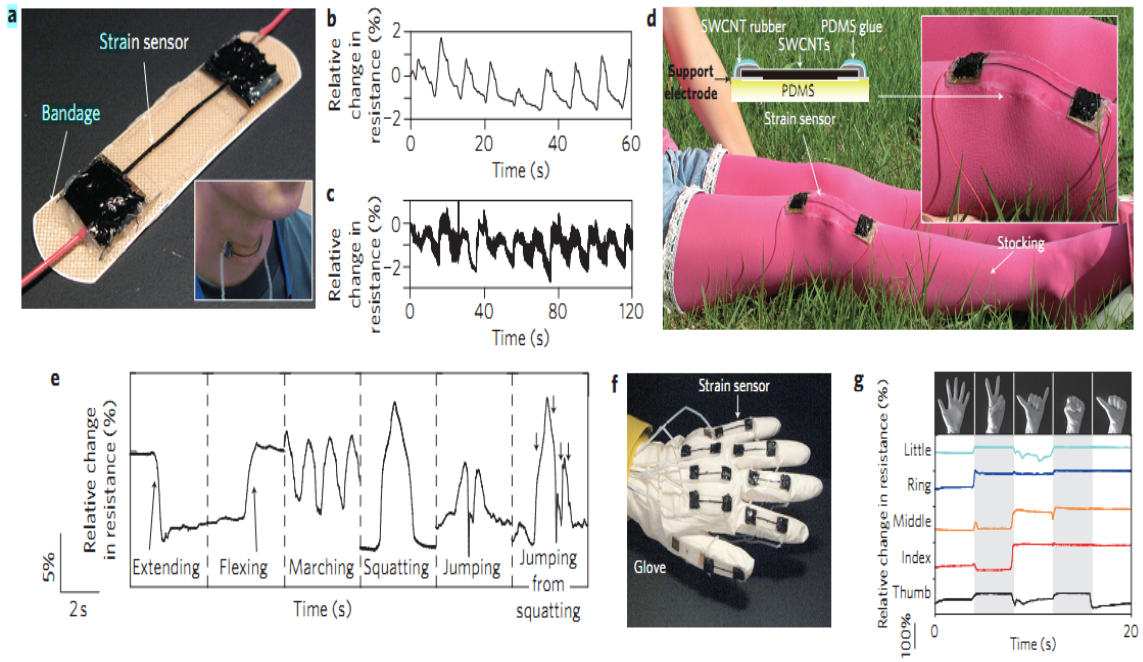

Figure 2.10 Wearable devices based on SWCNT strain sensor and their performances [54]

2.5.2 Conductive elastomeric composites

Most plastics or elastomers are insulating materials, after filled with conductive fillers, such as CNP, metallic particles, graphite powder (GP), carbon fiber (CF) or carbon nanotubes (CNTs), etc., the electrical resistivity of the composites decreases. Due to the electrically conductive behavior of the conductive composites, they have been intensively investigated for potential applications in electromagnetic interference shielding [55], electrostatic charge dissipation [56], electric switch [57], self-regulating heaters [58, 59] and sensors [49, 60-65]. Their perceived advantages include excellent flexibility, low weight, large deformability, high environmental stability, adjustable conductivity and Young's modulus as well as relatively low manufacturing cost.

The concentration of conductive fillers is one of the important parameters affecting

electrical properties of the conductive composites. When the filler loading is low, the electrical resistivity of the composites is similar to that of insulating matrix. With the increase of conductive filler, the electrical resistivity of the conductive composites decreases and it is significantly decreased by several orders of magnitude when the concentration of conductive filler is beyond a critical value, i.e. percolation threshold. With further increase of the filler loading, the changing in electrical resistivity of the composites is getting moderate.

The obvious change in electrical resistivity of the composites beyond percolation threshold can be achieved not only by the changing of conductive filler loadings but also by applied mechanical forces. The corresponding piezo-resistive effect of conductive elastomeric composites has been studied by many researchers [66-76]. If there is a definite relationship between electrical resistance and mechanical deformation or pressure, the composites especially elastomeric ones, can be used as flexible strain sensors to measure large repeated strain or displacement, which are very important units for wearable electronics and human-machine interaction devices.

Among the commonly used conductive fillers, metallic materials can supply excellent conductivity, but the composites implanted with metals impose severe weight penalties as well as corrosion and degradation under external environments. GP and CF also have good conductivity and have been studied in conductive composites for sensor applications [77-79]. However, drawbacks of sliding wear behavior of GP and crisp of CF result worse repeatability of electromechanical properties under cyclic measurement.

CNTs have very high aspect ratio and when used as conductive filler, a very low loading

is needed for percolation threshold. The ethylene propylene diene M-class rubber (EPDM)/CNT composites have been studied to measure the bending and compressive large beam deflection [80], as shown in Figure 2.11. Filler loading dependable sensitivity from 5.1 to 1.1 with CNT loading from 10 wt% to 50 wt% were achieved with a relative good linearity between resistance and strain, but the strain measuring range is only 0.4%. Employing electro spinning fabrication scheme, the strain sensing performance of CNT-based piezoelectric fabric strain sensor was studied in structural vibration experiments [81]. The change in measured voltage across the sensor increased by a dramatic 35 times, from 2.4 to 84.5 mV for CNT loading of 0.05 wt%. The dominant mechanism responsible for such performance was found to be the alignment of dipoles in the piezoelectric material. CNT filled polymethyl methacrylate (PMMA) composites have also been studied with melt processing or solution casting methods for strain sensing applications, and the results demonstrated that the strain sensitivity of the conductive films can be tailored by controlling the loadings of nanotube, degree of nanotube dispersion and film fabrication process [82], benefit for the development of sensors with different purposes, but the strain measuring range is less than 1%. The same materials were used to fabricate flexible strain sensor for respiration rhythm measurement, but the strain working range achieved is even smaller [83].

Figure 2.11 CNT/EPDM based sensor [80]

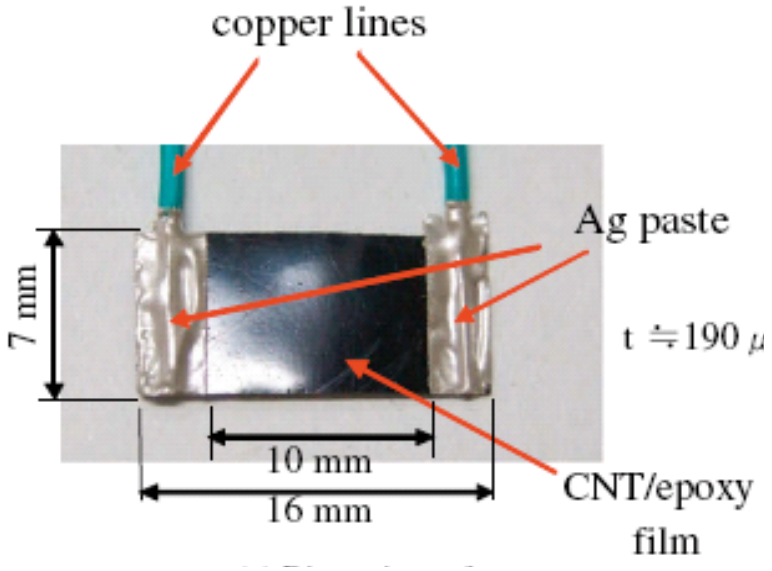

Figure 2.12 Photo of CNT/polymer based strain sensor. [84]

As conductive fillers, carbon nanotubes [84] and graphene [85] can be fabricated into composites for sensing applications with far lower loadings than other conductive fillers to achieve a very high sensitivity, one example is shown in Figure 2.12. However, the high price, complex fabricating process, uncertainty of safety effect on humans, small strain measuring range as well as the difficulty of large scaled industrial production still limited their further application as flexible, large working range strain sensors in smart textiles.

Compared to CNT and graphene, the price of conductive CNP is much lower, and the zero dimensional structure of CNP after good dispersion make them less constrict on the deformation of matrix materials in composites compared to one dimensional CNT, which is benefit for fabricating conductive composites with large deformation and low Young's modulus. Furthermore, chemical resistance property as well as low density of CNP compared to other conductive fillers make it more preferred electrically conductive filler in composites for flexible strain sensors with large and repeated strain measuring ability [86].

The electromechanical properties of low structured CNP (Ketjenblack EC) filled SE composite under axial stretching with single and cyclic loading was studied [72, 87, 88], the results demonstrated that the relative electrical resistance of the composite increased with tensile strain, that can be potentially used as flexible strain sensors. Under cyclic measurement, the composite showed irreversible resistance changes between first and successive cycles as tensile strain was 40%. However, the irreversible behavior of the composites can be stabilized with mechanical pre-conditioning at a higher strain beyond its working range. The composite also showed maximum strain amplitude and strain rate dependence behavior, which limited their industrial application.

To compare the effect of CNP structure on mechanical and electrical properties of CNP filled elastomers, CNPs with low and high structures were filled into ethylene-octene (EO) elastomers, respectively [89]. Under extension, the composite filled with low structured CNP showed an increase in resistivity with strain in the first loading period. While for the following measurement, similar behavior that composite exhibited irreversible change in

both mechanical and electrical properties even with low strains appeared. Different from the low structure CNP filled composite, the conductive composite consisting of high structure CNP showed a decrease in electrical resistance at low strains (2–4%), and then followed by reversible resistance-strain behavior upon cyclic loading to 20% strain. When the tensile strain was further increased, the decrease in resistivity at low strains (20%) and the weak increase at intermediate strains (up to about 300%) can be observed for high structured CNP filled EO composite [69]. The increase in resistance was believed related to recoverable damage of conductive paths in 100% strain, while the unrecoverable increase was due to de-percolation of conductive paths at even higher strain. For the requirement of good repeatability, the composite can be potentially used as strain sensor in the strain working range between 0- 20% for its high reversibility. The electrical and mechanical behavior of high structured CNP (HAF N330) filled natural rubber (NR) and acrylonitrile butadiene rubber (NBR) composites at large strains in tension was also studied [76], the results showed that the resistance of the composites increased with tensile strain under moderate extensions for unstrained specimen, but decrease at higher extension. The increase of resistance followed by tensile strain was ascribed to the breakdown of the CNP network, while decrease of resistance at higher extension was attributed to the alignment of the shaped CNP aggregates under large strain. In the unloading period, the resistivity was significantly higher than that measured in the unstrained elastomer, which may be caused by destroying of the specimen. When the composites were pressed, the resistance also increased with compressive strain. Xie et al. [75] simulated the electrical behavior of CNP filled NR at large strains based upon an infinite circuit model. Good agreement was achieved between the simulations and the experimental data of Yamaguchi [76]. The simulated results confirmed the change of electrical resistivity under strain was contributed to the breakdown of CNP network and

the alignment of CNP aggregates.

With acetylene black as conductive filler, conductive composites with different types of insulating matrix such as ethylene-vinyl acetate (EVA), NBR and ethylene-propylenediene rubber (EPDM) were studied [68, 90]. The electrical behavior of these composites depend on processing parameters like mixing time, rotor speed, mixing temperature, vulcanization time and other service conditions like pressure and temperature applied [91]. A very similar percolation behavior was observed for these composites, the variation of their percolation threshold depended on the polarity and viscosity of matrix. Both the mechanical and electrical behavior of the composites synchronously changed with tensile strain, demonstrating the feasibility of them in the application of flexible strain sensors.

Dependence of CNP loadings on reversible piezo-resistive effects of CNP/polyisoprene composite was studied by Knite et al. [92]. The resistance showed an increase of about 4 orders of magnitude upon 40% strain for composite at percolation threshold of about 10 wt% CNP loading. Though maximum sensitivity could be achieved at percolation threshold, the higher resistance is usually out of the measurement range of many ordinary instruments. The balance between sensitivity and measured resistance was considered for sensor applications [67], where composites with CNP loading well beyond percolation threshold was selected and a monotone increase in resistance followed by strain was achieved.

The flexible and large deforming properties of CNP filled elastomers are good candidates for strain sensors to measure deformation of textile materials for their low modulus, good

elastic properties and piezo-resistive behavior, though the sensing behavior of them are affected by many parameters like CNP structures, elastomer types, CNP concentrations, fabrication methods, etc.. The composites have been studied by integrated with textile materials. Rubber solution containing micro disperse phases of carbon on polyester/Lycra jersey fabric have been studied to measure the respiratory rate of human-being [93]. Based on the results, different fabrication routes were further studied.

Conductive fabrics knitted by cotton/ Lycra threads with carbon loaded rubber on surface [32] and directly smeared CNP loaded elastomer [33, 94] were fabricated, and the gauge factor of 2.5 and 2.8 was achieved for them, respectively. The sensor has negligible capacitive effects up to 100 MHz and diminished long transient time for the latter one; Prototypes of upper limb kinesthetic garment and sensing glove fabricated using graphite filled silicone rubber over Lycra fabric as strain sensor were also studied by the same group as shown in Figure 2.13 [95-97] .

(a) (b)

Figure 2.13 (a) Upper limb kinesthetic garment (ULKG) prototype and (b) sensorized glove based on carbon loaded elastomer [95, 97].

By comparing the conventional melt mixing method and solvent aided method, high

structured CNP filled thermoplastic Evoprene 007 (styrene-butadiene-styrene co-polymer) composites were fabricated using solvent aided method to produce strain sensor with flexible property, as shown in Figure 2.14 [98]. The CNP loading of 27.6 vol %, which is much higher than percolation threshold, was selected to achieve a promise performance between low initial resistance and high sensitivity. Under extension, a nonlinear electrical resistance vs. strain curve was observed for the sensor, which can be divided into a nonlinear zone with strain below 15% and linear zone with strain from 15% to 45% with correlation coefficient $R^2 > 0.99$, and gauge factor about 31 and 80 was calculated for the two ranges, respectively [67, 98]. The exceptionally higher gauge factor of the sensor can be attributed to combination of geometry change of the sensor and variation of percolation network of the system. The effect of climate conditions on the sensor performance was tested and the results showed that with increase of humidity, the electrical resistance of the sensor significantly increased about 40% when humidity increased from 15% to 90% under the fixed temperature of 40 ^{0}C, while the effect of temperature is relatively smaller compared to the effect of humidity. Further study showed that the relative resistance of the sensor increased about 42% at strain of 25% when strain rate increased from 0.125/min to 12.5/min. The electrical resistivity of the sensor was also tested under cyclic elongation with maximum strain of 4%, the electrical resistance is stable at maximum strain but slowly increased at minimum strain [99].

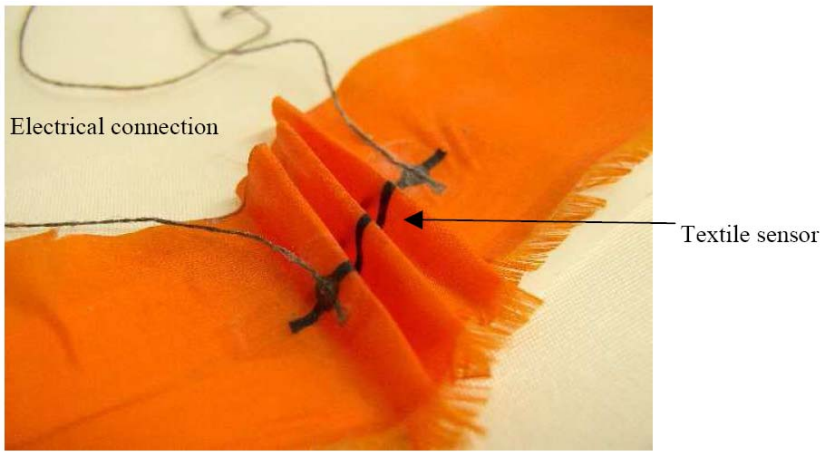

Figure 2.14 Textile strain sensor with electrical connection based on CNP filled thermoplastic elastomer [67, 98].

Conductive composite consists of 50wt% thermoplastic elastomer (TPE) and 50wt% CNP fabricated by melt mixing method was also studied as strain sensor with fiber shape configuration to measure large strain up to 80% in textiles, as shown in Figure 2.15 [100]. Study on the performance of the sensor showed that the relative resistance increased about 11% when strain rate increased from 2.5 /min to 30/min; the sensitivity expressed by gauge factor was about 20 as resistance relaxed 8.8% in 2 min with maximum strain of 80%; the maximum hysteresis error of ±3.5% (7%) and the mean hysteresis error over the working range of ±2.25% (4.5%) showed its potential industrial applications, and a prototype to measure upper body posters was build with the sensors integrated into textiles.

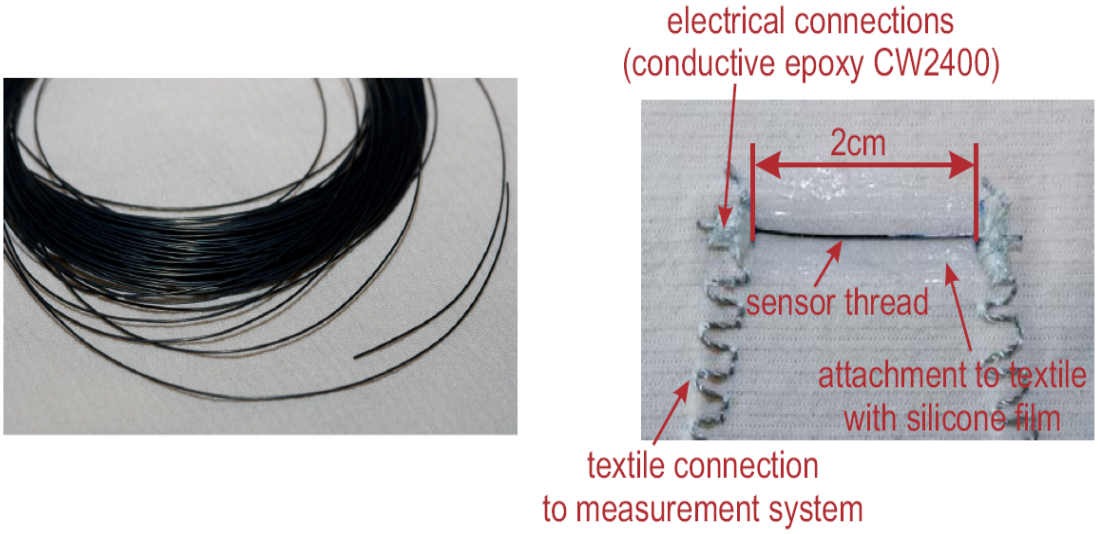

Figure 2.15 CNP filled thermoplastic elastomer composite sensor (a) sensor thread after extrusion (b) sensor thread attached to the textile with a silicone film. [100]

Conductive elastomeric composites are soft and own good flexibility that compatible with textile substrates without affecting their original physical properties. They also show large deformability and piezo-resistivity if the materials, filler loadings, and fabrication parameters were carefully selected and optimized, which can be made into flexible strain sensors for smart textiles. Though many researches on flexible strain sensors have been focused on conductive elastomeric composites materials, the existing problems such as repeatability in cyclic measurement, fatigue resistance, obvious temperature and humidity effect, reliability of sensor connection with substrate and data gathering circuit and unclear conductive and sensing mechanisms etc. reserve further study.

2.6 Comparison of different flexible strain sensors

In the above mentioned flexible strain sensors, the inductive ones, capacitive ones and polymer optical fibers are difficult to achieve the large deformations beyond 20% with good repeatability in cyclic measurement simultaneously using the existing materials and

structures though they can be made flexible, while some of the resistive ones show potential to obtain these performances. The resistive flexible strain sensors developed by various research groups have been summarized and tabulated in Table 2.2. In these flexible strain sensors, there are advantages and disadvantages for all of them. PPy is an inelastic conductive polymer while knitted fabric has large deformability, when coated PPy on knitted fabric, the deformability of the formed conductive fabrics is very small. To achieve a high strain measuring range, the continuous PPy film will be broken, as described in Figure 2.3, which counteract the efforts in stabilizing the long-term environmental stability of PPy. High sensitivity and large deformation were obtained for conductive fabrics knitted by conductive fiber. However, the data achieved is instable and the accuracy of measurement is not high enough. The strain working range of CNT filled elastomers are too small to fulfill the requirements of textile applications while sensors made by adhere CNT to elastomer is too complex and expensive though very good sensing performances was achieved. CNP filled elastomer seems to have the highest potential to be used as strain sensors with required performances, but the reliability and repeatability in cyclic measurement should be improved. In the next part, the materials and fabrication methods will be reviewed for the flexible strain sensors based on knitted fabric integrated with CNP filled elastomers.

Table 2.2 Summary of resistive flexible strain sensors and their performance

Research Groups	Materials and Fabrication Methods	Performances		Merits and disadvantages	Literature
		Repeated cycles	Strain sensitivity (GF) and range		
Farringdon (Philips Lab, UK)	Knitted fabric	-	9.5 at 42% strain	Wide strain working range Nonlinearity and instability	[41, 101, 102]
Tao XM (Hong Kong Polytechnic University, Hong Kong)	Knitted string/fabric with stainless steel filament/carbon fiber	-	2.2~5.6 at 10% strain, maximum strain range about 15~32% according to fabric density 12 ohm to 1ohm when elongated to 20% 3.0 with maximum strain of 30% for carbon tubular fabric 5.6 with strain of 15% for single warp gauge	Working temperature up to 200 ^{0}C Poor reliability	[45-48, 103-105]
	Ppy coated knitted fabric by screen printing method with chemical vapor deposition under low temperature	-	210 at maximum strain of 50%	High sensitivity Poor long-term stability	[14, 28, 29, 34, 37]
Troster (ETH Zürich, Switzerland)	50wt% thermoplastic elastomer (TPE) and 50wt% CNP fabricated by melt mixing method	3800	20 with resistance relaxed 8.8% in 2 min under maximum strain of 80%	Fiber structure is beneficial for measuring Reliability of connection is not good	[100, 106]
Koncar (Laboratoire de Génie et Matériaux Textiles, ENSAIT, France)	35 wt% CNP filled 65 wt% thermoplastic elastomers by solvent process	-	~31 at strain 0-10% and ~ 80 at strain between 15% -45%	High sensitivity and large working range Nonlinear behavior; obvious affected by humidity; resistance increased about 42% at strain of 25% when strain rate increased from 0.125/min to 12.5/min	[67, 98, 99]
De Rossi D (University of Pisa, Italy)	PPy-coated Lycra fabric or Lycra/cotton by chemical polymerization	-	~13 at 1.2% fabric strain	High sensitivity Variation of sensor resistance with time and long response time in several minutes	[32]
	Graphite loaded rubber	-	~2.5 at 10% fabric strain;	Nonlinearity	[32, 93-97,

	coated on cotton/lycra threads and knitted into fabric; Graphite loaded rubber smearing or screen printed on fabric		~2.8 for strain greater than 40%	Obvious resistance relaxation about 30% at 30% in 20Sec Large hysteresis about 13.6% at 80% strain	107-111]
G.G Wallace (University of Wollongong, Australia)	PPy coated Nylon/Lycra fabric using solution phase chemical polymerization method	-	~80 at 10-60% strain	High strain range; pre-strained 20% to ensure linearity Worse long-term stability	[35]
Wijesiriwardana (University of Manchester, England)	Carbon filled polymeric fibre laid in the course direction (rows of stitches) of the base structure of knitted fabric	-	~0.5 at 0-80% strain	Nonlinearity; worse reproducibility	[112]
Chang SH (National Taiwan University, Taiwan)	Twist piezoresistive carbon coated fibers on elastic core yarn	-	3-9 at 25% strain	High strain working range, good repeatability; Reliability is not good	[50, 51]
Hata Kenji (National Institute of Advanced Industrial Science and Technology, Japan)	Aligned CNT adhere to PDMS substrate	10,000	0.82 at 0 to 40% strain and 0.06 at 60 to 200% strain	Large working range; quick responding time Sophisticated fabrication process, low sensitivity	[54]
Seong Hun Kim (Hanyang University, Korea)	PPy coated PET/Spandex	30	-0.5 at 0-50% strain and 3 at 50% strain	High strain range; Worse long-term stability	[30, 31]

2.7 Materials

2.7.1 Carbon Nanoparticle

CNP is widely used reinforcing and conducting filler in rubber and plastic industry. It is an amorphous form of carbon with a structure similar to disordered graphite as discovered by X-ray diffraction [113]. Figure 2.16 shows the microstructure models of a typical crystallite (Figure 2.16a), random orientation of crystallites in one carbon particle (Figure 2.16b) and unit cell of graphite (Figure 2.16c) based on the X-ray diffraction results, respectively. Further investigation by dark field transmission electron microscopy (TEM) showed that hollow shell structure appeared in the oxidized CNP [114]. Diffracted beam SEM with higher resolution demonstrated that in the center regions of the CNP particle, either hollowness or lack of ordered graphitic layer segments may be exist while the orientation near the surface is more ordered [115]. Phase contrast images of CNP demonstrated that the continuous graphitic layers agreed well with the paracrystalline structure model, which is shown in Figure 2.17. Natural graphite single crystals behaved as semi-metal, therefore primary particle of the CNP showed similar properties. CNP was usually regarded as a promising conductive material for the forming of aggregates and agglomerations [116].

Aggregates and agglomerations are terminology describing CNP structure. Because CNPs are easily fused together to form continuous structure, the concept of CNP “structure” was introduced by Ladd and Wiegand [117] referring to the tendency of the CNP particles to be linked together in chains or clusters. The structure of CNP can be determined by the amount of primary particles in an aggregate. Where aggregate is defined as a discrete,

rigid colloidal entity that is the smallest dispersible unit while the primary particles of CNP can only be separated from aggregate by fracture. If many aggregates physical fused together, agglomerations are formed.

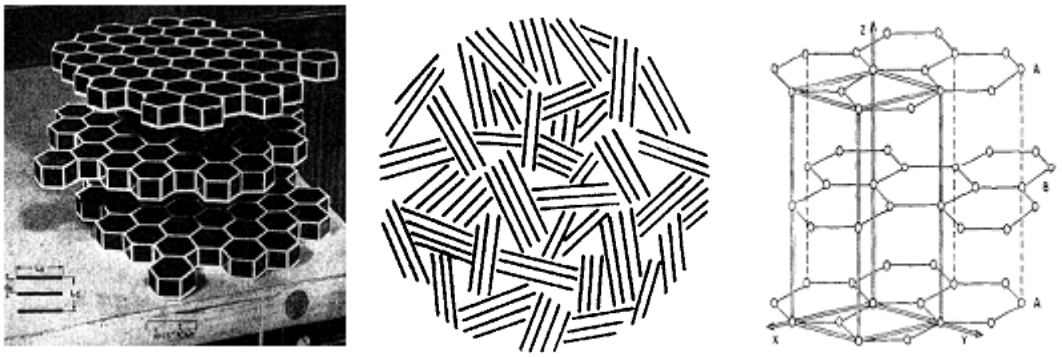

(a) [118] (b) [118] (c) [119]

Figure 2.16 Models of CNP structure based on X-ray observation and in comparison to graphite (a) typical crystallite, (b) crystallites orientation and (c) unit cell of graphite.

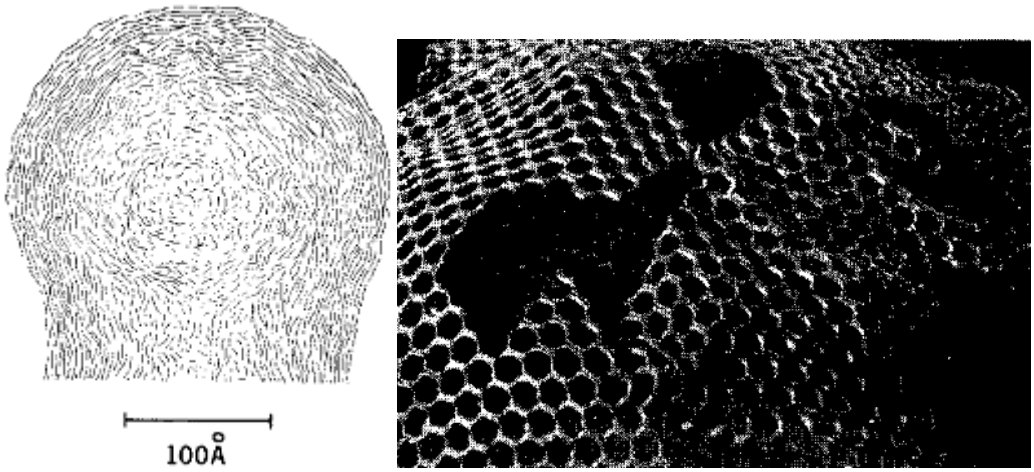

Figure 2.17 Paracrystalline structure model of CNP [120]

The structure affects not only physical properties, but also electrical properties of CNP. Since high structured CNP is easily to form agglomerates, their electrical conductivity is relatively higher than the low structured ones at same loading for the much smaller gaps between conductive aggregates, [121]. However, to separate them homogeneously, the energy consumption to overcome the Van der Walls forces between agglomerates is also

higher.

Generally speaking, particle size and distribution, surface area and porosity are also import parameters affecting the conductivity of CNPs besides structure [122, 123]. Diameter of CNP is usually measured using electron microscope method, colloidal technique and tinting strength method etc. [122]. Surface area refers to the amount of CNP surface available to interact with other spieces, it usually determined by adsorption of specified molecules on the CNP surface, such as nitrogen (ASTM D 3037), cetyltrimethyl ammonium bromide (CTAB) (ASTM D 3765) and iodine (ASTM D 1510) etc., higher adsorption means larger surface area and porosity [122]. Porosity is an import parameter for CNP characterization no matter in practical and theoretical viewpoint. It directly affects the surface area of CNP and then the physical and electrical properties in applications. Because of the aggregate tendency of CNP, the porosity of them can be divided into two categories, some porosity is open to external that can be accessible to surface, which lies in CNP particles or CNP surface in an aggregate, and can affect the result of surface area; others are close to the surface that will not reached by small molecular gas. The density of CNP is affected by both open and close pores while surface area is not related to close pores. CNPs with high structure, small diameter, large surface area, and large porosity are suitable as filler to denote the composite with higher electric conductivity, some CNPs used in conductive elastomer composites are shown in Table 2.3. Verhelst et al. [124] compared the effect of density and structure of CNP on electrical properties of conductive composites, and the resistivity-strain curves for three types of CNP filled elastomers were shown in Figure 2.18, in which the HAF CNP has low structure and low porosity, Vulcan XC 72 has high structure and low porosity, EC black has low structure and very high porosity. The results showed that EC black with the

lowest density (highest porosity) caused by the presence of a large number of hollow-shells [125] and lower structure can achieve lowest resistivity compared to other ones with relative lower density and high structure.

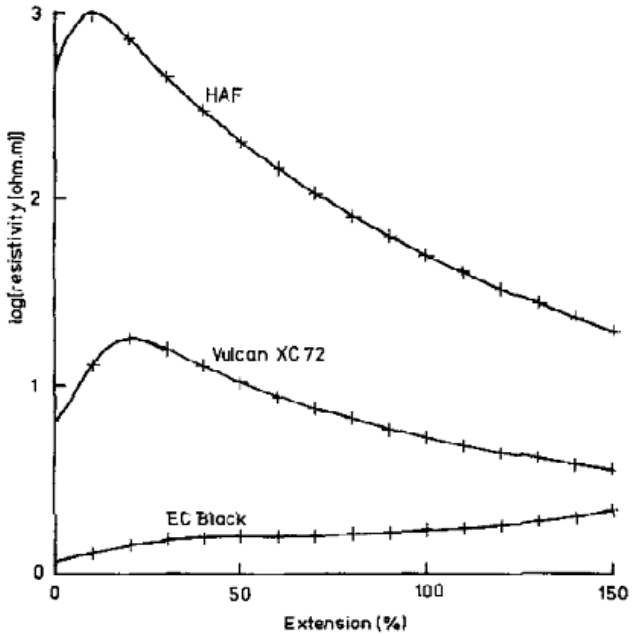

Figure 2.18 Change of resistivity on extension for SBR vulcanizates [124].

In composites, it is difficult to separate CNP particles homogeneously for high structured ones for the formation of aggregates or agglomerates, while for low structured CNP, it is much easier. Considering the application of CNP as conductive filler in elastomers for flexible strain sensors, a monotonous increase or decrease of resistivity with tensile strain is preferred. The composite filled with low structured CNP can achieve the required performance for the elimination of structure orientation process. CNP with low structure, but very high porosity can be good candidate for the sensing conductive composites in flexible strain sensor applications.

Table 2.3 Physical Properties of selected CNPs for Electrical Conductivity

Name	Diameter (nm)	Nitrogen surface area (m^2/g)	DBP absorption ($cm^3/100g$)	Resistivity (Ohm·cm)	References
Vulcan XC-72	29	180	178	-	[126, 127]
Conductex 975U	21	242	170	-	[128]
Acetylene black	42	70	250	2.6	[90, 129, 130]
BP2000	15	1475	330	-	[127]
HAF N330	27	82	102	-	[127]
Ketjenblack EC600JD	30	1270	480	-	[131]
HG1P	33	-	586	0.27	[132]
SL20	-	140	-	0.5	[133]
V4	-	220	-	-	[134]
Monarch 880	-	220	105	-	[135]
FEF N550	40	40	-	-	[136]
Vulcan 7H-N234	20-25	-	125	-	[137]
Vulcan 7H-N339	26-30	-	120	-	[137]
Sterling SO-N550	40-48	-	121	-	[137]
Printex L6	18	250	122	-	[67]

Printex 30	27	80	102	-	[128]
Lampblack	60-200	14-24	-	-	[138]
MS-TS	300	8	33	-	[128]
GPF 660	70	39	70	-	[127]

2.7.2 Elastomers

Elastomers, also named rubbers, are insulating materials with elastic properties. Elastomers are amorphous polymers existing above their glass transition temperature, so that considerable segmental motion is possible with flexibility and deformable properties, their molecular structure can be imagined as a 'spaghetti and meatball' structure, with the meatballs signifying cross-links. The elasticity is derived from the ability of the long chains to reconfigure them to distribute an applied stress. The covalent cross-linkages ensure that the elastomer will return to its original configuration when the stress is removed. As a result of this extreme flexibility, elastomers can reversibly extend from 5 to 700%, depending on the specific material. By hybrid conductive CNP, insulating properties of elastomer can be transformed to conductive and the resistance decreased with increase of CNP loading, external conditions such as force and temperature, etc. can also change the electrical resistance of the CNP filled elastomers.

Various elastomers have been used for preparation of CNP filled composites, including NR [138, 139], EPDM [140, 141], EVA [142, 143], SBR [144], NR [74, 90, 128, 130, 145-148], EO [69, 89], PDMS [149], Polyisoprene [150], SE [151] and blends of two or more immiscible elastomers [90, 130, 148]. The performance of elastomers has obvious influence on the conductive composites from dispersion to performance of end products [152, 153]. Since the introduction of CNP will significantly increase the viscosity of mixtures, resulting in difficulty of dispersion and higher Young’s modulus. So elastomer with lower viscosity is benefit for composites fabrication. The interaction between elastomers and CNP also affect CNP dispersion. If the interaction between CNP and elastomer is higher than that between CNP and CNP, the dispersion will get easier. However, the percolation threshold will correspondingly increase for the good interaction

between elastomer and CNP that reduced the contact between CNP particles until a higher CNP concentration was reached.

Considering the application of flexible strain sensor close to human body, the room vulcanized SE will be preferred elastomer for its good biocompatibility, low viscosity and low vulcanization temperature along with excellent mechanical properties.

2.7.3 Fabrics

Fabrics are essential element of clothing, they have high surface area, wide range of mechanical properties, high flexibility, and large-scale deform availability, making them adequate for substrate of strain gauges to measure the large scale deformation. Fabrics can be classified into woven fabric, knitted fabric and nonwoven fabric, in which the mechanical properties of nonwoven fabric are poor. The woven fabric is nearly inelastic without the use of elastic yarn, and the deformation is smaller than 10% for most woven fabrics even when elastic yarns are used. Knitted fabric is usually knitted with elastic yarn/filament and has the most significant elasticity and large deforming ability of more than 100% for its structure and the elastic yarn/filament adopted, and excellent mechanical behavior under cyclic loading-unloading cycles. Many researches on smart textiles have integrated conductive yarn into knitted fabrics as flexible strain sensors [45, 48], or to be substrate by attaching flexible strain sensors on knitted fabrics [100]. These efforts have greatly enhanced the working range of flexible strain sensors. However, sensors with better performances can be achieved if the materials, structure of knitted fabric are well examined, and the fabric was used as part of the flexible strain sensor.

2.8 Fabrication Methods

To fabricate CNP filled elastomers with uniform mechanical and electrical properties, the CNP particles should be uniformly dispersed into elastomers, and then vulcanized. The performance of the composite system is obviously affected by mixing and fabrication methods [154, 155].

Though the processing parameters of CNP filled elastomers have been studied by some researchers and the composites with better conductivity can be achieved with relatively lower CNP loadings by uneven dispersion of CNP particles without destroying their structure was concluded [91]. However, the inhomogeneous mixture will affect the stability and reproducibility of the composites under cyclic measurement for both mechanical and electrical properties.

Various dispersion methods (e.g., stirring, extrusion, kneading, etc.) for the distribution of CNPs in elastomers have been used by considering the categories of polymer matrix and the processing methods. Sonication technique is a common technique to disperse CNPs in composites; it can exfoliate agglomerates and disperse CNPs in the matrix effectively by a pulsed ultrasound. However, this method is only manageable for small batches due to the extreme reduction of the vibrational energy with increasing distance from the sonic tip. The use of calendars is the most common technique for the dispersion of micro-scaled particles in industry (e.g., cosmetics, paints and coatings, rubber, etc.) and also seems to be an appropriate method for the distribution of nanoparticles like CNP into elastomers. As schematically shown in Figure 2.19, the shearing forces act on CNP agglomerates at the interfaces of laminar flow and break them into primary aggregates [156]. According to the type and viscosity of elastomers, three methods can be used for dispersion.

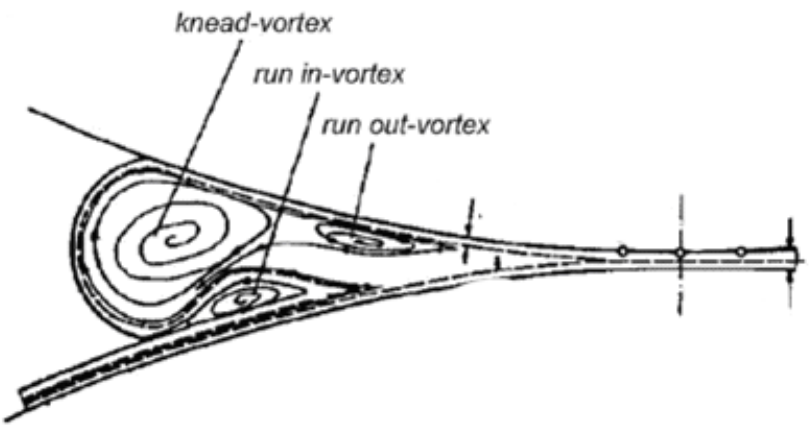

Figure 2.19 Schematic of small particles dispersed into elastomer by three-roll mill [157].

2.8.1 Dry Mixing

Dry mixing is usually adopted to mix CNP and low viscosity of gum elastomer blends at room temperature by using two-roll mill, three-roll mill, internal mixers or extruders [90]. It is one of the most frequently used techniques to disperse CNP into elastomers. During mixing, the CNP agglomerates at the interface of laminar flow were broken down to primary aggregates by shear force. The mixing process is very simple; however, it is difficult to uniformly mix the high porous CNP filled elastomers for sensor application for the high viscosity of mixtures.

2.8.2 Melt Mixing

For thermoplastic elastomers under solid states, melt mixing can be used for CNP dispersing. For example, fillers can be added into melted EO elastomer to fabricate CNP/EO composite [89]. The same method was also used to fabricate nano-particle CNP/ thermoplastic elastomer (TPE) composite[67] [100]. The viscosity of elastomer under melted status was still not sufficient low to completely wet and disperse high volume

fraction of CNP, which deteriorate the dispersion effect. Moreover, the energy consumed under high shear mixing condition is high, which increased the cost of production.

2.8.3 Solution Aided Mixing

Most elastomers exist with morphology of gum before vulcanization and the viscosity of them increases dramatically with the addition of CNP loading, which deteriorates the dispersion characteristics of elastomer. By diluting elastomers into organic solvent (Hexane, toluene, chloroform, and ethylene chloride, etc.) that can be volatilize after mixing, the dispersing of CNP is getting easier [158]. To disperse CNP fillers into silicone rubber, hexane was selected as solvent and mechanical stirring along with ultrasonic vibration was used to aided for better particle dispersion [159] [160], while the same method but different sequences was adopted to disperse CNP in NBR and SBR [135, 137]. By compare the melt mixing and solution aided mixing method, the latter one was selected by Cochrane [67] for EVO/CNP composite because this method can disperse CNP better than melt mixing method due to the lower viscosity of the solution. The long fabrication time and toxic material used as solvent are the disadvantage of this method, but by changing solvent and processing parameters, the defaults can be diminished.

After conductive CNP was well dispersed into elastomers, compression-molded [67, 132, 161] or extrusion methods [100] was usually used to fabricate the required composites according to the requirements of samples.

2.9 Summary

Smart textiles and clothing have great potential to be applied in fields like rehabilitation,

entertainment, sports, etc. Reliable flexible strain sensors that can be easily embedded into textiles with performances of low modulus less than 1MPa, large strain measuring range beyond 20%, good repeatability in cyclic measurement with fatigue life more than 100,000 and good sensing properties are essentially important for market and become the subject of many researches. Although there are many investigations concerned on the flexible strain sensors, it is still lack of studies on improving the mentioned properties of fabric strain sensors that can easily embedded into textile or clothing with low price. So it is evident that there is a critical need for comprehensive study on the materials, structures, fabricating parameters, treatment methods and sensing mechanisms towards the improvement and balance of sensor performances for reliable application in smart textiles.

The existing methods for developing the required flexible strain sensors have been reviewed and discussed in this chapter. Among the fabricating methods, the inductive, capacitive transducer and polymer optical fibers seem to be difficult in achieving the required performances, especially for the large strain working range and good repeatability in cyclic measurement as well as good fatigue resistance. In the resistive flexible strain sensors, the environmental stability of conductive fiber/yarn/fabrics coated intrinsically conductive polymers are still poor due to the instability of conductive material even though various methods have been investigate to increase their stability, while the reliability and accuracy of conductive fabrics knitted by conductive fiber/filament is not good enough. CNP filled elastomer seems to have the highest potential to achieve better performances. However, there is no sensor can fully satisfy the requirements of flexible strain sensor in smart textiles, especially the high fatigue resistance and repeatability in cyclic measurement, the accuracy, temperature and

humidity effect and reliability in connection with substrate and measuring circuit also need further improvement.

Based on the above consideration, CNP filled elastomers with low modulus and better electromechanical properties will be studied and optimized as conductive and sensing element of flexible strain sensor. Knitted fabric with good mechanical properties will be selected and integrated with conductive CNP filled elastomer as supporting element for the good fatigue resistance and elasticity. The materials, fabrication methods, structures and treatment methods of the sensor will be studied and optimized to achieve a flexible strain sensor with low modulus, large working range, good fatigue resistance and sensing performances. Based on the study, the sensing mechanism of the sensor will also be studied.

References

1. Wijesiriwardana, R., *Inductive fiber-meshed strain and displacement transducers for respiratory measuring systems and motion capturing systems.* Ieee Sensors Journal, 2006. **6**(3): p. 571-579.
2. Matsuzaki, R. and A. Todoroki, *Wireless strain monitoring of tires using electrical capacitance changes with an oscillating circuit.* Sensors and Actuators a-Physical, 2005. **119**(2): p. 323-331.
3. Tang, L.Q., X.M. Tao, W.C. Du, and C.L. Choy. *Reliability of fiber Bragg grating sensors embedded in textile composites*. in *7th International Conference on Composite Interfaces (ICCI-VII)*. 1998. Fujisawa, Japan.
4. Tao, X.M., L.Q. Tang, W.C. Du, and C.L. Choy, *Internal strain measurement by fiber Bragg grating sensors in textile composites.* Composites Science and Technology, 2000. **60**(5): p. 657-669.
5. Witt, J., M. Schukar, and K. Krebber, *Medicinal Textiles with Integrated Polymer-Optical Fibers for Respiration Monitoring.* Tm-Technisches Messen, 2008. **75**(12): p. 670-677.
6. Yang, B., X.M. Tao, J.Y. Yu, and H.L. Ho, *Compression force measured by fiber optic smart cellular textile composites.* Textile Research Journal, 2004. **74**(4): p. 305-313.
7. Yang, B., J.Y. Yu, X.M. Tao, and H.L. Ho, *Tangential load measurements by a smart textile composite.* Textile Research Journal, 2004. **74**(9): p. 810-818.
8. Yang, C.M., W.T. Huang, T.L. Yang, M.C. Hsieh, and C.T. Liu. *Textiles Digital Sensors for Detecting Breathing Frequency*. in *5th International Summer School*

and Symposium on Medical Devices and Biosensors. 2008. Hong Kong, PEOPLES R CHINA.

9. Yuan, J.M., M.A. El-Sherif, S. Khalil, and J. Fairneny. *Characterization of integrated fiber optic sensors in smart textiles*. in *Conference on Industrial and Highway Sensors Technology*. 2003. Providence, RI.
10. Yuan, S.F., R. Huang, and Y.J. Rao, *Internal strain measurement in 3D braided composites using co-braided optical fiber sensors.* Journal of Materials Science & Technology, 2004. **20**(2): p. 199-202.
11. Babchenko, A. and J. Maryles, *Graded-index plastic optical fiber for deformation sensing.* Optics and Lasers in Engineering, 2007. **45**(7): p. 757-760.
12. Neubert, H.K.P., *Instrument Transducers: An Introduction to Their Performance and Design*2003: Oxford University Press.
13. Wallace, G.G., G.M. Spinks, L.A.P. Kane-Maguire, and P.R. Teasdale, *Conductive Electroactive Polymers: Intelligent Materials Systems*. 2nd ed2003: CRC Press, Boca Raton, FL.
14. Li, Y., X.Y. Cheng, M.Y. Leung, J. Tsang, X.M. Tao, and M.C.W. Yuen, *A flexible strain sensor from polypyrrole-coated fabrics.* Synthetic Metals, 2005. **155**(1): p. 89-94.
15. Gregory, R.V., W.C. Kimbrell, and H.H. Kuhn, *Conductive Textiles.* Synthetic Metals, 1989. **28**(1-2): p. C823-C835.
16. Heisey, C.L., J.P. Wightman, E.H. Pittman, and H.H. Kuhn, *Surface and Adhesion Properties of Polypyrrole-Coated Textiles.* Textile Research Journal, 1993. **63**(5): p. 247-256.
17. Kuhn, H.H., *Characterization and Application of Polypyrrole-Coated Textiles*, in *Intrinsically Conducting Polymers : an Emerging Technology*, M. Aldissi, Editor 1993. p. 25-34.
18. Kuhn, H.H., W.C. Kimbrell, J.E. Fowler, and C.N. Barry, *Properties and Applications of Conductive Textiles.* Synthetic Metals, 1993. **57**(1): p. 3707-3712.
19. Child, A.D. and H.H. Kuhn, *Degradation of Conductivity in Polypyrrole Coated Textiles.* Abstracts of Papers of the American Chemical Society, 1994. **207**: p. 247-POLY.
20. Kuhn, H.H., A.D. Child, and W.C. Kimbrell, *Toward Real Applications of Conductive Polymers.* Synthetic Metals, 1995. **71**(1-3): p. 2139-2142.
21. Avlyanov, J.K., H.H. Kuhn, J.Y. Josefowicz, and A.G. MacDiarmid, *In-situ deposited thin films of polypyrrole: Conformational changes induced by variation of dopant and substrate surface.* Synthetic Metals, 1997. **84**(1-3): p. 153-154.
22. Child, A.D. and H.H. Kuhn, *Enhancement of the thermal stability of chemically synthesized polypyrrole.* Synthetic Metals, 1997. **84**(1-3): p. 141-142.
23. Kuhn, H.H., *Adsorption at the liquid/solid interface: Conductive textiles based on polypyrrole.* Textile Chemist and Colorist, 1997. **29**(12): p. 17-21.
24. De Rossi, D., A. Della Santa, and A. Mazzoldi, *Dressware: Wearable piezo- and thermoresistive fabrics for ergonomics and rehabilitation*, in *Proceedings of the 19th Annual International Conference of the Ieee Engineering in Medicine and Biology Society, Vol 19, Pts 1-6: Magnificent Milestones and Emerging Opportunities in Medical Engineering*1997. p. 1880-1883.
25. Alici, G., G.M. Spinks, J.D. Madden, Y.Z. Wu, and G.G. Wallace, *Response characterization of electroactive polymers as mechanical sensors.* Ieee-Asme Transactions on Mechatronics, 2008. **13**(2): p. 187-196.
26. Kim, B., V. Koncar, E. Devaux, C. Dufour, and P. Viallier, *Electrical and morphological properties of PP and PET conductive polymer fibers.* Synthetic

Metals, 2004. **146**(2): p. 167-174.
27. Spinks, G.M., B.B. Xi, D.Z. Zhou, V.T. Truong, and G.G. Wallace, *Enhanced control and stability of polypyrrole electromechanical actuators.* Synthetic Metals, 2004. **140**(2-3): p. 273-280.
28. Wang, J.P., P. Xue, and X.M. Tao, *Strain sensing behavior of electrically conductive fibers under large deformation.* Materials Science and Engineering a-Structural Materials Properties Microstructure and Processing, 2011. **528**(6): p. 2863-2869.
29. Xue, P., X.M. Tao, and H.Y. Tsang, *In situ SEM studies on strain sensing mechanisms of PPy-coated electrically conducting fabrics.* Applied Surface Science, 2007. **253**(7): p. 3387-3392.
30. Oh, K.W., H.J. Park, and S.H. Kim, *Stretchable conductive fabric for electrotherapy.* Journal of Applied Polymer Science, 2003. **88**(5): p. 1225-1229.
31. Kim, H.A., M.S. Kim, S.Y. Chun, Y.H. Park, B.S. Jeon, J.Y. Lee, et al. *Characteristics of electrically conducting polymer-coated textiles*. in *13th Korea-Japan Joint Forum on Organic Materials for Electronics and Photonics*. 2002. Sendai, Japan.
32. Tognetti, A., F. Carpi, F. Lorussi, A. Mazzoldi, P. Orsini, E.P. Scilingo, et al. *Wearable sensory-motor orthoses for tele-rehabilitation*. in *25th Annual International Conference of the IEEE-Engineering-in-Medicine-and-Biology-Society*. 2003. Cancun, MEXICO.
33. Lorussi, F., W. Rocchia, E.P. Scilingo, A. Tognetti, and D. De Rossi, *Wearable, redundant fabric-based sensor arrays for reconstruction of body segment posture.* Ieee Sensors Journal, 2004. **4**(6): p. 807-818.
34. Tsang, J., S. Leung, X. Tao, M.C. Yuen, and P. Xue, *Effect of fabrication temperature on strain-sensing capacity of polypyrrole-coated conductive fabrics.* Polymer International, 2007. **56**(7): p. 827-833.
35. Campbell, T.E., B.J. Munro, G.G. Wallace, and J.R. Steele, *Can fabric sensors monitor breast motion?* Journal of Biomechanics, 2007. **40**(13): p. 3056-3059.
36. Tjahyono, A.P., K.C. Aw, J. Travas-Sejdic, and K.C. Li, *Flexible strain sensor for air muscles using Polypyrrole coated rubber*, in *Electroactive Polymer Actuators and Devices*, Y. BarCohen, Editor 2010.
37. Xue, P., X.M. Tao, H.Y. Tsang, and M.Y. Leung. *PPy-coated electrically conducting fabrics with high strain sensitivity*. in *Symposium on Smart Nanotextiles held at the 2006 MRS Spring Meeting*. 2006. San Francisco, CA.
38. Kim, M.S., H.K. Kim, S.W. Byun, S.H. Jeong, Y.K. Hong, J.S. Joo, et al., *PET fabric/polypyrrole composite with high electrical conductivity for EMI shielding.* Synthetic Metals, 2002. **126**(2-3): p. 233-239.
39. Harlin, A., P. Nousiainen, A. Puolakka, J. Pelto, and J. Sarlin, *Development of polyester and polyamide conductive fibre.* Journal of Materials Science, 2005. **40**(20): p. 5365-5371.
40. Kim, B., V. Koncar, and C. Dufour, *Polyaniline-coated PET conductive yarns: Study of electrical, mechanical, and electro-mechanical properties.* Journal of Applied Polymer Science, 2006. **101**(3): p. 1252-1256.
41. Farringdon, J., A.J. Moore, N. Tilbury, J. Church, and P.D. Biemond, *Wearable sensor badge and sensor jacket for context awareness*, in *The 3rd International Symposium on Wearable Computers*1999: San Francisco, California, USA
42. Gibbs, P. and H.H. Asada. *Wearable conductive fiber sensor arrays for measuring multi-axis joint motion*. in *26th Annual International Conference of the IEEE Engineering in Medicine and Biology Society*. 2004. San Francisco, CA.

43. Farringdon, J., A.J. Moorea, N. Tilburyb, J. Churchb, and P.D. Biemond. *Wearable Sensor Badge & Sensor Jacket for Context Awareness*. in *ISWC '99 Proceedings of the 3rd IEEE International Symposium on Wearable Computers*. 1999. IEEE Computer Society Washington, DC, USA.
44. Farringdon, J. and S. Nashold. *Continuous body monitoring*. in *Workshop on Ambient Intelligence for Scientific Discovery*. 2004. Vienna, AUSTRIA.
45. Yang, B., X.M. Tao, and J.Y. Yu, *A study on the relation between resistance and strain based on stainless steel fabric.* Rare Metal Materials and Engineering, 2006. **35**(1): p. 96-99.
46. Zhang, H., X.M. Tao, S.Y. Wang, and T.X. Yu, *Electro-mechanical properties of knitted fabric made from conductive multi-filament yarn under unidirectional extension.* Textile Research Journal, 2005. **75**(8): p. 598-606.
47. Zhang, H., X.M. Tao, T.X. Yu, and S.Y. Wang, *Conductive knitted fabric as large-strain gauge under high temperature.* Sensors and Actuators a-Physical, 2006. **126**(1): p. 129-140.
48. Zhang, H., X.M. Tao, T.X. Yu, S.Y. Wang, and X.Y. Cheng, *A novel sensate 'string' for large-strain measurement at high temperature.* Measurement Science & Technology, 2006. **17**(2): p. 450-458.
49. Xue, P., X.M. Tao, K.W.Y. Kwok, M.Y. Leung, and T.X. Yu, *Electromechanical behavior of fibers coated with an electrically conductive polymer.* Textile Research Journal, 2004. **74**(10): p. 929-936.
50. Huang, C.T., C.F. Tang, M.C. Lee, and S.H. Chang, *Parametric design of yarn-based piezoresistive sensors for smart textiles.* Sensors and Actuators a-Physical, 2008. **148**(1): p. 10-15.
51. Huang, C.T., C.L. Shen, C.F. Tang, and S.H. Chang, *A wearable yarn-based piezo-resistive sensor.* Sensors and Actuators a-Physical, 2008. **141**(2): p. 396-403.
52. Riekeberg, S., J. Buttner, and J. Muller, *A Carbon Nanotube Based Temperature Independent Strain Sensor on a Flexible Polymer*, in *2010 Ieee Sensors* 2010. p. 647-651.
53. Zhao, H.B., Y.Y. Zhang, P.D. Bradford, Q.A. Zhou, Q.X. Jia, F.G. Yuan, et al., *Carbon nanotube yarn strain sensors.* Nanotechnology, 2010. **21**(30).
54. Yamada, T., Y. Hayamizu, Y. Yamamoto, Y. Yomogida, A.I. Najafabadi, D.N. Futaba, et al., *A stretchable carbon nanotube strain sensor for human-motion detection.* Nature Nanotechnology, 2011.
55. Mahapatra, S.P., V. Sridhar, and D.K. Tripathy, *Impedance analysis and electromagnetic interference shielding effectiveness of conductive carbon black reinforced microcellular EPDM rubber vulcanizates.* Polymer Composites, 2008. **29**(5): p. 465-472.
56. Aal, N.A., F. El-Tantawy, A. Al-Hajry, and M. Bououdina, *New antistatic charge and electromagnetic shielding effectiveness from conductive epoxy resin/plasticized carbon black composites.* Polymer Composites, 2008. **29**(2): p. 125-132.
57. Vilcakova, J., M. Paligova, M. Omastova, P. Saha, and O. Quadrat, *"Switching effect" in pressure deformation of silicone rubber/polypyrrole composites.* Synthetic Metals, 2004. **146**(2): p. 121-126.
58. Park, E.S., L.W. Jang, and J.S. Yoon, *Resistivity and thermal reproducibility of carbon black and metallic powder filled silicone rubber heaters.* Journal of Applied Polymer Science, 2005. **95**(5): p. 1122-1128.
59. Song, Y.H., Y. Pan, Q. Zheng, and X.S. Yi, *The electric self-heating behavior of graphite-filled high-density polyethylene composites.* Journal of Polymer Science,

Part B: Polymer Physics, 2000. **38**(13): p. 1756-1763.
60. Cheng, X.Y., H.Y.J. Tsang, Y. Li, M.Y. Leung, X.M. Tao, X.X. Cheng, et al., *Polypyrrole-coated large deformation strain fabric sensor and its properties study*, in *Smart Nanotextiles*, X. Tao, G. Troster, and D. Diamond, Editors. 2006. p. 127-133.
61. Xue, P. and X.M. Tao, *Morphological and electromechanical studies of fibers coated with electrically conductive polymer.* Journal of Applied Polymer Science, 2005. **98**(4): p. 1844-1854.
62. Godfrey, T.A., *Strain effects on percolation conduction in conductive particle filled composites.* Journal of Materials Science, 2008. **43**(3): p. 1128-1134.
63. Luo, Y.L., Y.L. Li, and Z.Q. Li, *Investigation into the vapor sensing behavior and mechanism of a reactive hydroxyl-terminated polybutadiene liquid rubber/carbon black conductive film.* Smart Materials & Structures, 2006. **15**(6): p. 1979-1985.
64. Carrillo, A., I.R. Martin-Dominguez, and A. Marquez-Lucero, *Modeling and experimental testing of the effect of solvent absorption on the electric properties of styrene butadiene rubber/carbon black chemical sensors.* Sensors and Actuators B-Chemical, 2006. **113**(1): p. 477-486.
65. Dong, X.M., R.W. Fu, M.Q. Zhang, B. Zhang, and M.Z. Rong, *Electrical resistance response of carbon black filled amorphous polymer composite sensors to organic vapors at low vapor concentrations.* Carbon, 2004. **42**(12-13): p. 2551-2559.
66. Busfield, J.J.C., A.G. Thomas, and K. Yamaguchi, *Electrical and mechanical behavior of filled rubber. III. Dynamic loading and the rate of recovery.* Journal of Polymer Science, Part B: Polymer Physics, 2005. **43**(13): p. 1649-1661.
67. Cochrane, C., V. Koncar, M. Lewandowski, and C. Dufour, *Design and development of a flexible strain sensor for textile structures based on a conductive polymer composite.* Sensors, 2007. **7**(4): p. 473-492.
68. Das, N.C., T.K. Chaki, and D. Khastgir, *Effect of axial stretching on electrical resistivity of short carbon fibre and carbon black filled conductive rubber composites.* Polymer International, 2002. **51**(2): p. 156-163.
69. Flandin, L., A. Hiltner, and E. Baer, *Interrelationships between electrical and mechanical properties of a carbon black-filled ethylene-octene elastomer.* Polymer, 2001. **42**(2): p. 827-838.
70. Kluppel, M., *The role of disorder in filler reinforcement of elastomers on various length scales*, in *Filler-Reinforced Elastomers Scanning Force Microscopy*2003, Springer-Verlag Berlin: Berlin. p. 1-86.
71. Knite, M., V. Teteris, A. Kiploka, and J. Kaupuzs. *Polyisoprene-carbon black nanocomposites as tensile strain and pressure sensor materials*. in *EUROSENSORS XVI Conference*. 2002. Prague, Czech Republic.
72. Kost, J., A. Foux, and M. Narkis, *Quantitative Model Relating Electrical-Resistance, Strain, and Time for Carbon-Black Loaded Silicone-Rubber.* Polymer Engineering and Science, 1994. **34**(21): p. 1628-1634.
73. Oliveira, F.A., N. Alves, J.A. Giacometti, C.J.L. Constantino, L.H.C. Mattoso, A. Man, et al., *Study of the thermomechanical and electrical properties of conducting composites containing natural rubber and carbon black.* Journal of Applied Polymer Science, 2007. **106**(2): p. 1001-1006.
74. Pramanik, P.K., D. Khastagir, and T.N. Saha, *Effect of Extensional Strain on the Resistivity of Electrically Conductive Nitrile-Rubber Composites Filled with Carbon Filler.* Journal of Materials Science, 1993. **28**(13): p. 3539-3546.
75. Xie, Z.M., Y.J. Yum, and C.K. Lee, *Simulation of electrical resistivity of carbon*

black filled rubber under elongation. Journal of Macromolecular Science Part B-Physics, 2007. **46**(3): p. 561-567.
76. Yamaguchi, K., J.J.C. Busfield, and A.G. Thomas, *Electrical and mechanical behavior of filled elastomers. I. The effect of strain.* Journal of Polymer Science, Part B: Polymer Physics, 2003. **41**(17): p. 2079-2089.
77. Beruto, D.T., M. Capurro, and G. Marro, *Piezoresistance behavior of silicone-graphite composites in the proximity of the electric percolation threshold.* Sensors and Actuators A-Physical, 2005. **117**(2): p. 301-308.
78. Chen, X.D., Y.D. Jiang, Z.M. Wu, D. Li, and J.D. Yang. *Morphology and gas-sensitive properties of polymer based composite films*. in *7th International Meeting on Chemical Sensors (IMCS-7)*. 1998. Beijing, Peoples R China.
79. Das, N.C., T.K. Chaki, and D. Khastgir, *Carbon fiber-filled conductive composites based on EVA, EPDM and their blends.* Journal of Polymer Engineering, 2002. **22**(2): p. 115-136.
80. Kim, J.H., Y.J. Kim, W.K. Baek, K.T. Lim, and I. Kang, *Flexible Strain Sensor Based on Carbon Nanotube Rubber Composites*, in *Nanosensors, Biosensors, and Info-Tech Sensors and Systems 2010*, V.K. Varadan, Editor 2010.
81. Laxminarayana, K. and N. Jalili, *Functional nanotube-based textiles: Pathway to next generation fabrics with enhanced sensing capabilities.* Textile Research Journal, 2005. **75**(9): p. 670-680.
82. Pham, G.T., Y.B. Park, Z. Liang, C. Zhang, and B. Wang, *Processing and modeling of conductive thermoplastic/carbon nanotube films for strain sensing.* Composites Part B-Engineering, 2008. **39**(1): p. 209-216.
83. Abraham, J.K., L. Aryasomayajula, A. Whitchurch, and V.K. Varadan, *Carbon nanotube strain sensors for wearable patient monitoring applications*, in *Nanosensors and Microsensors for Bio-Systems 2008*, V.K. Varadan, Editor 2008. p. J9310-J9310.
84. Hu, N., Y. Karube, M. Arai, T. Watanabe, C. Yan, Y. Li, et al., *Investigation on sensitivity of a polymer/carbon nanotube composite strain sensor.* Carbon, 2010. **48**(3): p. 680-687.
85. Yu, T., Z.H. Ni, C.L. Du, Y.M. You, Y.Y. Wang, and Z.X. Shen, *Raman mapping investigation of graphene on transparent flexible substrate: The strain effect.* Journal of Physical Chemistry C, 2008. **112**(33): p. 12602-12605.
86. Novak, I., I. Krupa, and I. Janigova, *Hybrid electro-conductive composites with improved toughness, filled by carbon black.* Carbon, 2005. **43**(4): p. 841-848.
87. Kost, J., M. Narkis, and A. Foux, *Resistivity Behavior of Carbon-Black-Filled Silicone-Rubber in Cyclic Loading Experiments.* Journal of Applied Polymer Science, 1984. **29**(12): p. 3937-3946.
88. Kost, J., M. Narkis, and A. Foux, *Effects of Axial Stretching on the Resistivity of Carbon-Black Filled Silicone-Rubber.* Polymer Engineering and Science, 1983. **23**(10): p. 567-571.
89. Flandin, L., A. Chang, S. Nazarenko, A. Hiltner, and E. Baer, *Effect of strain on the properties of an ethylene-octene elastomer with conductive carbon fillers.* Journal of Applied Polymer Science, 2000. **76**(6): p. 894-905.
90. Sau, K.P., T.K. Chaki, and D. Khastgir, *The change in conductivity of a rubber carbon black composite subjected to different modes of pre-strain.* Composites Part A-Applied Science and Manufacturing, 1998. **29**(4): p. 363-370.
91. Das, N.C., T.K. Chaki, and D. Khastgir, *Effect of processing parameters, applied pressure and temperature on the electrical resistivity of rubber-based conductive composites.* Carbon, 2002. **40**(6): p. 807-816.

92. Knite, M., V. Teteris, A. Kiploka, and I. Klemenoks, *Reversible tenso-resistance and piezo-resistance effects in conductive polymer-carbon nanocomposites.* Advanced Engineering Materials, 2004. **6**(9): p. 742-746.
93. Scilingo, E.P., A. Gemignani, R. Paradiso, N. Taccini, B. Ghelarducci, and D. De Rossi. *Performance evaluation of sensing fabrics for monitoring physiological and biomechanical variables*. in *International Workshop on New Generation of Smart Wearable Health Systems and Applications*. 2003. Lucca, ITALY.
94. Tognetti, A., F. Lorussi, M. Tesconi, and D. De Rossi. *Strain sensing fabric characterization*. in *IEEE Sensors 2004 Conference*. 2004. Vienna, AUSTRIA.
95. Tognetti, A., F. Lorussi, R. Bartalesi, M. Tesconi, G. Zupone, and D. De Rossi. *Analysis and synthesis of human movements: Wearable kinesthetic interfaces*. in *IEEE 9th International Conference on Rehabilitation Robotics*. 2005. Chicago, IL.
96. Tognetti, A., N. Carbonaro, G.Z. Pone, and D. De Rossi. *Characterization of a novel data glove based on textile integrated sensors*. in *28th Annual International Conference of the IEEE-Engineering-in-Medicine-and-Biology-Society*. 2006. New York, NY.
97. Tognetti, A., R. Bartalesi, F. Lorussi, and D. De Rossi, *Body segment position reconstruction and posture classification by smart textiles.* Transactions of the Institute of Measurement and Control, 2007. **29**(3-4): p. 215-253.
98. Koncar, V., C. Cochrane, M. Lewandowski, F. Boussu, and C. Dufour. *Electro-conductive sensors and heating elements based on conductive polymer composites*. in *3rd International Technical Textiles Congress*. 2007. Istanbul, TURKEY.
99. Cochrane, C., M. Lewandowski, and V. Koncar, *A Flexible Strain Sensor Based on a Conductive Polymer Composite for in situ Measurement of Parachute Canopy Deformation.* Sensors, 2010. **10**(9): p. 8291-8303.
100. Mattmann, C., F. Clemens, and G. Troster, *Sensor for measuring strain in textile.* Sensors, 2008. **8**(6): p. 3719-3732.
101. Krause, A., D.P. Siewiorek, A. Smailagic, and J. Farringdon. *Unsupervised, dynamic identification of physiological and activity context in wearable computing*. in *7th International Symposium on Wearable Computers*. 2003. White Plains, Ny.
102. Farringdon, J. and S. Nashold, *Continuous body monitoring*, in *Ambient Intelligence for Scientific Discovery: Foundations, Theories, and Systems*, Y. Cai, Editor 2005. p. 202-223.
103. Yang, B., X.M. Tao, and J.Y. Yu. *A study on textile structure used as strain sensor made of stainless steel fiber*. in *83rd Textile-Institute World Conference*. 2004. Shanghai, PEOPLES R CHINA.
104. Zhang, H., X.M. Tao, and S.Y. Wang. *Modeling of elecro-mechanical properties of conductive knitted fabrics under large uniaxial deformation*. in *83rd Textile-Institute World Conference*. 2004. Shanghai, PEOPLES R CHINA.
105. Yang, B., X.M. Tao, J.Y. Cai, and T.X. Yu. *Strain sensing behavior of textile structures made of stainless steel continuous filament yarns under uni-axial tensile loading*. in *International Conference on Smart Materials and Nanotechnology in Engineering*. 2007. Harbin, PEOPLES R CHINA.
106. Mattmann, C., O. Amft, H. Harms, and G. Troster. *Recognizing upper body postures using textile strain sensors*. in *11th International Symposium on Wearable Computers*. 2007. Boston, MA.
107. Lorussi, F., E.P. Scilingo, M. Tesconi, A. Tognetti, and D. De Rossi. *Strain sensing fabric for hand posture and gesture monitoring*. in *International Workshop on*

New Generation of Smart Wearable Health Systems and Applications. 2003. Lucca, ITALY.
108. Bartalesi, R., F. Lorussi, M. Tesconi, A. Tognetti, G. Zupone, and D. De Rossi. *Wearable kinesthetic system for capturing and classifying upper limb gesture*. in *1st Joint Eurohaptics Conference/Symposium on Haptic Interfaces for Virtual Environment and Teleoperator Systems*. 2005. Pisa, ITALY.
109. Tognetti, A., F. Lorussi, M. Tesconi, R. Bartalesi, G. Zupone, and D. De Rossi. *Wearable kinesthetic systems for capturing and classifying body posture and gesture*. in *27th Annual International Conference of the IEEE-Engineering-in-Medicine-and-Biology-Society*. 2005. Shanghai, PEOPLES R CHINA.
110. De Rossi, D., R. Bartalesi, F. Lorussi, A. Tognetti, and G. Zupone. *Body gesture and posture classification by smart clothes*. in *1st IEEE RAS-EMBS International Conference on Biomedical Robotics and Biomechatronics (BioRob 2006)*. 2006. Pisa, ITALY.
111. Ferro, M., G. Pioggia, A. Tognetti, N. Carbonaro, and D. De Rossi, *A Sensing Seat for Human Authentication.* Ieee Transactions on Information Forensics and Security, 2009. **4**(3): p. 451-459.
112. Wijesiriwardana, R., T. Dias, and S. Mukhopadhyay. *Resistive fibre-meshed transducers*. in *7th International Symposium on Wearable Computers*. 2003. White Plains, Ny.
113. Warren, B.E., *X-Ray Diffraction Study of Carbon Black.* The Journal of Chemical Physics, 1934. **2**(551).
114. Ladd, W.A. and M.W. Ladd, *Modern Role of the Electron Microscope in Rubber Research.* Rubber Chemistry & Technology, 1961. **34**(697).
115. Hess, W.M., L.L. Ban, F.J. Eckert, and V. Chirico, *Microstructural Variations in Commercial Carbon Blacks.* Rubber Chemistry and Technology, 1968. **41**(356).
116. Hwang, J.S., *Carbon black filled electrospun fiberweb: electrical and mechanical properties*, 2006, North Carolina State University.
117. Ladd, W.A. and W.B. Wiegand, Rubber Age, 1945. **57**(299).
118. Sweitzer, C.W. and G.L. Heller, *The formation of carbon black in hydrocarbon flames.* Rubber World, 1954. **134**: p. 855-865.
119. Warren, B.E. *X-ray study of the graphitization of carbon black*. in *Proceedings of 1st Conference on Carbon*. 1956. Buffalo University, New York.
120. Harling, D.F. and F.A. Heckman, Mater. Plast. Elastomeric, 1969. **35**(80).
121. Accorsi, J. and E. Romero, *Special carbon blacks for plastics.* Plastics Engineering, 1995. **51**(4): p. 29-32.
122. Donnet, J.-B., R.C. Bansal, and M.-J. Wang, *Carbon Black*1993, NEW YORK: MARCEL DEKKER, INC.
123. Huang, J.C., *Carbon black filled conducting polymers and polymer blends.* Advances in Polymer Technology, 2002. **21**(4): p. 299-313.
124. Verhelst WF, W.K., Voet A, et al, *Role of Morphology and Structure of Carbon-blacks in Electrical Conductance of Vulcanizates.* Rubber Chemistry and Technology, 1977. **50**(4): p. 735-746.
125. Tashima, D., K. Kurosawatsu, M. Uota, T. Karashima, Y.M. Sung, M. Otsubo, et al. *Space charge behaviors of electric double layer capacitors with nanocomposite electrode*. in *5th Asian/European International Conference on Plasma Surface Engineering*. 2005. Qingdao, PEOPLES R CHINA.
126. Das, N.C., T.K. Chaki, D. Khastgir, and A. Chakraborty, *Electromagnetic interference shielding effectiveness of ethylene vinyl acetate based conductive*

composites containing carbon fillers. Journal of Applied Polymer Science, 2001. **80**(10): p. 1601-1608.
127. Zhang, J. and S.Y. Feng, *Temperature effects of electrical resistivity of conductive silicone rubber filled with carbon blacks.* Journal of Applied Polymer Science, 2003. **90**(14): p. 3889-3895.
128. Pramanik, P.K., D. Khastgir, and T.N. Saha, *Effect of Some Processing Parameters on the Resistivity of Conductive Nitrile Rubber Composites.* Plastics Rubber and Composites Processing and Applications, 1992. **17**(3): p. 179-185.
129. Sau, K.P., D. Khastgir, and T.K. Chaki, *Electrical conductivity of carbon black and carbon fibre filled silicone rubber composites.* Angewandte Makromolekulare Chemie, 1998. **258**: p. 11-17.
130. Sau, K.P., T.K. Chaki, and D. Khastgir, *The effect of compressive strain and stress on electrical conductivity of conductive rubber composites.* Rubber Chemistry and Technology, 2000. **73**(2): p. 310-324.
131. Kim, I., *Investigation of electrically conductive alcrylonitrile-butadiene rubber.* Journal of Vinyl & Additive Technology, 2007. **13**(2): p. 71-75.
132. Wang, X.L. and G. Zhang, *PTC effect of carbon fiber filled EPDM rubber composite.* Journal of Materials Science-Materials in Electronics, 2008. **19**(11): p. 1105-1108.
133. Ding, T.H., L.H. Wang, and P. Wang, *Changes in electrical resistance of carbon-black-filled silicone rubber composite during compression.* Journal of Polymer Science, Part B: Polymer Physics, 2007. **45**(19): p. 2700-2706.
134. Wang, L.H., T.H. Ding, and P. Wang, *Effects of compression cycles and precompression pressure on the repeatability of piezoresistivity for carbon black-filled silicone rubber composite.* Journal of Polymer Science, Part B: Polymer Physics, 2008. **46**(11): p. 1050-1061.
135. Kawazoe, M. and H. Ishida, *A new concept for, nanoparticle distribution in SBR/NBR blend solution and films via molecular confinement.* Macromolecules, 2008. **41**(8): p. 2931-2937.
136. Bishai, A.M., A.M. Ghoneim, A.A.M. Ward, and A.F. Younan, *Electrical conductivity of styrene-butadiene rubber/polyester short-fiber reinforced with different types of carbon black.* Polymer-Plastics Technology and Engineering, 2003. **42**(4): p. 701-710.
137. Wan, Y. and D.J. Wen, *Thermo-sensitive properties of carbon-black-loaded styrene butadiene rubber composite membranes.* Smart Materials & Structures, 2004. **13**(5): p. 983-989.
138. Job, A.E., F.A. Oliveira, N. Alves, J.A. Giacometti, and L.H.C. Mattoso. *Conductive composites of natural rubber and carbon black for pressure sensors*. in *International Conference on Science and Technology of Synthetic Metals (ICSM 2002)*. 2002. Shanghai, Peoples R China: Elsevier Science Sa.
139. Das, N.C., D. Khastgir, T.K. Chaki, and A. Chakraborty, *Electromagnetic interference shielding effectiveness of carbon black and carbon fibre filled EVA and NR based composites.* Composites Part A-Applied Science and Manufacturing, 2000. **31**(10): p. 1069-1081.
140. Ghosh, P. and A. Chakrabarti, *Conducting carbon black filled EDPM vulcanizates: assessment of dependence of physical and mechanical properties and conducting character on variation of filler loading.* European Polymer Journal, 2000. **36**(5): p. 1043-1054.
141. Ghosh, P. and A. Chakrabarti, *Effect of incorporation of conducting carbon black as filler on melt rheology and relaxation behaviour of ethylene-propylene-diene*

monomer (EPDM). European Polymer Journal, 2000. **36**(3): p. 607-617.
142. Ghosh, P. and A. Chakrabarti, *Conducting carbon black filled EVA vulcanizates: Assessment of dependence of physical and mechanical properties and conducting character on variation of filler loading.* Journal of Polymer Materials, 2000. **17**(3): p. 291-304.
143. Ghosh, P. and A. Chakrabarti, *Effects of incorporation of conducting carbon black as filler on melt rheology and relaxation behavior of elastomeric EVA.* Journal of Polymer Materials, 2001. **18**(2): p. 187-200.
144. Le, H.H., M. Tiwari, S. Ilisch, and H.J. Radusch, *Online method for characterization of the homogeneity of rubber compounds filled with non-conductive carbon black.* Rubber Chemistry and Technology, 2006. **79**(4): p. 610-620.
145. Pramanik, P.K., D. Khastgir, S.K. De, and T.N. Saha, *Pressure-Sensitive Electrically Conductive Nitrile Rubber Composites Filled with Particulate Carbon-Black and Short Carbon-Fiber.* Journal of Materials Science, 1990. **25**(9): p. 3848-3853.
146. Pramanik, P.K., D. Khastgir, and T.N. Saha, *Effect of Filler Blend Composition and Temperature on the Properties of Electrically Conductive Rubber Composites.* Plastics Rubber and Composites Processing and Applications, 1991. **15**(3): p. 189-194.
147. Pramanik, P.K., D. Khastgir, and T.N. Saha, *Conductive Nitrile Rubber Composite Containing Carbon Fillers - Studies on Mechanical-Properties and Electrical-Conductivity.* Composites, 1992. **23**(3): p. 183-191.
148. Sau, K.P., T.K. Chaki, and D. Khastgir, *Electrical and mechanical properties of conducting carbon black filled composites based on rubber and rubber blends.* Journal of Applied Polymer Science, 1999. **71**(6): p. 887-895.
149. Engel, J.M., J. Chen, N. Chen, S. Pandya, and C. Liu. *Development and characterization of an artificial hair cell based on polyurethane elastomer and force sensitive resistors*. in *4th IEEE Conference on Sensors*. 2005. Irvine, CA: Ieee.
150. Knite, M., G. Podins, S. Zike, and J. Zavickis. *Prospective robotic tactile sensors - Elastomer-carbon nanostructure composites as prospective materials for flexible robotic tactile sensors*. in *5th International Conference on Informatics in Control, Automation and Robotics*. 2008. Funchal, PORTUGAL: Insticc-Inst Syst Technologies Information Control & Communication.
151. Princy, K.G., R. Joseph, and C.S. Kartha, *Studies on conductive silicone rubber compounds.* Journal of Applied Polymer Science, 1998. **69**(5): p. 1043-1050.
152. Tchoudakov, R., O. Breuer, M. Narkis, and A. Siegmann, *Conductive polymer blends with low carbon black loading: Polypropylene/polyamide.* Polymer Engineering and Science, 1996. **36**(10): p. 1336-1346.
153. Tchoudakov, R., O. Breuer, M. Narkis, and A. Siegmann, *Conductive polymer blends with low carbon black loading: Polypropylene/polycarbonate.* Polymer Networks & Blends, 1996. **6**(1): p. 1-8.
154. Kluppel, A. and J. Meier. *Carbon black networking in elastomers monitored by dynamic-mechanical and dielectric spectroscopy*. in *5th European Conference on Constitute Models for Rubber*. 2007. Paris, FRANCE: Taylor & Francis Ltd.
155. Le, H.H., S. Ilisch, H.J. Radusch, and H. Steinberger, *Macro- and microdispersion of carbon black in liquid silicone rubbers.* Plastics Rubber and Composites, 2008. **37**(8): p. 367-375.
156. Gojny, F.H., M.H.G. Wichmann, U. Kopke, B. Fiedler, and K. Schulte, *Carbon*

nanotube-reinforced epoxy-compo sites: enhanced stiffness and fracture toughness at low nanotube content. Composites Science and Technology, 2004. **64**(15): p. 2363-2371.

157. Schwarz, O., F.W. Ebeling, and B. Furth, *Kunststoffverarbeitung*2002: Vogel Verlag.
158. Huang, Y., B. Xiang, X.H. Ming, X.L. Fu, and Y.J. Ge. *Conductive Mechanism Research Based on Pressure-Sensitive Conductive Composite Material for Flexible Tactile Sensing*. in *IEEE International Conference on Information and Automation*. 2008. Changsha, PEOPLES R CHINA: Ieee.
159. Hussain, M., Y.H. Choa, and K. Niihara, *Fabrication process and electrical behavior of novel pressure-sensitive composites.* Composites Part A-Applied Science and Manufacturing, 2001. **32**(12): p. 1689-1696.
160. Wang, L.H., T.H. Ding, and P. Wang, *Thin Flexible Pressure Sensor Array Based on Carbon Black/Silicone Rubber Nanocomposite.* Ieee Sensors Journal, 2009. **9**(9): p. 1130-1135.
161. Kader, M.A., D. Choi, S.K. Lee, and C. Nah, *Morphology of conducting filler-reinforced nitrile rubber composites by electrostatic force microscopy.* Polymer Testing, 2005. **24**(3): p. 363-366.

CHAPTER 3

FABRICATION AND CHARACTERIZATION OF CNP/SE/SO COMPOISTES

3.1 Introduction

Elastomers filled with electrically conductive fillers show piezo-resistivity and are promising candidates for flexible strain sensors [1, 2]. The matrix materials studied including synthetic and natural rubbers [3-5], thermoplastic elastomers [6, 7] and silicone elastomers (SE) [8-11], where high temperature and pressure are employed to vulcanizing them [10, 12], which significantly limits their applications in textiles that are easily damaged under such high temperature [13]. Room temperature vulcanized (RTV) SE that has low viscosity, low vulcanizing temperature and pressure, along with good biocompatibility, excellent mechanical properties and thermal/chemical resistance, is a promising matrix material for flexible conductive composites for smart textiles.

Among the three major groups of conductive fillers, i.e., metallic fillers, carbonaceous fillers, and intrinsically conductive polymers, the second group is more attractive because of their low density, high environmental stability and good chemical stability. Conductive composites with graphite powders and carbon fibers have been studied for strain sensing

applications [14, 15]. However, a higher filler loading was required, and sliding wear behavior of graphite and brittleness of carbon fiber composites resulted in poor repeatability in electromechanical responses under cyclic mechanical tests. Though carbon nanotube [16] and graphene [17] composites can be applied in strain sensing applications with a low concentration, the high price, uncertain safety effect on humans, as well as the availability of large scale industrial production hinder their usage as compared to low priced conductive CNP.

In order to achieve good conductivity, a high concentration of CNP has to be used. Great challenge occurs in mixing high concentrations of CNP with SE in the post-percolation threshold region, since the viscosity of the mixtures increases drastically with increasing of CNP concentrations. One possible way to solve the problem is to add some organic solvents like hexane to reduce their viscosity. However, the Young's modulus of resultant composites increases significantly [11], leading to the undesirable high rigidity. Conductive composites with CNP loadings in percolation range have a high sensitivity. However, the significant resistance changes of several orders of magnitude in small strain ranges make them difficult to be measured.

In the present work, high porous but low structured CNP nano-particles filled SE composites were fabricated with dimethyl silicone oil (SO) as a diluting agent and plasticizer. Electrical, mechanical and thermal properties of the composites are studied experimentally. The performances of the conductive composites were identified with consideration of their potential applications as flexible strain sensors.

3.2 Experimental

3.2.1 Materials

Low structure but high porous (more than 80%) CNP nano-particles (Carbon® ECP600JD, Akzo Nobel, diameter of about 30 nm) were heated at 80 ^{0}C for 24 hours to remove the moisture for further uses as conductive fillers. The surface area of the CNP particles is ca. 440-510 ml/100g expressed by dibutylphthalate (DBP) absorbing value. SE (ELASTOSIL®LR6200 A and B, Wacker Chemie AG, Germany) was used as received. Nontoxic dimethyl SO with kinetic viscosity of 5.0 mm^2/s at 25 ^{0}C (Che Scientific Co., Hong Kong) was used as solvent to reduce the viscosity of the mixture paste and plasticizer to reduce the modulus of the composites. Figure 3.1 and Figure 3.2 show the vulcanization reaction of SE and the molecular structure of SO, respectively. Silver coated nylon yarn (70D/24F/2, Xiamen Unibest Import and Export Co., Ltd.) was used as conductive connecting wire between conductive composite and measuring equipment.

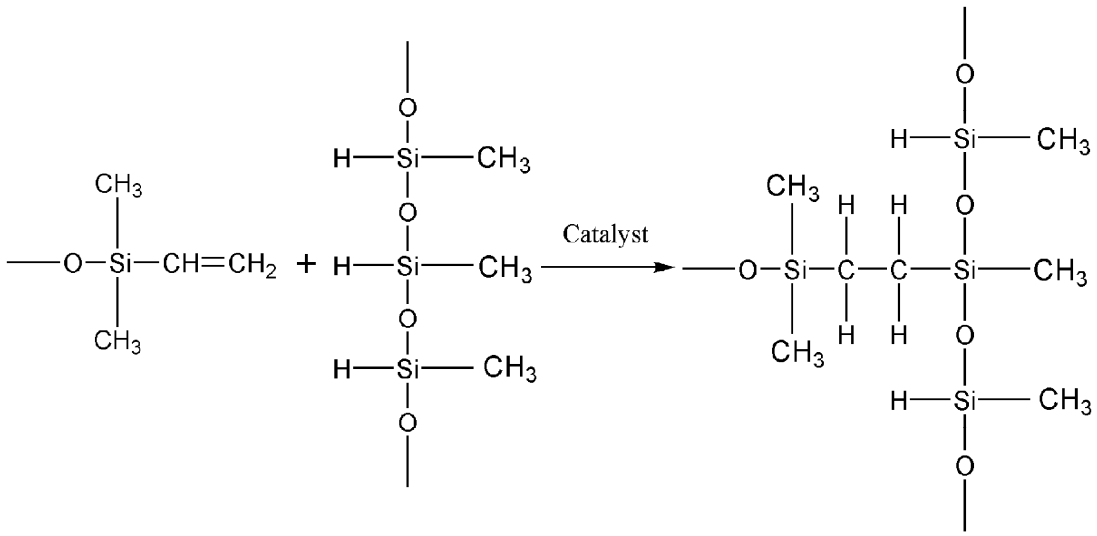

Figure 3.1 Formation process of SE

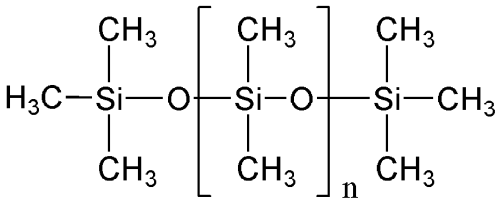

Figure 3.2 Molecular composition of SO

3.2.2 Fabrication

CNP, SE (with equal weight of the two parts), and SO were weighted and mixed in a plastic beaker, and then further blended on a three-roll miller (PTR 65, Pühler (Guangzhou) Machinery and Equipment Co., Ltd.) for 15 minutes under ambient temperature. The mixture was cast into a polytetrafluoroethylene (PTFE) mold and degassed in a vacuum oven for 10 minutes. Then, silver coated nylon yarns were embedded parallel in the film as conductive wire with a distance of 12 mm and vulcanized at 100 ^{0}C for 2 hours to obtain the specimens (whole size is 20 mm×10 mm×1 mm). For I-V characterization, pellet shaped samples with a diameter of 13 mm and thickness of 2 mm were fabricated with two parallel stainless steel electrodes pasted on both sides of the composites before curing to reduce the contact resistance. The compositions and codes of all samples are listed in Table 3.1. The samples were heated at 100 ^{0}C for 100 hours in a vacuum oven to release stress and volatilize excessive SO before further characterization.

Table 3.1 Composition of samples

Sample Code	*Composition (Weight ratio)*	*Sample Code*	*Composition (Weight ratio)*
SE	CNP/SE/SO 0.0/100.0/0.0	2.5CNP	CNP/SE/SO 2.5/97.5/45.0
SE/SO	CNP/SE/SO 0.0/100.0/20.0	3.0CNP	CNP/SE/SO 3.0/97.0/50.0

1.0CNP	CNP/SE/SO 1.0/99.0/45.0	4.5CNP	CNP/SE/SO 4.5/95.5/75.0
1.5CNP	CNP/SE/SO 1.5/98.5/45.0	6.0CNP	CNP/SE/SO 6.0/94.0/100.0
2.0CNP	CNP/SE/SO 2.0/98.0/45.0	9.0CNP	CNP/SE/SO 9.0/91.0/150.0
2.3CNP	CNP/SE/SO 2.3/97.7/45.0	12.0CNP	CNP/SE/SO 12.0/88.0/200.0

3.2.3 Characterization

3.2.3.1 Morphology

Scanning electron microscopy (SEM) observation of the CNP/SE/SO composites was performed on a field emission scanning electron microscope (JEOL JSM-6335F, JEOL Ltd., Japan). The specimens were prepared by freeze-fracturing in liquid nitrogen and followed by a gold coating.

3.2.3.2 Thermal Analysis

The CNP/SE/SO mixture paste was heated at 100 ^{0}C for 200 hours and its weight was recorded every 2 hours in the first 50 hours and with interval of 10 hours after the 50th hour. Thermo-gravimetric analysis (TGA) of the materials and the heat treated composite samples were carried out from 35 to 1300 ^{0}C (900 ^{0}C for CNP) under nitrogen atmosphere by using a NETZSCH TGA/DSC instrument with a heating rate 20 ^{0}C /min.

3.2.3.3 Current-voltage (I-V) Characteristics and Impedance Analysis

I-V curves of the pellet shaped composite samples were measured with a 814 photomultiplier detection system (Photon Technology International) with the voltage gradually increasing from -50 to 50 V under ambient temperature. The impedance analysis was performed by Solartron SI 1287 electrochemical interface combined with

1252A frequency response analyzer with voltage and current controlled at 10 V and 0.1 A, respectively. The frequency varied from 10^5 Hz to 10^{-1} Hz with an interval of 1Hz.

3.2.3.4 Coupled Electromechanical Measurement

The electrical resistance of the samples without strain was measured with a digital multi-meter (Keithley 2010, Keithley Instruments Inc. USA) using the 2-wire method for resistance lower than 10^8 Ω, while insulation resistance tester (YD 2683, Yangzi Electronics, China) was used for higher resistance. The volume resistivity, ρ , is calculated by

$$\rho = R \cdot w \cdot d / l \tag{3-1}$$

where R is the resistance (Ω), l, w and d are the length, width and thickness of the samples, respectively.

The measurement setup for coupled electromechanical properties of the composites is shown in Figure 3.3. The force and displacement were achieved from Universal Material Tester (Instron 5566), and resistance from the digital multi-meter (Keithley 2010), simultaneously. The gauge length was set as 10 mm for the tensile strain measurement and cross-head speed was 50 mm/min if not further specified.

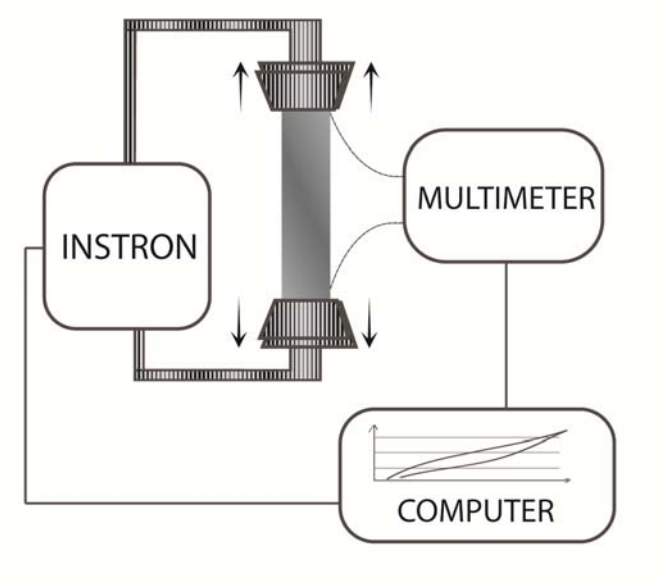

Figure 3.3 Experimental setup for coupled electromechanical measurement of CNP/SE/SO composites under tensile strain

3.2.3.5 Temperature Effect

The samples were fixed on the clamps of a strain frame by two ends, and tested in a climate chamber with fixed humidity of 65%. The resistance were measured between the low and high temperature (0 ^{0}C to 60 ^{0}C) for 3 cycles with step of 20 ^{0}C, and at each step the temperature was kept 2 hours for balancing, the process was schematically shown in Figure 3.4. Resistance of the samples was continuously recorded by Agilent data acquisition system (34970A Data Acquisition Switch Unit) during the whole experiment and resistance of the composites at endpoint of each temperature was used for calculation.

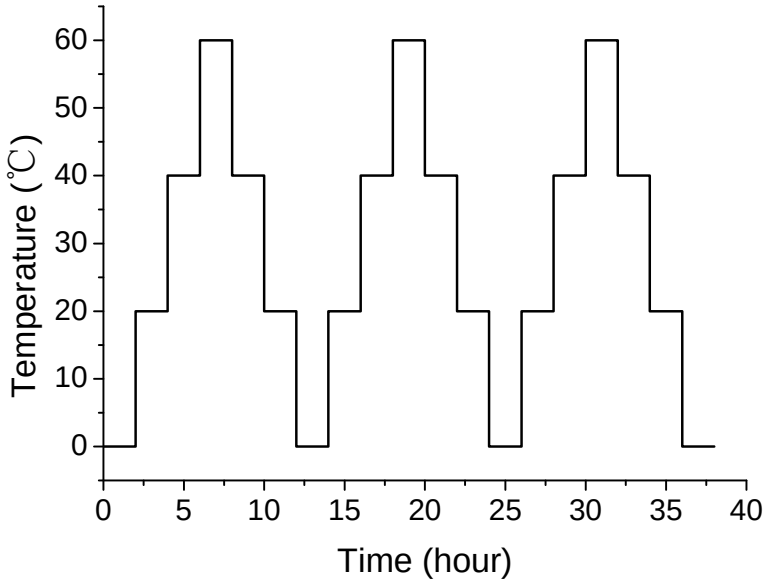

Figure 3.4 Schematic diagram of the conductive composites for temperature effect evaluation.

To evaluate the sensing behavior of the composites under different temperatures, the composites were loading and unloading for 3 cycles at each balanced temperature, and the dependence of electrical resistance on both temperature and strain were recorded.

3.2.3.6 Humidity Effect

The experimental setup for evaluating the humidity effect of the composite is the same as that used in the temperature experiment. The temperature was fixed at 20^0C, and the humidity varied between 90% and 10% for one cycle with step of 10%, and at each level the humidity was balanced for 2 hours. The resistance of the composites at balanced humidity was used for calculation.

3.3. Results and Discussion

3.3.1 Morphology

Figure 3.5 shows the SEM images of the CNP and fractured composites in cross-section. The spherical CNP particles are uniformly dispersed into the matrix. The size of the CNP in composites increases with CNP concentration and they still show quasi-spherical configurations, meaning that the CNP or small CNP aggregates are covered with SE and the interface between them is good. Compared to other dispersing methods [6, 18], the facile dispersion of CNP without high temperature or pressure can greatly reduce the production cost of the composites and make it possible to process with textile materials simultaneously.

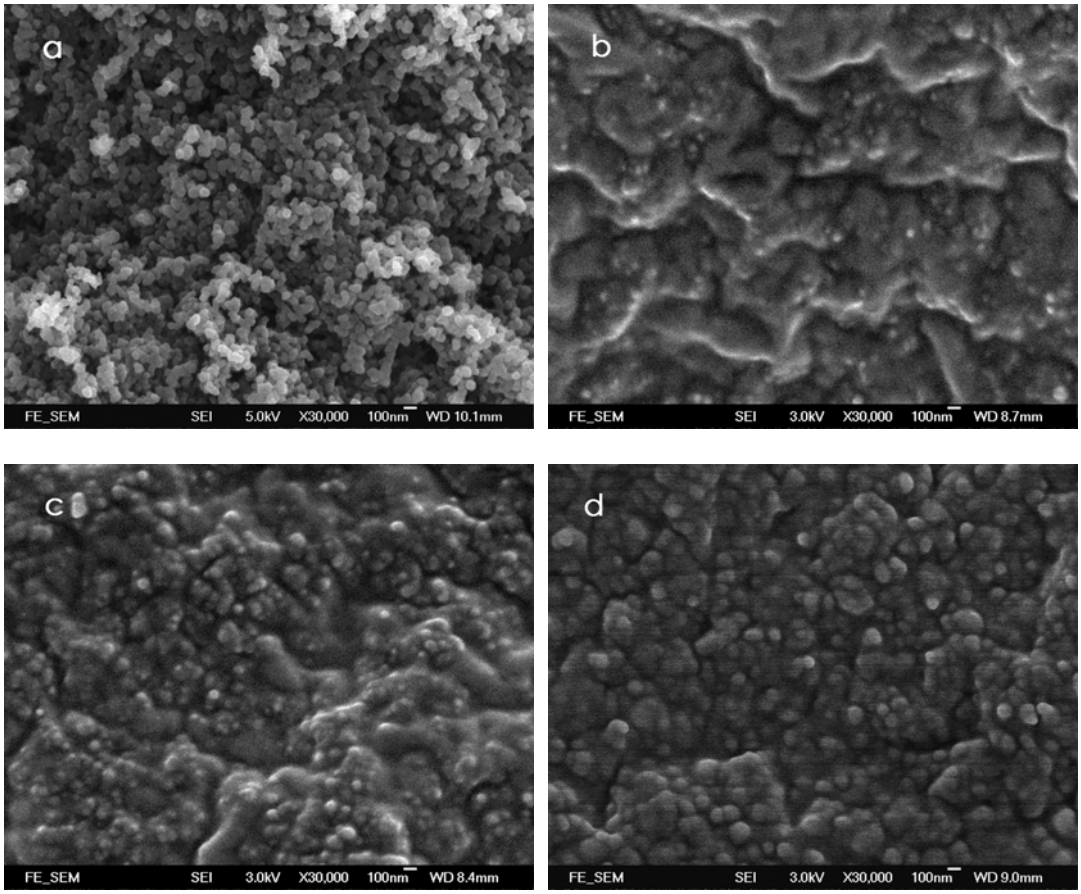

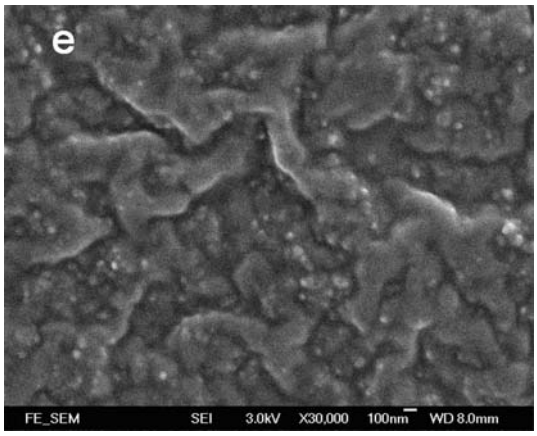

Figure 3.5 SEM images of (a) pure CNP particles and CNP/SE/SO composites of (b) 1.0CNP, (c) 3.0CNP, (d) 6.0CNP and (e) 9.0CNP

3.3.2 Thermal Analysis

The weight variation of SO with time in CNP/SE/SO mixture paste and comparative mixtures of CNP/SO and SE/SO as well as pure SO, when heated in a vacuum oven at 100 ^{0}C, was continuously monitored and the result is shown in Figure 3.6. Almost all the pure SO was lost in 70 hours while there was a substantial amount of SO left in the mixtures after a prolonged heating. For instance, approximately 70% SO remained in the SE/SO mixture after heat treated for 200 hours, while the value for SO in the CNP/SO mixture and CNP/SE/SO mixture is about 35% and 30%, respectively. The results can be attributed to the adsorption of CNP and shielding effect of vulcanized SE, which reduced the diffusion and volatilization of SO. The SO molecule has a volume of 225.64 Å^3, while the CNP particle is approximately 30 nm in diameter (1.1×10^8 Å^3 in volume) and with a void volume more than 80%. Thus it is easy for the SO or part of SE molecules to penetrate into the CNP particles (schematically shown in Figure 3.7) before vulcanization and to form a good interface between the CNP and the matrix after vulcanize as described in the SEM observation. After 100 hours heat treatment, the weight of SO in the composite is relatively stable, which means the heat treatment is effective to stabilize the

samples.

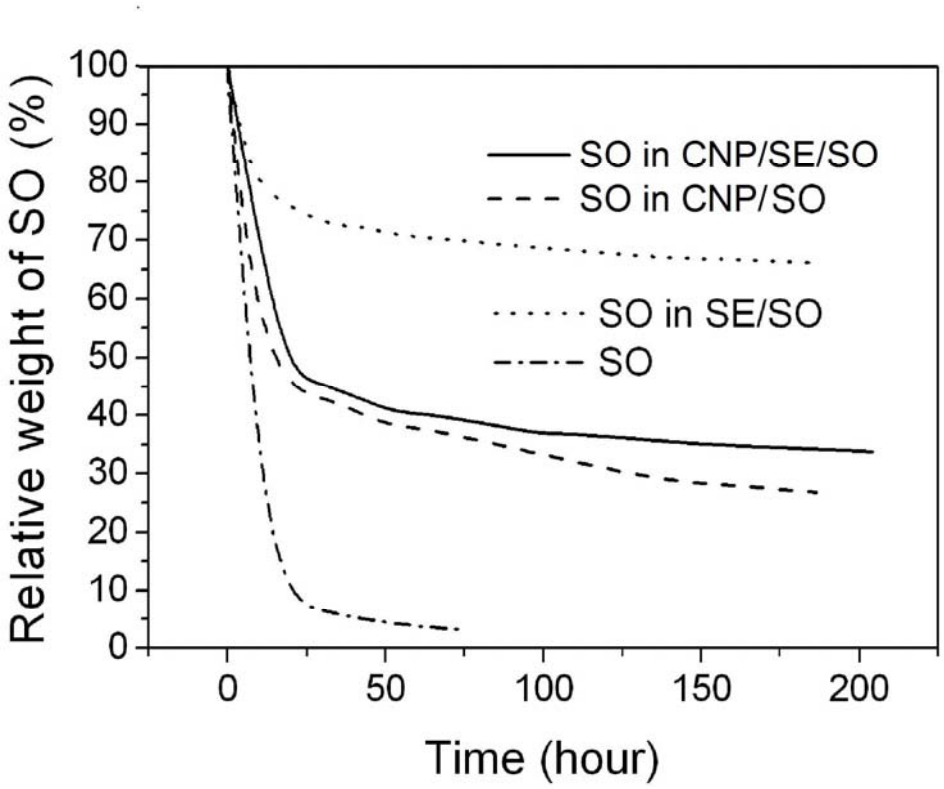

Figure 3.6 Weight variation of SO in CNP/SO, SE/SO and CNP/SE/SO composites (9.0CNP) heated at 100 ^{0}C

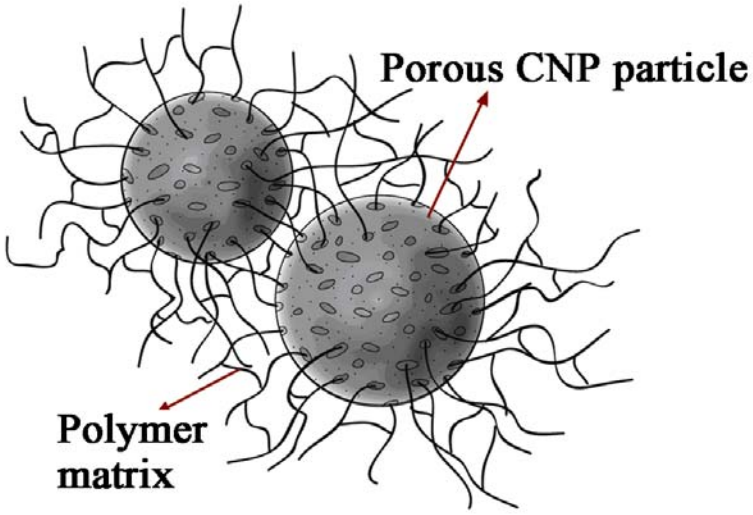

Figure 3.7 Schematic of matrix material molecules penetrate into porous CNP particles

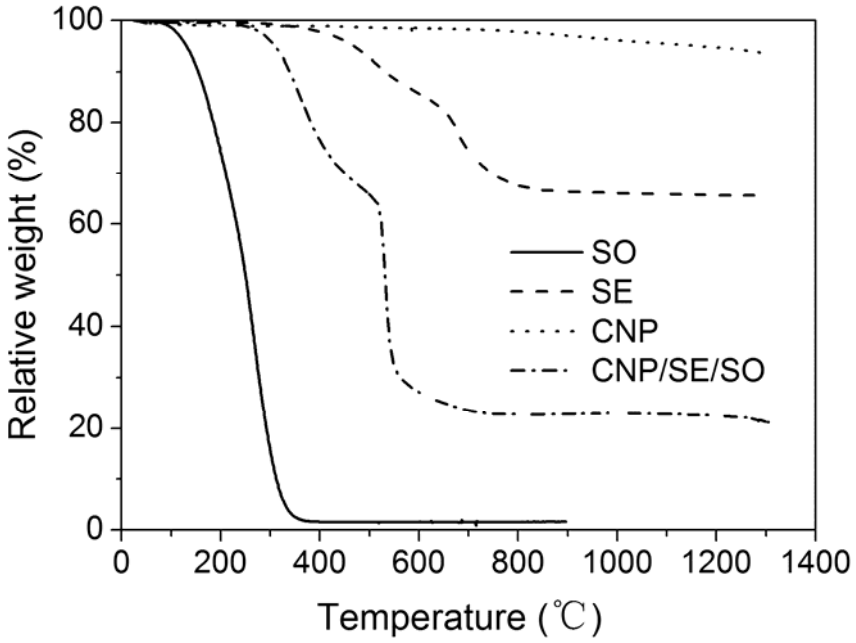

Figure 3.8 TGA curves of SO, SE, CNP and heat treated CNP/SE/SO composite

Figure 3.8 shows the dependence of weight loss on temperature for pure SO, SE, CNP and heat treated CNP/SE/SO composite, respectively. The CNP is very stable for temperatures under 600 ^{0}C, while SO begin to volatilize and decompose at temperature around 100 ^{0}C and lost most of weight with temperature lower than 400 ^{0}C. SE is relatively stable below 300 ^{0}C, then decompose with further increase of temperature, and about 33% weight lost when temperature is higher than 800 ^{0}C. The CNP/SE/SO composite is stable below 250 ^{0}C due to the excessive SO already volatilized in the heat treatment process. Beyond 250 ^{0}C, the weight of the composite quickly decreases due to the decomposition of SE and volatilization of SO original adsorption by CNP and sealed by SE. The results show the existence of SO in the heat treated composite and further confirms that it is stably conserved in the composite to play a role as plasticizer to decrease the modulus of the composite for flexible strain sensors.

3.3.3 Percolation Threshold

As shown in Figure 3.9, the SE/SO composite is a good insulating material with volume resistivity of about 10^{13} Ω·cm. With increase of CNP concentration, the volume resistivity of the composite decreases by approximately 7 orders of magnitude as CNP loading is increased from 0.5 wt% to 2.5 wt%, which is called percolation phenomenon [10, 19]. When CNP loading further increased, the resistivity decreased slowly. Based on the variation of resistivity with CNP loading, three ranges are separated by CNP loading of 0.5 wt% and 2.5 wt%, that is, the insulating, percolation and post-percolation ranges. The achieved percolation threshold is much lower than that of normal CNPs, which is due to the higher porosity (DBP absorbing value of 440-510 ml/100g comparing to others in the range of 98-330 ml/100g [20]). The electrical conductive behavior of the CNP/SE/SO composite can be expressed with an equivalent circuit consisting of series of resistor and capacitor units, one equivalent unit is schematically shown in Figure 3.10 [21].

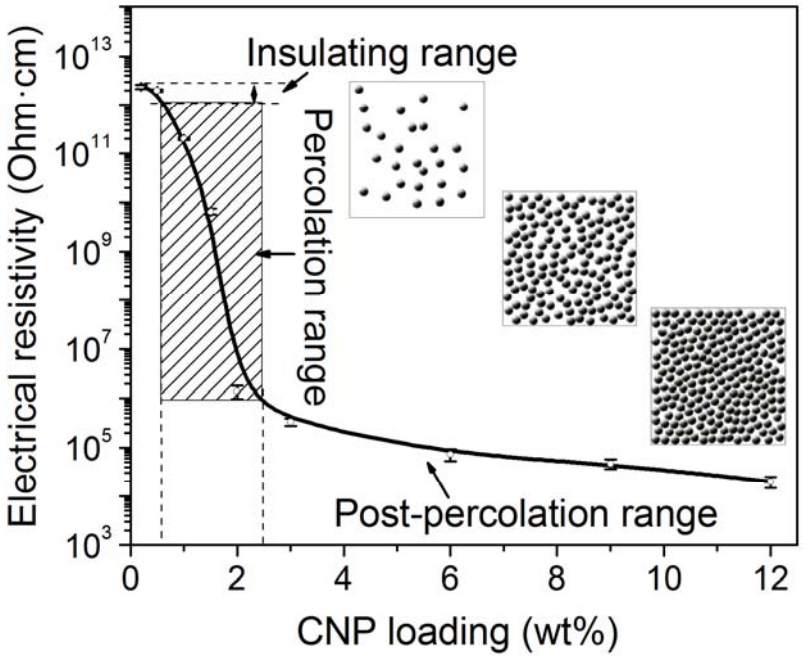

Figure 3.9 Relationship between resistivity and CNP concentrations of CNP/SE/SO

composites. The insets show the schematic diagrams of composites in (a) insulating range, (b) percolation range and (c) post-percolation range

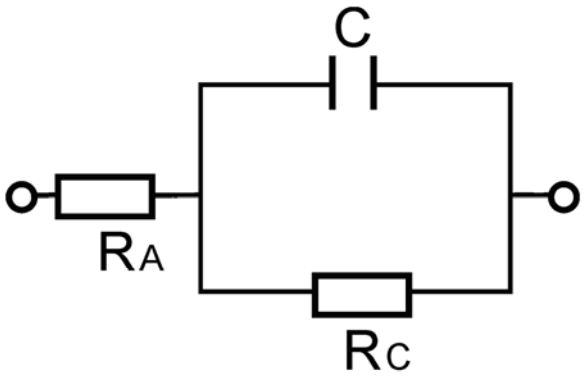

Figure 3.10 Equivalent circuit for CNP/SE/SO composites

where R_A denotes the resistance within one conductive domain, which is one conductive CNP or small CNP aggregates consist of several CNPs, while R_C and C represent the resistance and capacitance between two neighboring conductive domains, respectively. Many of the resistor and capacitor units combine together and form a continuous conductive network. Under direct voltage, the capacitor blocks the transfer of electrons as an open circuit and the electrons can only transfer through the resistors. The equivalent resistance of the conductive composites unit can be calculated as $R_A + R_C$. Because resistance in one conductive domain (R_A) is composed of resistance of CNPs or small CNP aggregates, it is relatively less influenced by CNP concentration. The resistance between conductive domains (R_C) is mainly consist of contact resistance or hopping resistance between the conductive domains according to CNP concentration, which is more sensitive to distances between them. When the CNP loading is very small, in other word, in the insulating range, the conductive domains (CNP or small aggregates) are separated by insulating polymer matrix and few of them can hop to form continuous conductive pathways through the composite. With the increase of CNP concentration, the

space occupied by conductive domains increases, and the distance between them decreases to a level that permits electrons to pass through by hopping if the concentration of CNP is beyond the percolation threshold. The corresponding resistance R_C decreases with further increase of CNP loading and accompany by the increase of large amount of conductive pathways dominated by electron hopping, resulting a significantly decrease of electrical resistivity with CNP loading. Beyond the percolation range, physical contact of the conductive particles or aggregates begin to play a dominant role instead of electron hopping, the resistance R_C further decreases with CNP loading but the amount of continuous conductive pathways increase slowly, and the corresponding resistivity decreases slowly with further increase of CNP loading.

3.3.4 I-V Characteristics and Impedance Spectra

The hopping of electrons in a conductive composite is governed by the energy barrier, and it is also affected by voltage or frequency applied. On the other hand, ohmic type conductive behavior is little influenced by the voltage or frequency. Hence I-V curves and impedance spectra can be used to examine the conductive mechanisms of the composite. Figure 3.11 shows the I-V relationship of the conductive composites with different CNP loadings. For composite 2.0CNP, the I-V curve is nearly linear when the voltage increased from -50 to 50 V (-25 to 25 V/mm) but the current is very small. Though the CNP loading is in percolation range, the gaps between adjacent conductive domains are still relatively large thus the increased voltage cannot break the insulator down to generate more continuous conductive pathways. With the increase of CNP loading, the gaps between conductive domains decreases, which means that many of the original capacitors transferred to resistors when the distance between two electrodes of the capacitor decreased to a level that permit electrons hopping through, leading to the nonlinear I-V

characteristic of the conductive composites at high voltages. The exciting voltage also decreases with increase of CNP loading. When the CNP loading further increased, a large amount of ohmic conductive pathways formed with the domination of physical contact between conductive particles or domains, which is less affected by the voltage variation, and the I-V curves begin to show better linearity again.

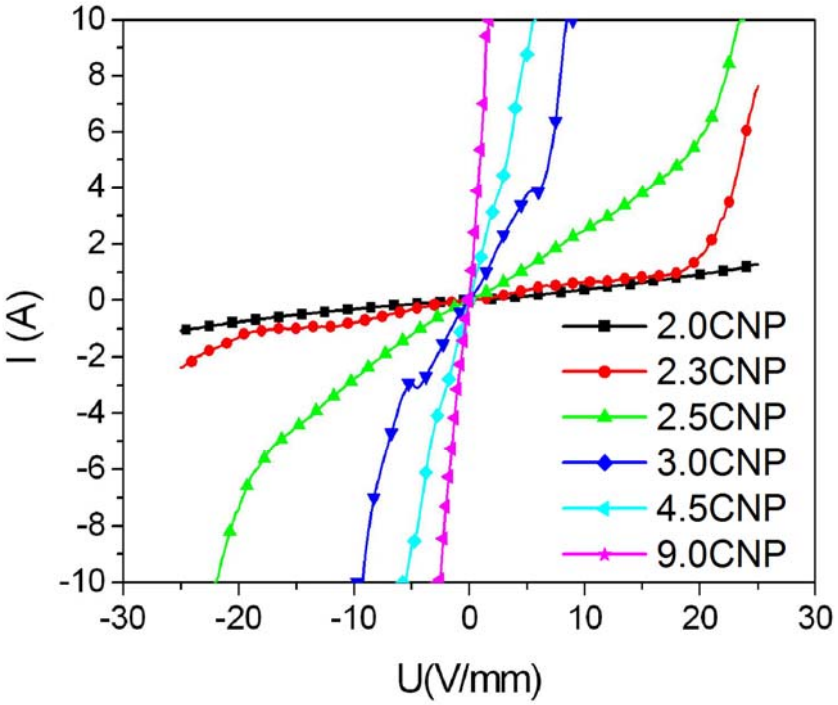

Figure 3.11 I-V curves of CNP/SE/SO composites

Figure 3.12 illustrates the dependence of impedance magnitude and phase angle on frequency for conductive composites with different CNP loadings. At frequency below 400Hz, the composite of 2.3CNP shows pure resistive property, with the increase of frequency, capacitive behavior appears and getting obvious. However, with the increase of CNP loading, the impedance of the conductive composite is less affected by frequency, and there is no capacitive behavior observed for 9.0CNP at the frequency range of 10^{-1}-10^{5} Hz, which means physical contacted CNP particle dominant in the composite of 9.0CNP. Under AC measurement, the electrons in conductive composites are permitted to

flow through the capacitors shown in Figure 3.10 by charging and discharging process. The impedance of the capacitor is:

$$Z = -j/2\pi fC \tag{3-2}$$

where Z is the impedance, j is the imaginary unit, f is frequency and C is capacitance of the capacitor, respectively. The capacitance can be expressed by:

$$C = \varepsilon A/d \tag{3-3}$$

where ε is dielectric permittivity, A is area of conductive domains and d is the distance between two conductive domains. Integrated formula 3-2 and 3-3, we can draw:

$$Z = -jd/2\pi f\varepsilon A \tag{3-4}$$

The impedance of the capacitor increased with distance between conductive domains and decreased with frequency and areas of conductive domains. For the conductive composites, the distance between conductive domains decreased and the area of conductive domains increased with CNP concentration, and the value of capacitance correspondingly decreased with increase of CNP concentration at a fixed frequency.

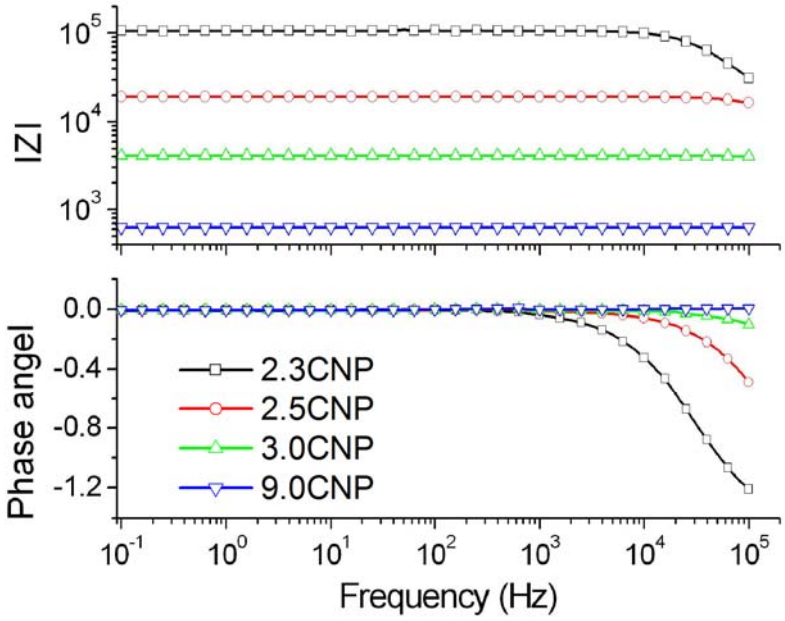

Figure 3.12 Impedance spectra of CNP/SE/SO composites

The effect of tensile strain on the impedance spectra of the composites is shown in Figure 3.13. The composites with CNP concentrations beyond percolation transition range show relative good ohmic behavior without extension. However, the ohmic conductive behavior transferred to capacitive behavior with the increase of tensile strain at high frequencies, especially for composites with lower CNP concentrations. The results confirmed that the distance between conductive domains increased with tensile strain, and the conductive mechanism of the composites transferred from physical contact of conductive domains to mixture of physical contact with electron hopping, meaning the effect of tensile strain plays a similar role on resistance change as decreasing CNP concentrations.

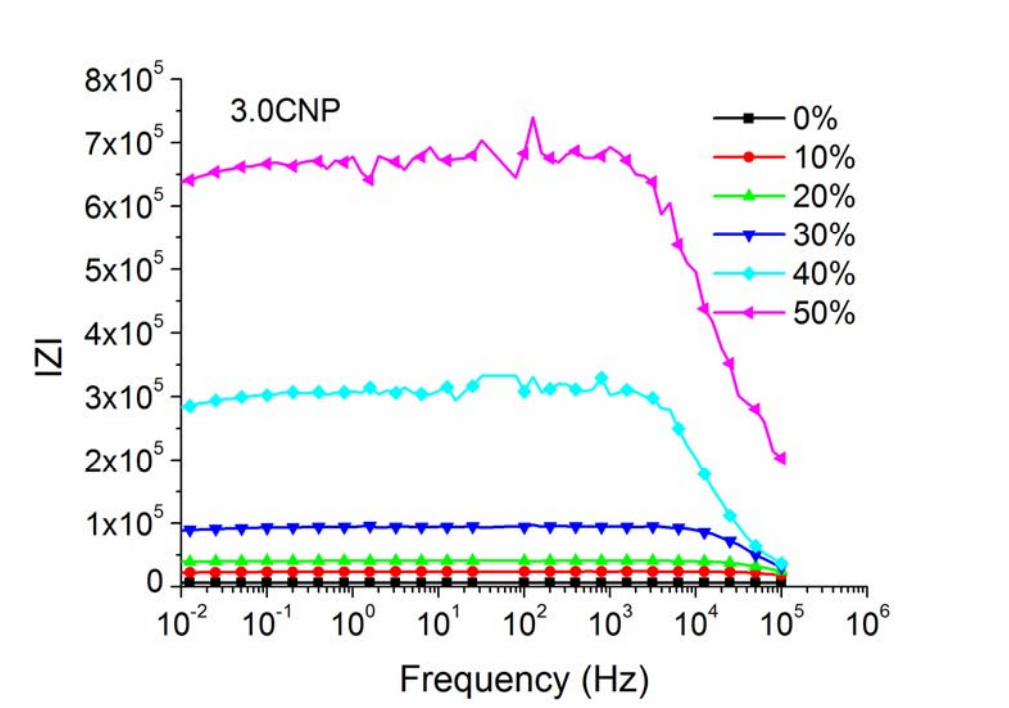

(a)

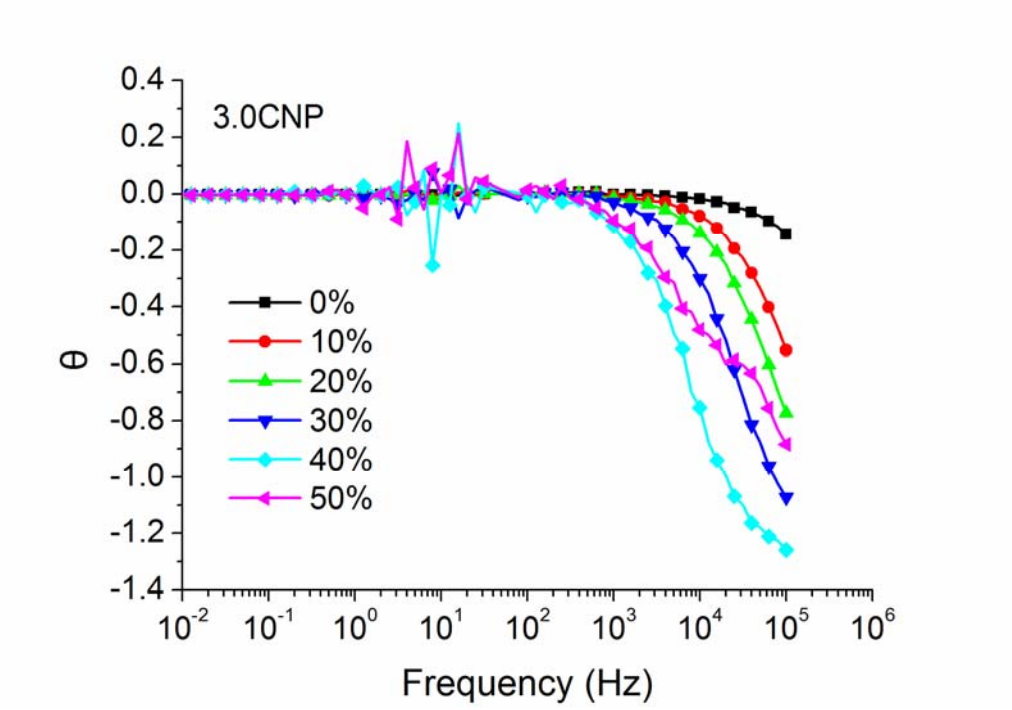
3.0CNP
θ
0%
10%
20%
30%
40%
50%
Frequency (Hz)

(b)

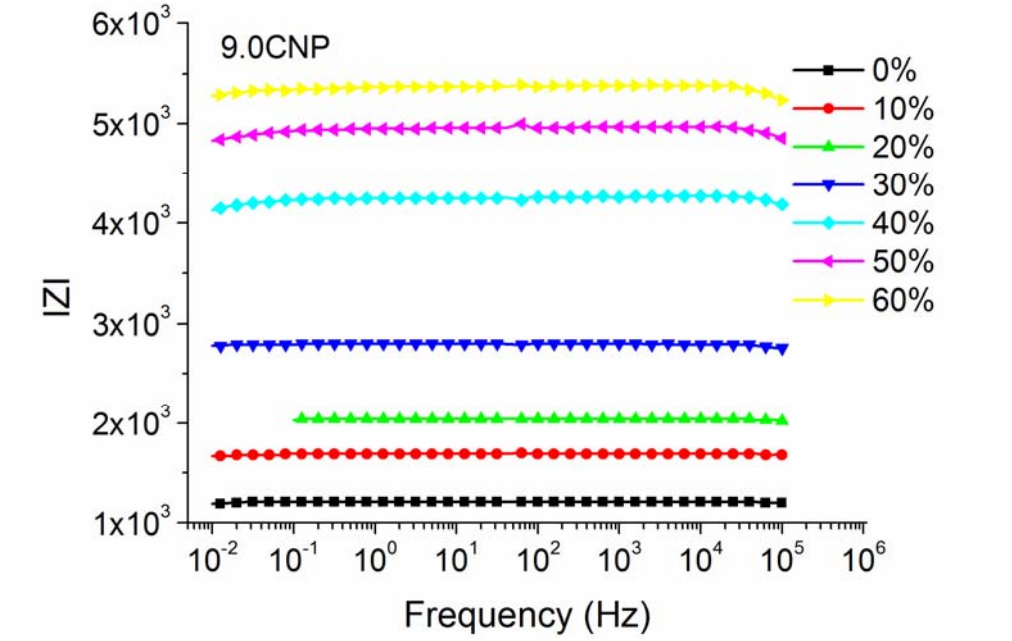
9.0CNP
|Z|
0%
10%
20%
30%
40%
50%
60%
Frequency (Hz)

(c)

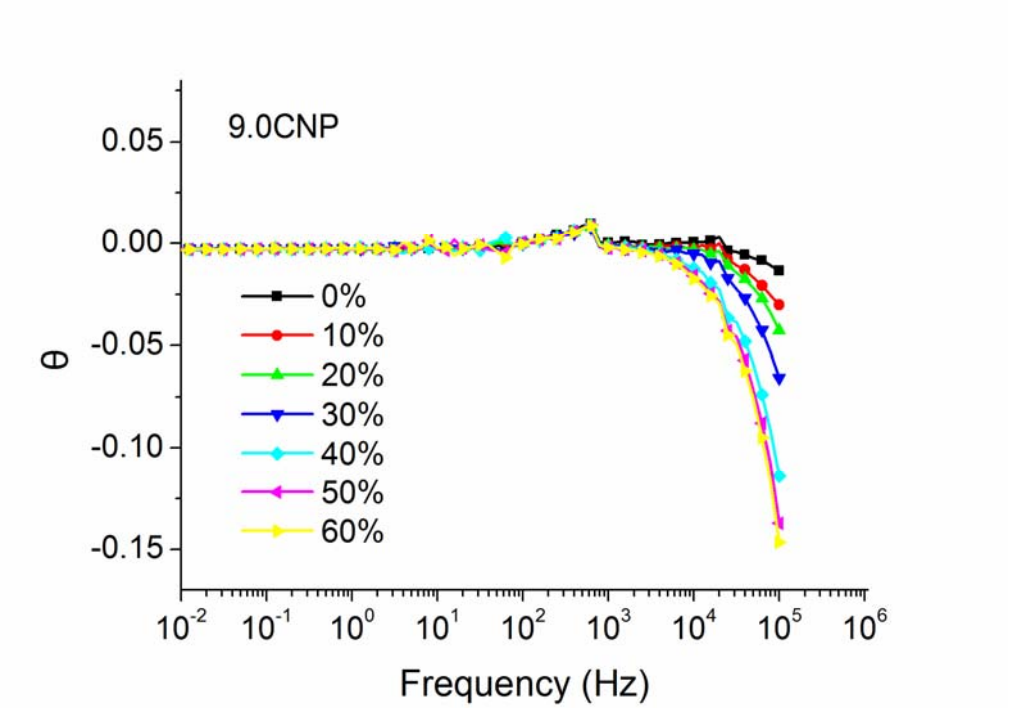

(d)

Figure 3.13 Impedance spectra of CNP/SE/SO composites under various tensile strains (a) (c) magnitude and (b) (d) phase angle for 3.0CNP and 9.0CNP, respectively

3.3.5 Mechanical Properties

The modulus and rigidity of the elastomeric matrix usually increases due to the presence of CNP particles for the strong interfacial adhesion between them [22], and the processing difficulties also increased when the CNP loading increased. Low rigidity and high flexibility of a sensor is preferred for strain measurement to ensure minimum interference of the sensor to the measured objectives. Strength is not critical as the strain sensors should deform within its working range. It was expected that the incorporation of SO as a plasticizer would balance the reinforcing effect of CNP particles and benefit the flexibility of the composites by facilitating the segmental movement of the polymer chains.

Figure 3.14 (a) shows the representative stress-strain curves for the CNP/SE/SO composites under extension. Stress monotonically increased with tensile strain can be observed. Table 3.2 is a summary of the measured mechanical properties of SE, SE/SO and CNP/SE/SO composites. The Young's modulus of SE is 1.38MPa and it decreases to 0.85 MPa with the addition of 20 wt% SO. The more the SO used, the lower the modulus of the composites. The low modulus is particularly beneficial for strain sensing applications for soft materials, as the deformation of conductive composites will not influence the original strain filed of the materials to be measured. The elongation at break for the conductive composites is approximately 150%, which is not affected by the addition of SO. The tensile strength is less than 0.7 MPa for all CNP/SE/SO composites, much lower than that of pure SE and other CNP filled elastomers reported [23, 24].

Table 3.2 Mechanical properties of SE, SE/SO and CNP/SE/SO composites

Sample	Young's modulus (MPa)	Tensile strength (MPa)	Elongation at break (%)
SE	1.38	0.94	150
SE/SO	0.85	0.55	201
2.5CNP	0.76	0.66	163
3.0CNP	0.63	0.55	158
4.5CNP	0.59	0.44	154
9.0CNP	0.49	0.30	154

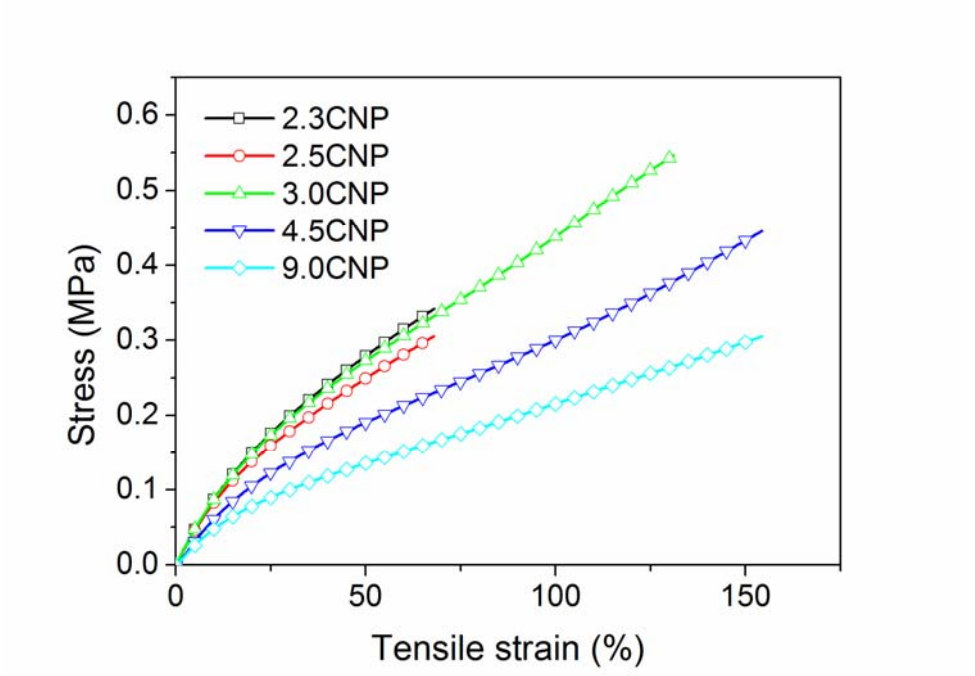

(a)

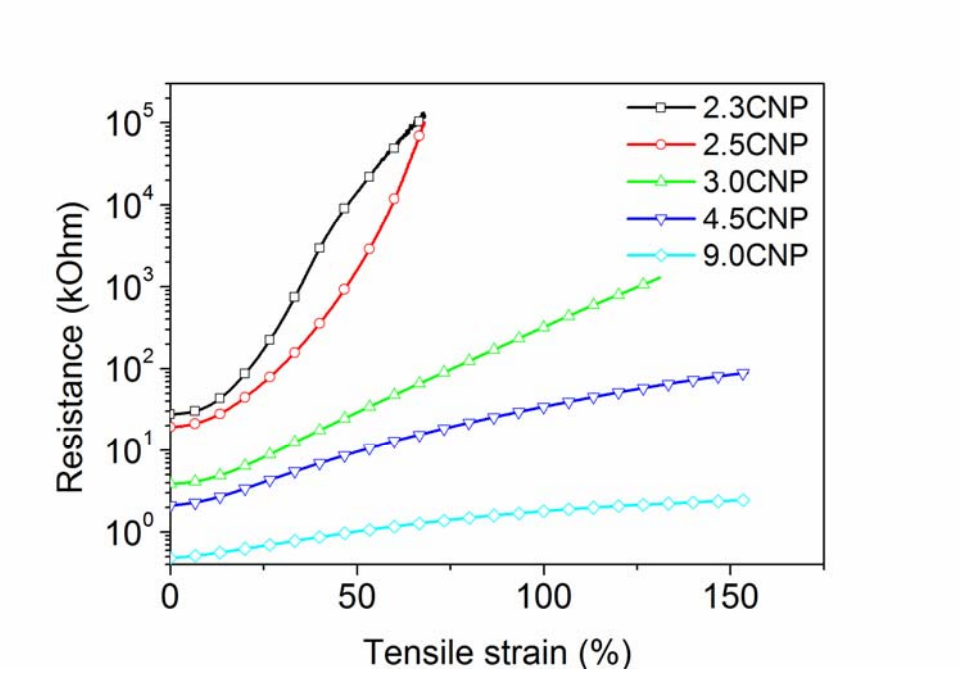

(b)

Figure 3.14 (a) Stress-strain curves and (b) resistance-strain curves of CNP/SE/SO composites

3.3.6 Electrical Properties

3.3.6.1 Effect of CNP Concentration

Figure 3.14 (b) shows the relationship between electrical resistance and tensile strain for the CNP/SE/SO composites with various CNP loadings. The resistance of sample 2.3CNP, which is in the percolation range, significantly increases approximately 10^4 orders of magnitude when the tensile strain increases to 70% and the value of electrical resistance is beyond the measurement range of the instrument when the tensile strain further increased. With increase of CNP concentration, though the resistance of the composites still monotonically increases with tensile strain, the resistance change, thus the strain sensitivity, is getting moderate. This is because in the percolation range, the continuous conductive pathways mainly contributed to hopping electrons, which are sensitive to the distances between conductive domains. When the composite is stretched, some of the conductive pathways broken as the distances between the conductive domains increase to a level larger than that permitted for electron hopping, resulting significant increase of resistance. While in the post-percolation range, the conductive networks consist of large amount of continuous pathways dominated by physical contact of the conductive domains. Though some of them may be broken under extension, the formation of new ones will compensate the destroyed ones and resulting in much smaller resistance changes under extension. The insignificant alignment of aggregates in the CNP/SE/SO composites due to the low structured CNP particles contributed to the monotonously increased electrical resistance with tensile strain, which is benefit for strain sensing application.

3.3.6.2 Cyclic Measurement

Considering the electrical and mechanical properties of the conductive composites, the

ones with CNP loading beyond percolation transition range is preferred for flexible strain sensors. Figure 3.15 shows the dependence of relative resistance on tensile strain for the samples of 2.5CNP, 3.0CNP and 9.0CNP under cyclic measurement. The electrical resistance increases during extension, then decreases and almost return to their respective initial values in the unloading process. The synchronously change of electrical resistance with tensile strain demonstrating the conductive composites have an evident reversibility. The repeatability of the resistance-strain curves of the CNP/SE/SO composites are much better than that of elastomers filled with high structured CNP particles [24, 25]. The improvement may be explained by the uniformly dispersion of low structured CNP in SE matrix due to the existence of SO, and the morphology of small particles or aggregates instead of agglomerates in high structured CNP filled elastomers, which significantly reduce the energy dispersion during the transformation and rotation of CNP agglomerates. Furthermore, the strong interfacial adhesion between the porous CNP nano-particles and SE matrix is also a benefit for the good repeatability. The resistance hysteresis between the loading and unloading curves can be ascribe to the viscosity and internal friction of the composites, due to which the conductive particles or aggregates cannot return from a transient position to balanced position instantaneously during unloading process. The change of resistance with tensile strain, that implies the strain sensitivity, is getting smaller with the increase of CNP loading, from nearly 70 decreases to 3.5 when CNP loading increases from 2.5 wt% to 9.0 wt%. However, the linearity and working range of the conductive composite improved a lot, demonstrating that the composites with higher CNP loadings are more preferred for sensing applications in smart textiles.

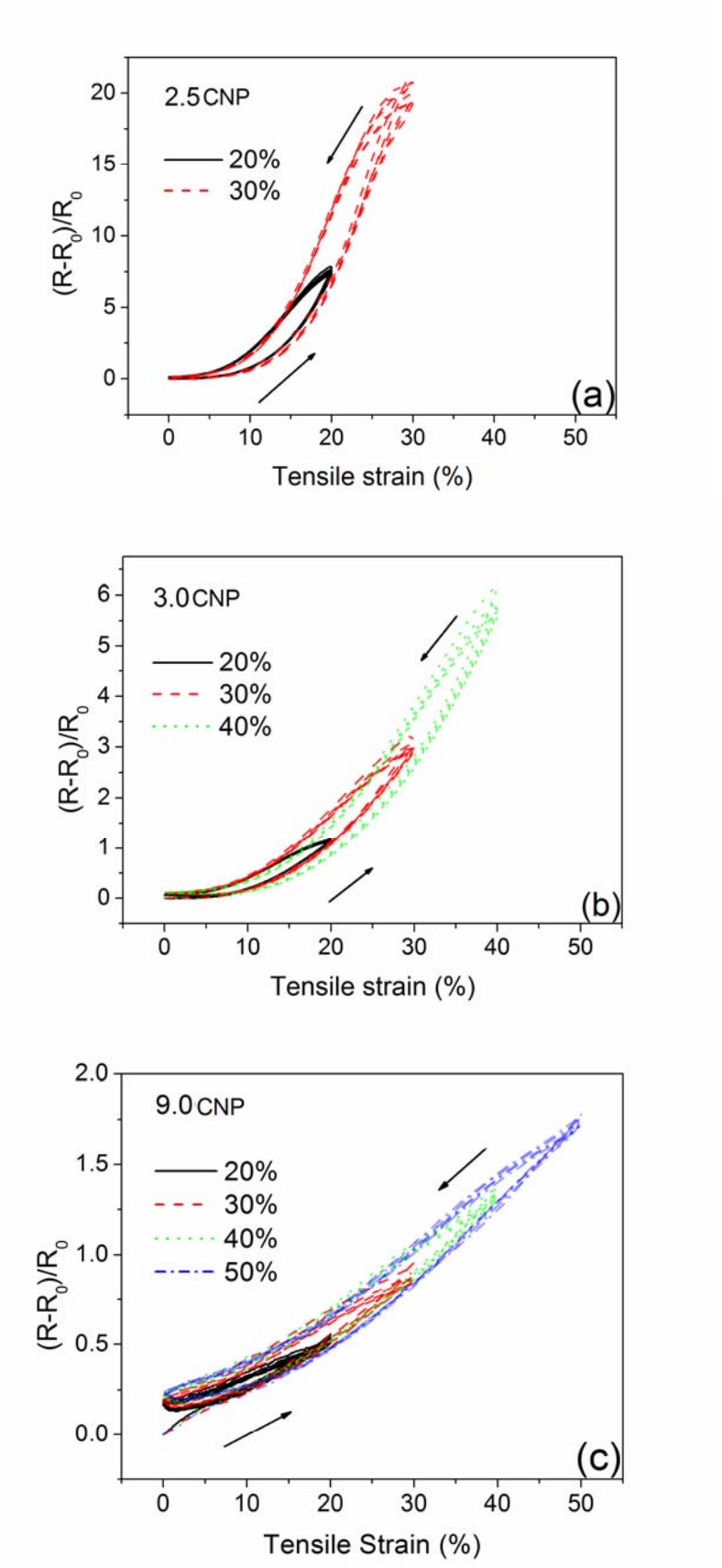

Figure 3.15 Dependence of relative resistance on tensile strain under cyclic measurement for composite of (a) 2.5CNP, (b) 3.0CNP and (c) 9.0CNP

Figure 3.16 shows the electrical fatigue behavior of conductive composite 9.0CNP with tensile strain of 40%. The electrical resistance is instable and increased with tensile cycles which may be due to the permanent destruction of the conductive pathways resulted from defect in the composite and the worse reliability in conductive connection.

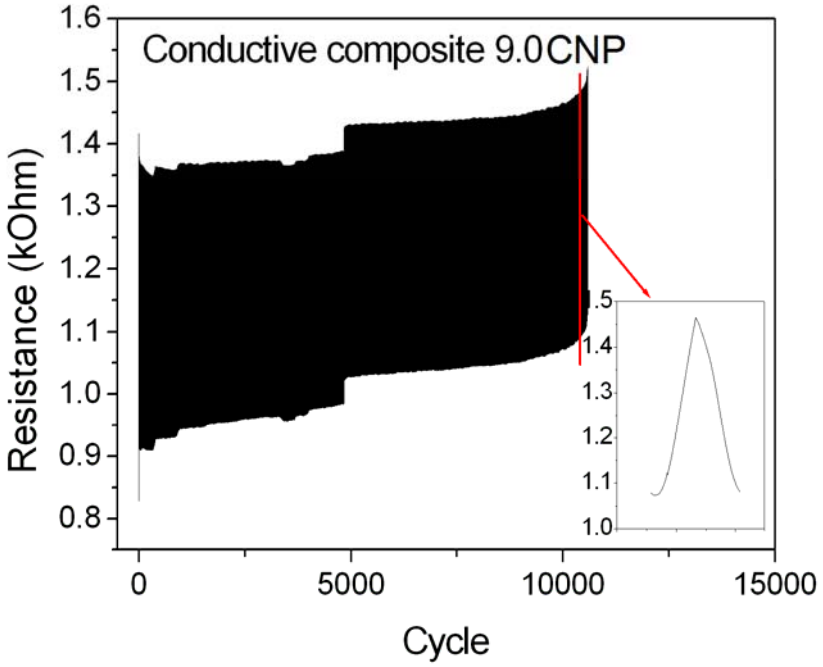

Figure 3.16 Fatigue resistance of the conductive composite 9.0CNP

3.3.6.3 Effect of Strain Rate

The effect of strain rate on resistance is another important factor that should be considered when a material is used for strain sensing applications. Figure 3.17 shows the strain rate dependence of the conductive composites with sample codes of 3.0CNP and 9.0CNP for one cycle. The electrical behavior of the composites is only marginal dependent on strain rate in the range of 0.1-10/min for both of them. The reason can be ascribed to the presence of SO and uniformly dispersion of CNP particles with small agglomerates that eliminating the time consuming alignment process under deformation.

Comparing to the obvious influences of strain rate on electrical resistance reported for CNP/SE composite [26], the smaller strain rate dependent property of the conductive composite can make them find a wider applications in the fields of health monitoring in sports, gesture and posture simulation, etc.

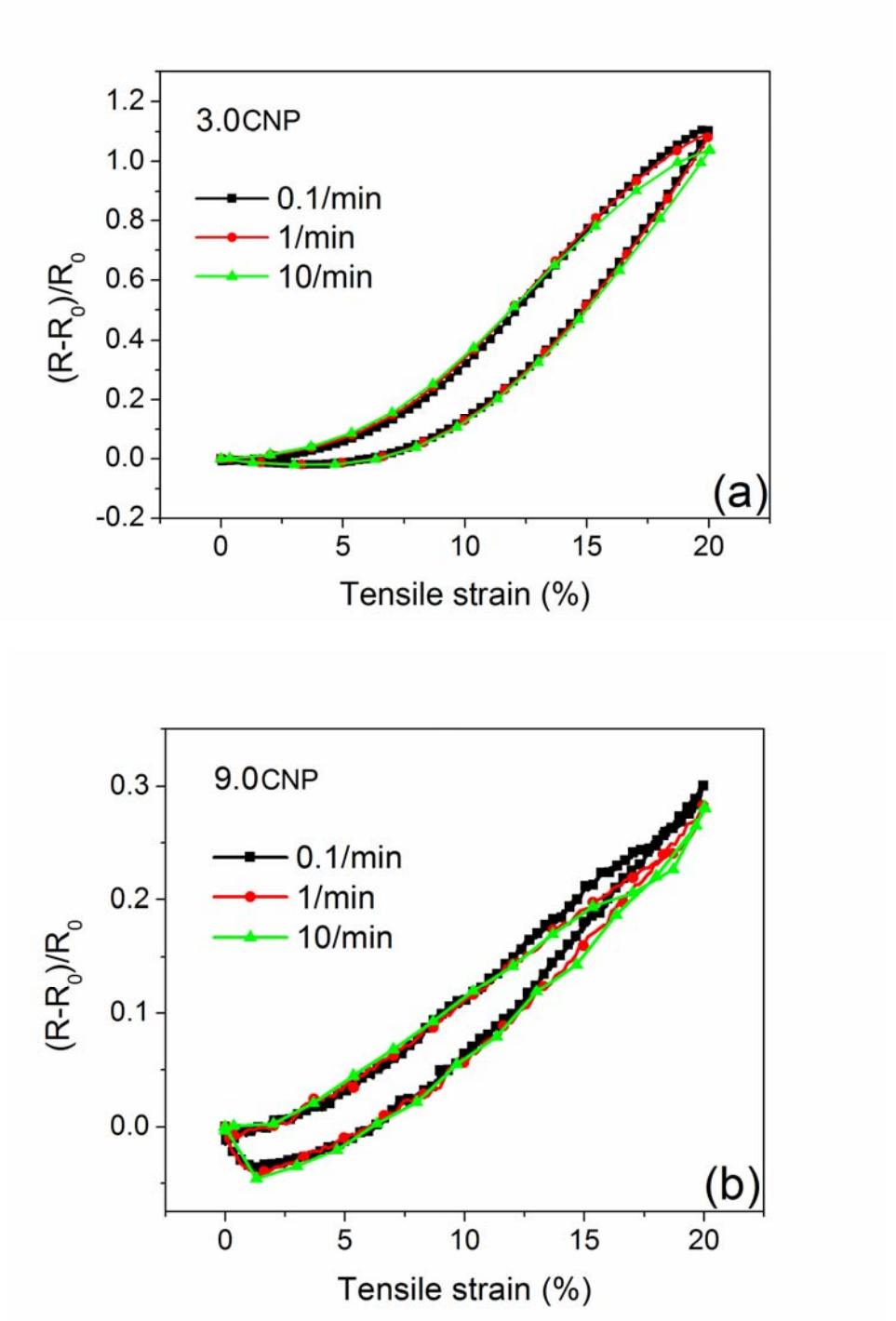

Figure 3.17 Effect of tensile strain rate on resistance variation of CNP/SE/SO composites (a) 3.0CNP and (b) 9.0CNP

3.3.7 Effect of Temperature

Reversible temperature effect on the CNP/SE/SO composites is very important for sensor performance. The effect of temperature on resistance drift and sensing accuracy should be defined and taken into account. If the transfer function of sensors change with temperature is significant, special temperature compensation should be considered. Figure 3.18 shows the temperature effect of CNP/SE/SO composite under cyclic temperature tests between 0 ^{0}C and 60 ^{0}C for samples 3.0CNP, 4.5CNP and 9.0CNP. The resistance hysteresis decreases with temperature cycles for all of them. The maximum hysteresis of initial resistance is less than 2.5% for all the cycles, approximately 1% if excluding the first cycle, implying that the temperature effect is reversible. Furthermore, within the experimental range, the temperature effect is relatively small (less than 5%). There is a weak negative coefficient of temperature (NTC) effect, which means the effect of temperature is well defined and can be calibrated. The monotonous change in resistance with temperature is beneficial for temperature compensation. The temperature coefficient of resistance (approximately -1.17 $^0C^{-1}\times10^{-3}$) is much lower than that reported previously [6, 12]. The NTC effect is the combined result of two competing phenomena: (1) gap changes result from difference in thermal expansion of the polymer matrix and the fillers [27], and (2) flocculation of CNP and excitation of electrons in the CNP particles at elevated temperatures. When the CNP concentration is in the post-percolation range, the conductive networks are mainly contributed to the physical contact of conductive particles or domains, the destruction of the conductive pathways, which results from differential thermal expansion of filler and matrix, is not obvious, while the porous CNP particles facilitate more electron emission, resulting in a weak and repeatable NTC effect.

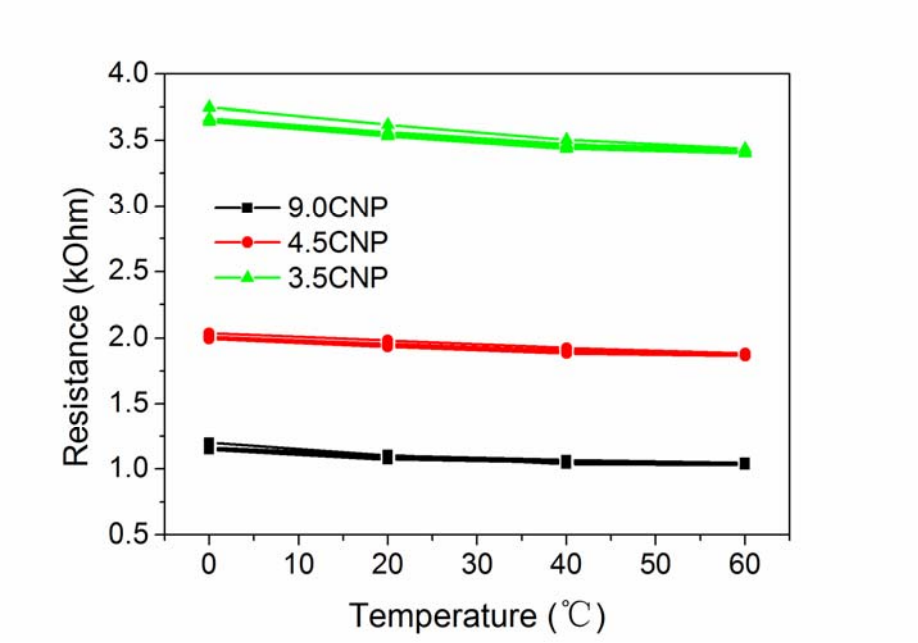

Figure 3.18 Variation of initial resistance of CNP/SE/SO composites in cyclic temperature tests

Figure 3.19 shows the dependence of electrical resistance on strain and temperature for the conductive composite 3.0CNP, 4.5CNP and 9.0CNP, respectively, in 3 temperature cycles. The electrical resistance decreases with the increase of temperature at the same tensile strain, which means the sensitivity of the composites decreases with increase of temperature. The result is due to the resistance relaxation behavior the composites, for which the value is high at high temperature. The repeatability of the resistance-strain curves is relative good for composite 3.0CNP and 4.5CNP at same temperature, while for composite 9.0CNP, the repeatability is not good at 0 ^{0}C. The results demonstrate that the temperature effect should be compensated when the composites are used in strain sensing applications.

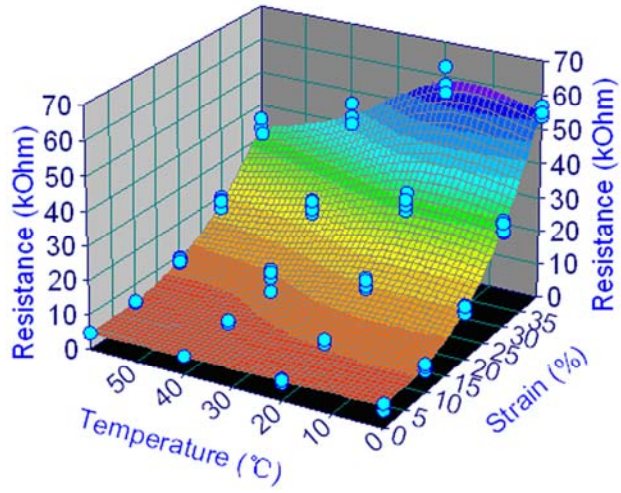
Resistance (kOhm)
70
60
50
40
30
20
10
0
Temperature (℃)
50
40
30
20
10
0
Strain (%)
0
5
10
15
20
25
30
35

(a)

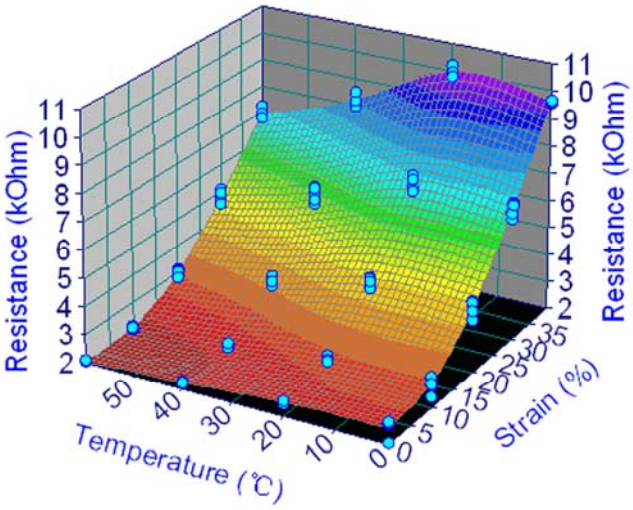
Resistance (kOhm)
11
10
9
8
7
6
5
4
3
2
Temperature (℃)
50
40
30
20
10
0
Strain (%)
0
5
10
15
20
25
30
35

(b)

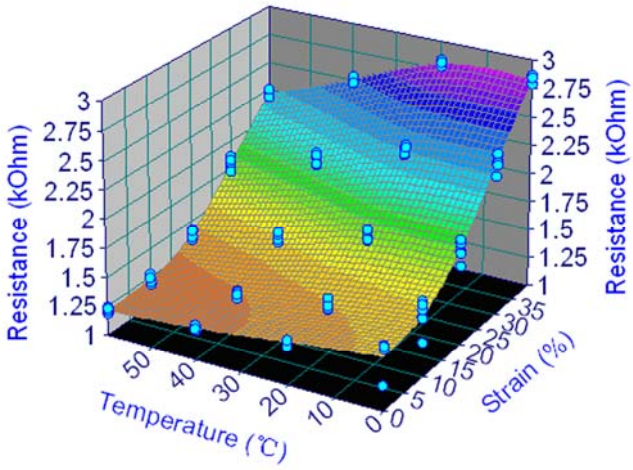
Resistance (kOhm)
3
2.75
2.5
2.25
2
1.75
1.5
1.25
1
Temperature (℃)
50
40
30
20
10
0
Strain (%)
0
5
10
15
20
25
30
35

(c)

Figure 3.19 Effects of temperature and strain on relative resistance change of CNP/SE/SO composite (a) 3.0CNP, (b) 4.5CNP and (c) 9.0CNP

3.3.8 Effect of Humidity

Figure 3.20 shows the dependence of relative resistance on humidity for composite 3.0CNP under fixed temperature of 20 ^{0}C. During the process of humidity decreases from 90% to 20% and then increases to 90%, the resistance continuously decreases for only about 2.37% in the whole process and 0.63% in the humidity increase process. SE and SO are water repellent materials, so the decrease of resistance probably results from the relaxation of the electrical resistance with long treatment time, but not the effect of humidity.

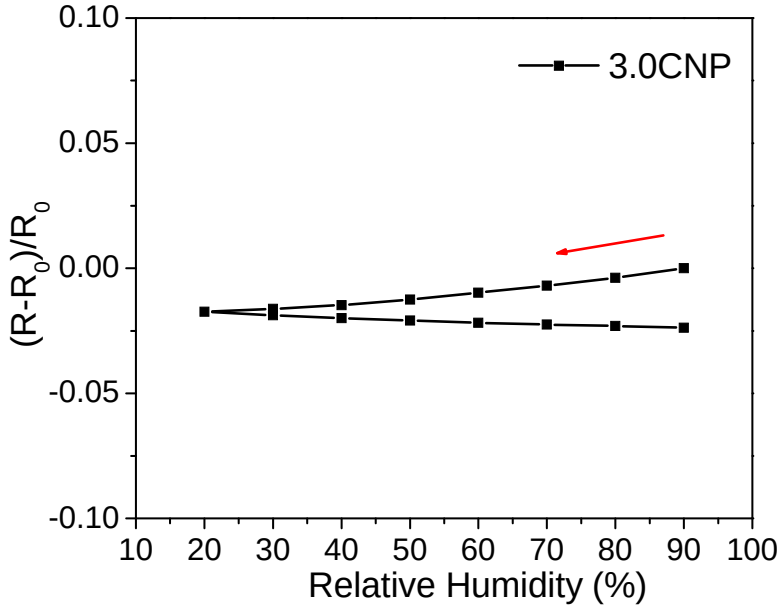

Figure 3.20 Dependence of resistance on relative humidity for composite 3.0CNP

3.4. Conclusions

The CNP/SE/SO conductive composites with sensing properties were fabricated. The

introduction of SO into the system decreases the modulus of the materials to less than 1 MPa without affecting their elongation property. After volatilization of the excessive SO with heat treatment, the composites show good stability, which is confirmed by thermal gravimetric analysis. Study on the dependence of CNP loading on electrical resistivity demonstrates that the conductive composite can be divided into insulating range, percolation range and post-percolation range at the CNP loadings of 0.5 wt% and 2.5 wt%. Electron hopping conduction endows the composites with a very high sensitivity when CNP loading was in percolation range. However, the lower working range and obvious nonlinear electromechanical behavior limited their applications in smart textiles where a large working range is essentially necessary. The sensitivity of the composites decreases with the increase of CNP loading beyond percolation range to post-percolation range. However, both the working range and linearity improved a lot. The conductive composite of 9.0CNP shows a low modulus, marginal strain rate dependent, small humidity effect, better linearity and repeatability in strain up to 50% for several cycles, illustrating a strong promise as flexible strain sensors for applications in smart textiles, but the fatigue resistance of the conductive composite limited their direct application in smart textiles as strain sensors.

References

1. Chen, W., X.M. Tao, P. Xue, and X.Y. Cheng, *Enhanced mechanical properties and morphological characterizations of poly(vinyl alcohol)-carbon nanotube composite films.* Applied Surface Science, 2005. **252**(5): p. 1404-1409.
2. Xue, P., X.M. Tao, H.Y. Tsang, and M.Y. Leung, *PPy-coated electrically conducting fabrics with high strain sensitivity*, in *Smart Nanotextiles*, X. Tao, G. Troster, and D. Diamond, Editors. 2006. p. 97-101.
3. Das, N.C., T.K. Chaki, D. Khastgir, and A. Chakraborty, *Electrical and mechanical properties of conductive carbon black filled EVA, EPDM and their blends.* Kautschuk Gummi Kunststoffe, 2002. **55**(6): p. 300-306.

4. Das, N.C., D. Khastgir, T.K. Chaki, and A. Chakraborty, *Electromagnetic interference shielding effectiveness of carbon black and carbon fibre filled EVA and NR based composites.* Composites Part A-Applied Science and Manufacturing, 2000. **31**(10): p. 1069-1081.
5. Flandin, L., A. Hiltner, and E. Baer, *Interrelationships between electrical and mechanical properties of a carbon black-filled ethylene-octene elastomer.* Polymer, 2001. **42**(2): p. 827-838.
6. Cochrane, C., V. Koncar, M. Lewandowski, and C. Dufour, *Design and development of a flexible strain sensor for textile structures based on a conductive polymer composite.* Sensors, 2007. **7**(4): p. 473-492.
7. Mattmann, C., F. Clemens, and G. Troster, *Sensor for measuring strain in textile.* Sensors, 2008. **8**(6): p. 3719-3732.
8. Sau, K.P., T.K. Chaki, and D. Khastgir, *The effect of compressive strain and stress on electrical conductivity of conductive rubber composites.* Rubber Chemistry and Technology, 2000. **73**(2): p. 310-324.
9. Wang, L.H., T.H. Ding, and P. Wang, *Effects of instantaneous compression pressure on electrical resistance of carbon black filled silicone rubber composite during compressive stress relaxation.* Composites Science And Technology, 2008. **68**(15-16): p. 3448-3450.
10. Zhou, J.F., Y.H. Song, Q. Zheng, Q. Wu, and M.Q. Zhang, *Percolation transition and hydrostatic piezoresistance for carbon black filled poly(methylvinylsilioxane) vulcanizates.* Carbon, 2008. **46**(4): p. 679-691.
11. Wang, L.H., T.H. Ding, and P. Wang, *Influence of carbon black concentration on piezoresistivity for carbon-black-filled silicone rubber composite.* Carbon, 2009. **47**(14): p. 3151-3157.
12. Das, N.C., T.K. Chaki, and D. Khastgir, *Effect of processing parameters, applied pressure and temperature on the electrical resistivity of rubber-based conductive composites.* Carbon, 2002. **40**(6): p. 807-816.
13. Tao, X.M., *Smart fibres, fabrics and clothing*2001, Cambridge: Woodhead Pub Co.
14. Beruto, D.T., M. Capurro, and G. Marro, *Piezoresistance behavior of silicone-graphite composites in the proximity of the electric percolation threshold.* Sensors and Actuators A-Physical, 2005. **117**(2): p. 301-308.
15. Zhu, S. and D.D.L. Chung, *Analytical model of piezoresistivity for strain sensing in carbon fiber polymer-matrix structural composite under flexure.* Carbon, 2007. **45**(8): p. 1606-1613.
16. Hu, N., Y. Karube, M. Arai, T. Watanabe, C. Yan, Y. Li, et al., *Investigation on sensitivity of a polymer/carbon nanotube composite strain sensor.* Carbon, 2010. **48**(3): p. 680-687.
17. Yu, T., Z.H. Ni, C.L. Du, Y.M. You, Y.Y. Wang, and Z.X. Shen, *Raman mapping investigation of graphene on transparent flexible substrate: The strain effect.* Journal of Physical Chemistry C, 2008. **112**(33): p. 12602-12605.
18. Sau, K.P., T.K. Chaki, and D. Khastgir, *The change in conductivity of a rubber carbon black composite subjected to different modes of pre-strain.* Composites Part A-Applied Science and Manufacturing, 1998. **29**(4): p. 363-370.
19. Balberg, I., *A comprehensive picture of the electrical phenomena in carbon black-polymer composites.* Carbon, 2002. **40**(2): p. 139-143.
20. Huang, J.C., *Carbon black filled conducting polymers and polymer blends.* Advances in Polymer Technology, 2002. **21**(4): p. 299-313.
21. Sichel, E.K., *Carbon black- polymer composites*1982: Marcel dekker, Inc.

22. Novak, I., I. Krupa, and I. Janigova, *Hybrid electro-conductive composites with improved toughness, filled by carbon black.* Carbon, 2005. **43**(4): p. 841-848.
23. Das, N.C., T.K. Chaki, and D. Khastgir, *Effect of axial stretching on electrical resistivity of short carbon fibre and carbon black filled conductive rubber composites.* Polymer International, 2002. **51**(2): p. 156-163.
24. Yamaguchi, K., J.J.C. Busfield, and A.G. Thomas, *Electrical and mechanical behavior of filled elastomers. I. The effect of strain.* Journal of Polymer Science, Part B: Polymer Physics, 2003. **41**(17): p. 2079-2089.
25. Flandin, L., A. Chang, S. Nazarenko, A. Hiltner, and E. Baer, *Effect of strain on the properties of an ethylene-octene elastomer with conductive carbon fillers.* Journal of Applied Polymer Science, 2000. **76**(6): p. 894-905.
26. Kost, J., M. Narkis, and A. Foux, *Effects of Axial Stretching on the Resistivity of Carbon-Black Filled Silicone-Rubber.* Polymer Engineering and Science, 1983. **23**(10): p. 567-571.
27. Hindermann-Bischoff, M. and F. Ehrburger-Dolle, *Electrical conductivity of carbon black-polyethylene composites - Experimental evidence of the change of cluster connectivity in the PTC effect.* Carbon, 2001. **39**(3): p. 375-382.

CHAPTER 4
FABRICATION AND CHARACTERIZATION OF CONDUCTIVE FABRICS

4.1 Introduction

Previous studies on CNP/SE/SO composites presented in Chapter 3 have shown that the introduction of silicone oil into CNP filled conductive elastomers decreases the modulus of composites to less than 1 MPa, which is in the same level as human skin. Besides, the sensitivity of the composites can be adjusted to a high value by changing CNP concentration in the percolation range, where the composites have a high potential to be flexible strain sensors. However, at that CNP concentration, the initial resistance of the composite is high and resistance changes in several orders of magnitude in small strain ranges increased the difficulty in measurement and cannot fulfill the requirement of large strain sensing in smart textiles. The conductive composite with CNP loading well beyond the percolation range is preferred for sensor applications, but the corresponding sensitivity decreased simultaneously. Furthermore, it's difficult to make a conductive connection between the conductive composite and measuring circuit with good reliability, the fatigue life of the conductive composite is also not good. Knitted fabrics have good fatigue resistance properties and high elasticity; it is also easy being connected with other textile materials by sewing or pasting methods.

In this chapter, a conductive fabric based on the previous developed conductive CNP/SE/SO composites will be developed to solve the problems in CNP/SE/SO

composites for strain sensing application. The parameters affecting the performances of the conductive fabric will be discussed.

4.2 Experimental

4.2.1 Materials and Processing

CNP nano-particles (Carbon® ECP600JD, Akzo Nobel) were heated at 100 ^{0}C for 2 hour to remove the moisture and used as conductive filler. Their average particle diameter is about 30 nm while aggregate size of about 70nm can be observed from SEM image. Specific surface area of the CNP is ca. 440-510 ml/100g as expressed by dibutylphthalate (DBP) absorbing value.

Silicone elastomer (SE) (ELASTOSIL®LR6200 A and B, Wacker Chemie AG, Germany) was used as received. Dimethyl silicone oil (SO) with kinetic viscosity of 5.0 mm^2/s at 25 ^{0}C from Che Scientific Co. (Hong Kong) Ltd., China, was used as the diluting agent.

Plain knitted fabric with 83% Tactel and 17% Lycra (Sunikorn Knitters Limited, Hong Kong) was selected as substrate material for its good elasticity and low hysteresis. The weight of the knitted fabric is 195 g/m^2, the density is 43 courses/cm and 22 wales/cm, the linear density of the Tactel yarn is 702 denier/68 filaments and the Lycra yarn is 40 denier/5 filaments. The knitted fabric was cleaned with 1 g/L non-ionic detergent (Lentol B) at 60 ^{0}C for 30 minutes and then rinsed thoroughly, followed by dehydration and drying at 60 ^{0}C for 15 min. The knitted fabrics with size of 60 cm×30 cm were cut and ironed flat before fabrication.

4.2.2 Design and Fabrication of Conductive Fabric

CNP/SE/SO mixture pastes with CNP loadings beyond the percolation transition range were fabricated using the mechanical mixing method as described in Chapter 3. Knitted fabric was flatly pasted on a glass with self-adhesive glue with a pre-tension of 1.2 N. Then the fabric together with the glass was mounted on a screen printing machine with screen mesh size of 1000 holes per square inch. The distance between the squeegee blade and screen was fixed to 8mm and the angle between them to 60° to achieve an even coating. The mixture paste was uniformly coated on the knitted fabric to form series of stripes with width of 10 mm, then the paste was cured at 100 ^{0}C for 2 hours, which is shown in Figure 4.1. Conductive fabrics of stripes in both wale and course direction were fabricated. Three mixture pastes with CNP loadings beyond the percolation transition range were used, as shown in Table 4.1.

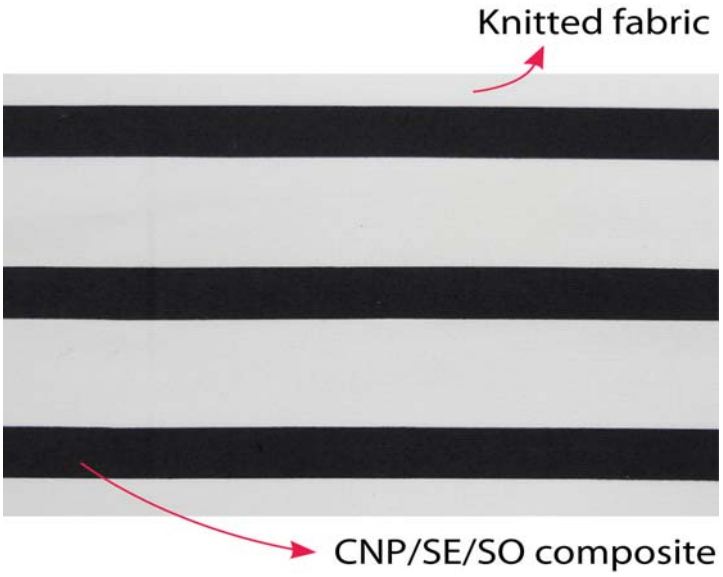

Figure 4.1 Photograph of conductive fabric

Irreversible stress-strain and resistance-strain behavior have been reported for many conductive composites or conductive composites based sensors [1, 2]. Due to the viscoelasticity of conductive composite and knitted fabric, their stress and resistance curves may show the same unrepeatable properties when a virgin conductive fabric was

stretched with sequence of increased strain levels. To compare the mechanical pretreatment on the performances of the conductive fabric, part of the samples were mechanical treated with a tensile strain of 70% for 1 time before further characterization.

Table 4.1 Ingredients of mixture pastes coated on knitted fabric

Sample Code	Composition of mixture pastes (Weight ratio)
3.5CNP	CNP/SE/SO 3.5/96.5/50.0
4.5CNP	CNP/SE/SO 4.5/95.5/75.0
9.0CNP	CNP/SE/SO 9.0/91.0/150.0

4.2.3 Characterization

4.2.3.1 Electrical Resistance

E-fabric Tester, developed in our laboratory with reference to ASTM D4496-04, was used to measure static resistance of the conductive fabric. Two copper bar electrodes were placed perpendicular to the direction of the conductive stripes with a space of 15 mm and the resistance was recorded. A predetermined weight of 10g was put on the electrodes to reduce the variation of contact resistance between electrodes and conductive fabric. The tests were carried out at 20 ^{0}C and relative humidity of 65% after the samples were conditioned at the same environment for 72 hours.

4.2.3.2 I-V Curves and Impedance Spectra

To examine the electrical properties of the conductive fabric, I-V curves and impedance spectra of them were measured. The specimen was fixed on a frame at two ends, as shown in Figure 4.2, the gauge length of the frame can be adjusted freely and the initial length was set to 10mm. The current value were measured using Solartron 1287

electrochemical interface system under ambient conditions with voltage gradually increased from -10 V to 10 V with an increasing speed of 100 mV/s. The impedance spectra was performed by Solartron SI 1287 electrochemical interface combined with 1252A frequency response analyzer with the frequency ranging between 10^{-2}-10^{5} Hz. I-V curves and impedance spectra of the conductive fabrics at different strains were achieved by increasing the gauge length of the frame with a step of 10% from 0 to 60%.

Figure 4.2 Conductive fabric mounted on a frame for characterizing I-V curve and impedance spectra

4.2.3.3 Coupled Electromechanical Properties

To measure the electromechanical properties of the conductive fabric, two copper plates were clamped on two sides of the conductive fabric as electrodes; the distance between the two electrodes was 10 mm. The force and displacement data were recorded by a computer connected to Universal Material Tester (Instron 5944), and resistance by the digital multi-meter (Keithley 2010) simultaneously using data acquisition system. All the measurements were conducted in a conditioned room with temperature of 20 ^{0}C and relative humidity of 65%. The experimental setup is the same as that shown in Chapter 3 and different protocols were used to characterize the conductive fabric.

For sensitivity characterization, the conductive fabric was stretched to 100% strain and

then released for 1 cycle. To characterize the responding time and resistance relaxation behavior, the conductive fabric was stretched to 40% strain with a tensile speed of 2400 mm/min, and then the load was released with the same speed after maintained for 10 minutes. To examine the repeatability of the responding behavior, the process was repeated for another time. When a flexible strain sensor was used for long-term health care and monitoring or athletic training, it should be able to resist cyclic loading-unloading for many times. To examine the fatigue life under these conditions, the conductive fabric was cyclic stretched to 40% strain for 10,000 times or failure was obviously observed. To compare the reproducibility of the conductive fabric at various strain levels, it was extended to strains of 20%, 40% and 60%, respectively for 1 cycle. To comparing the electrical behavior at different loading speeds, the conductive fabric was tested with strain rate from 12 mm/min to 2400 mm/min (the equivalent strain rate is 0.02 to 4 /s). In the electromechanical tests, the tensile speed of the strain gauge is 60 mm/min if not specially mentioned. In each experiment, 5 samples were used.

4.2.3.4 Temperature and Humidity Effect

The experimental setup to evaluate temperature and humidity effects of conductive fabrics is the same as that described in Chapter 3. The treatment method and evaluation process are also identical.

4.3 Results and Discussion

4.3.1 Electrically Resistance

The electrical resistance of the conductive fabric is affected by size, thickness and CNP concentration of conductive paste coating. During the fabrication process, the machine

parameters were fixed to precisely control the width and thickness of coating layer. After curing, the size of the conductive fabric can be controlled within 1%. The thickness of the coating layer was affected by the screen printing times. Table 4.2 shows the weight changes of conductive fabric after coated with CNP/SE/SO composites (the size of conductive fabric measured is 177 mm×126mm) for 1 time and 3 times respectively. It can be obviously observed that the weight variation of coating layer is much smaller for the conductive fabric coated for 3 times than that coated for 1 time, and the value can be controlled within 2.5%, meaning the 3 times coating process was suitable to fabricate the conductive fabric with better evenness.

Table 4.2 Weight of conductive composites coated on fabric

	Coated for 1 time		Coated for 3 times	
	Average weight increment (g)	CV (%)	Average weight increment (g)	CV (%)
Before curing	1.00	11.31	1.61	2.12
After curing	0.75	6.36	1.32	2.35

The electrical resistance of the conductive fabric with width of 10mm and length of 15mm was measured by E-Fabric Tester. In each conductive fabric, three paralleled conductive stripes were tested for 15 times at different locations as shown in Figure 4.3. Table 4.3 demonstrates the average electrical resistance and coefficient of variation for conductive fabrics with different CNP concentrations. The electrical resistance and the coefficient of variation of all conductive fabrics are at an acceptable level, which further confirmed the fabrication process is well controlled. The coefficient of variation decreases with increasing CNP concentration.

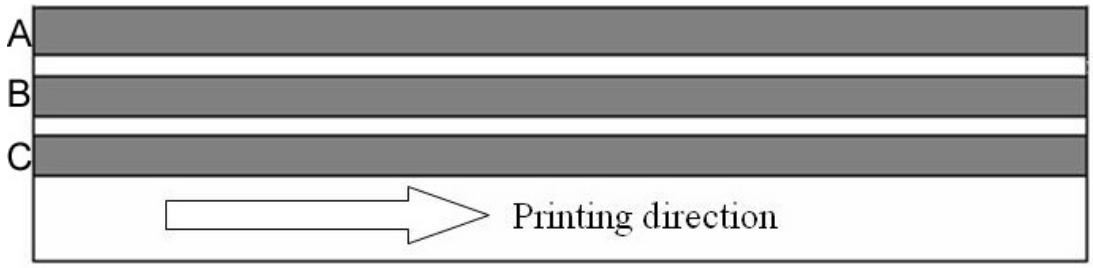

Figure 4.3 Location of the conductive stripes on the fabric

Table 4.3 Variation of the electrical resistance for conductive fabrics with different CNP concentrations

Sample code	R_0 (kΩ)	CV (%)
3.5CNP	115.90	5.24
4.5CNP	69.27	4.12
9.0CNP	10.29	3.50

4.3.2 I-V Characteristics and Impedance Spectra

To fabricate a piezoresistive strain sensor, a linear current-voltage (I-V) relationship within the working range is preferred for improving the accuracy and simplifies the measuring circuit. Figure 4.4 compares the I-V curves of conductive fabric (4.5CNP and 9.0CNP) and corresponding conductive composites. Although the slope of I-V curves are smaller for the conductive fabric than those of conductive composites due to the thinner coating layer, the linear I-V curves still demonstrate the conductive fabrics own ohmic conduction under the applied voltages if they are not stretched.

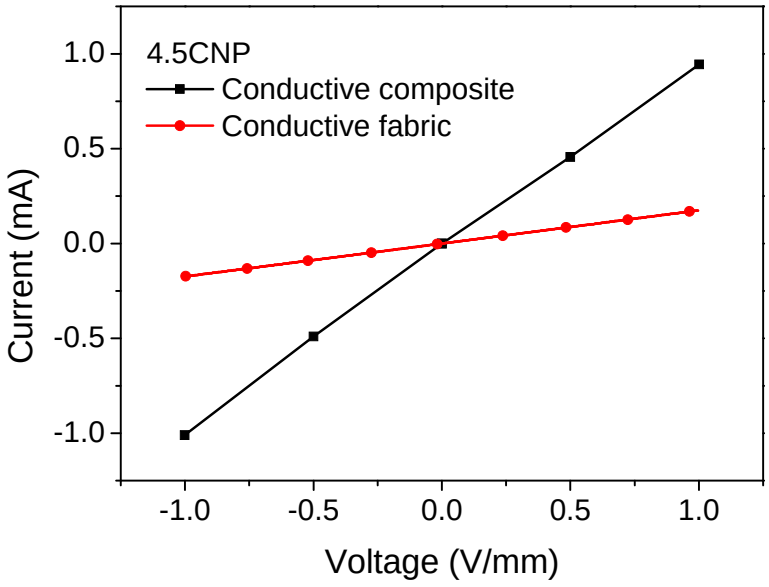

(a)

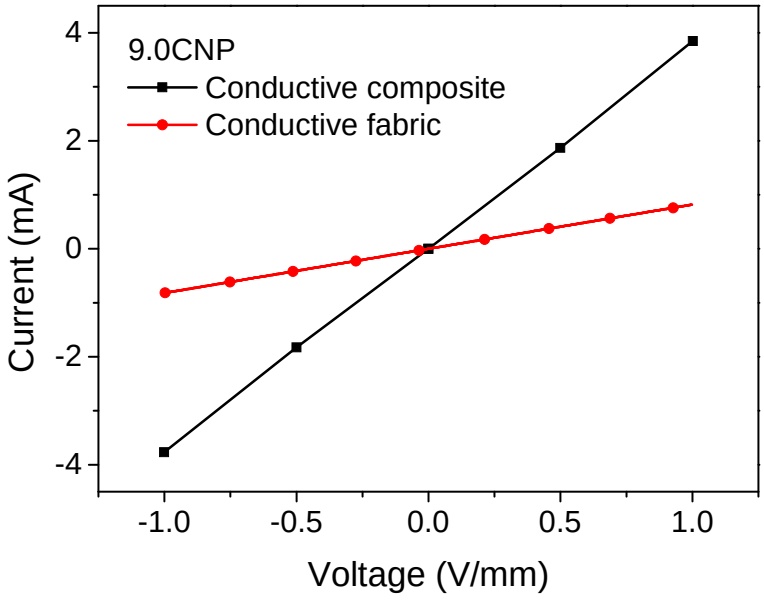

(b)

Figure 4.4 I-V curves of conductive fabrics and corresponding conductive CNP/SE/SO composites without extension (a) 4.5CNP (b) 9.0CNP

Figure 4.5 shows the I-V curves of the conductive fabrics at different strain levels. The

9.0CNP conductive fabric exhibits nearly linear I-V characteristic in strain ranges from 0 to 60%, indicating ohmic conduction still dominant after large extension under the applied voltages. For conductive fabric of 4.5CNP and 3.5CNP, there is still no obvious nonlinearity at strains up to 40% for the low voltage applied, at which the electrons that can be excited for hopping is relatively small.

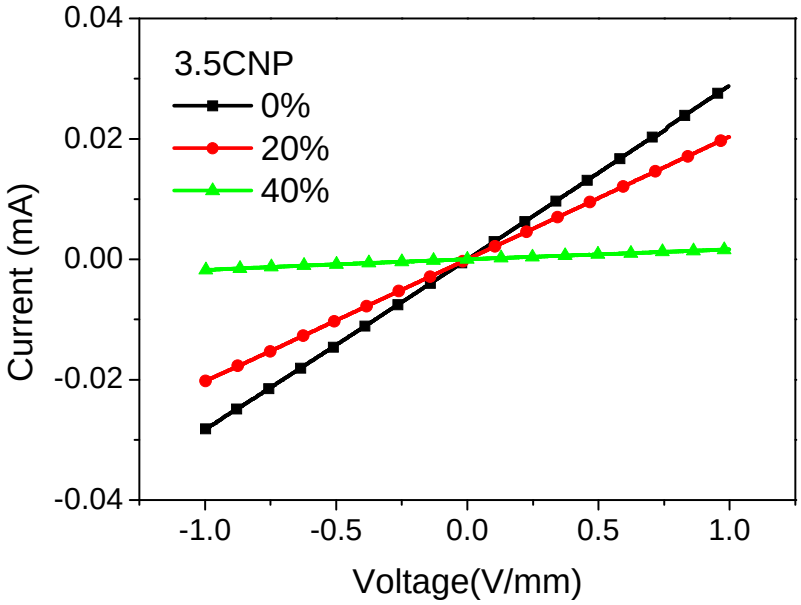

(a)

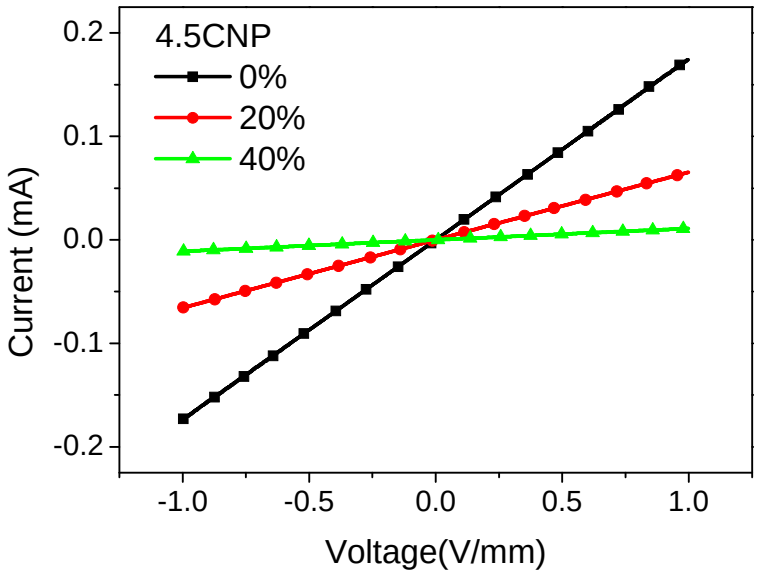

(b)

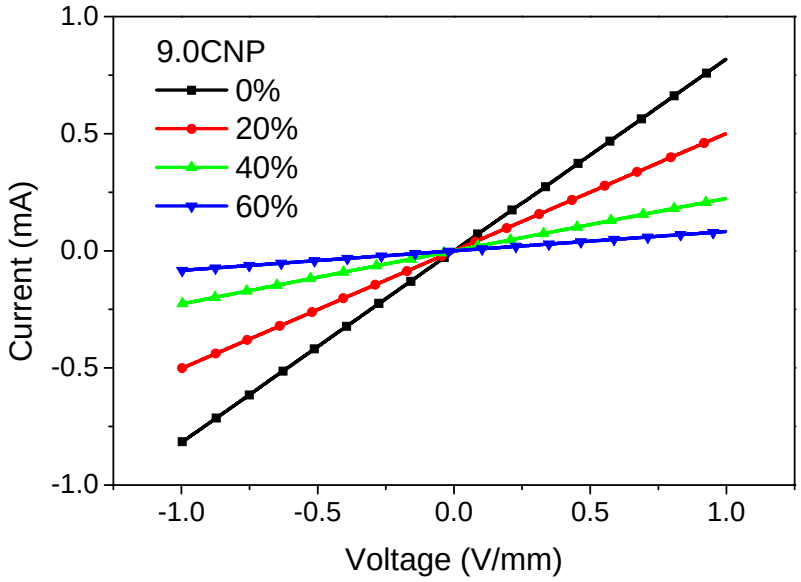

(c)

Figure 4.5 I-V characteristics of conductive fabrics at various tensile strains for samples of (a) 3.5CNP, (b) 4.5CNP and (c) 9.0CNP

Figure 4.6 compares the impedance spectra of conductive fabrics and composites with various CNP concentrations when there is no extension. From the plot it can be observed that the impedance of conductive fabrics is more dependent on frequency than that of composites, which may be due to the thinner conductive composite layer on knitted fabric. The frequency dependent impedance also decreased with increase of CNP concentration.

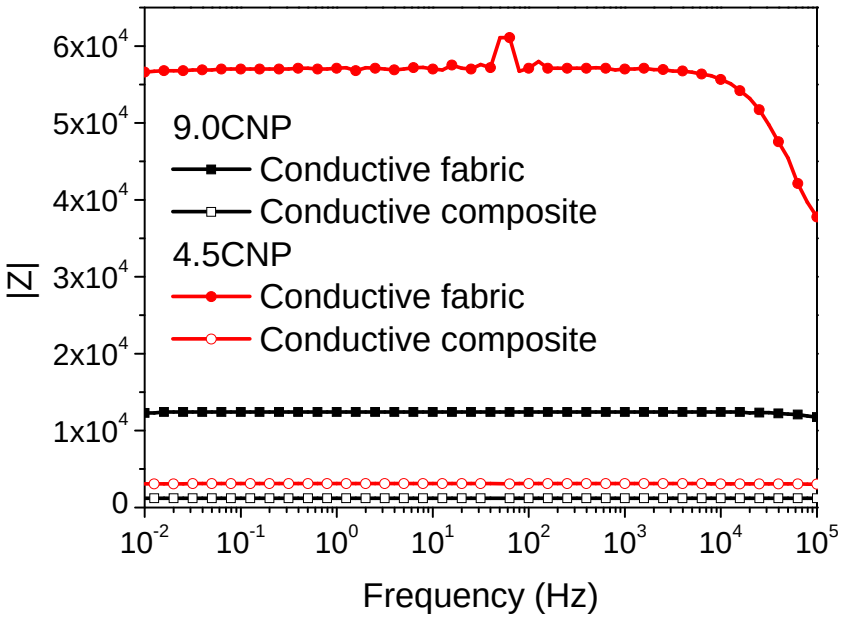

(a)

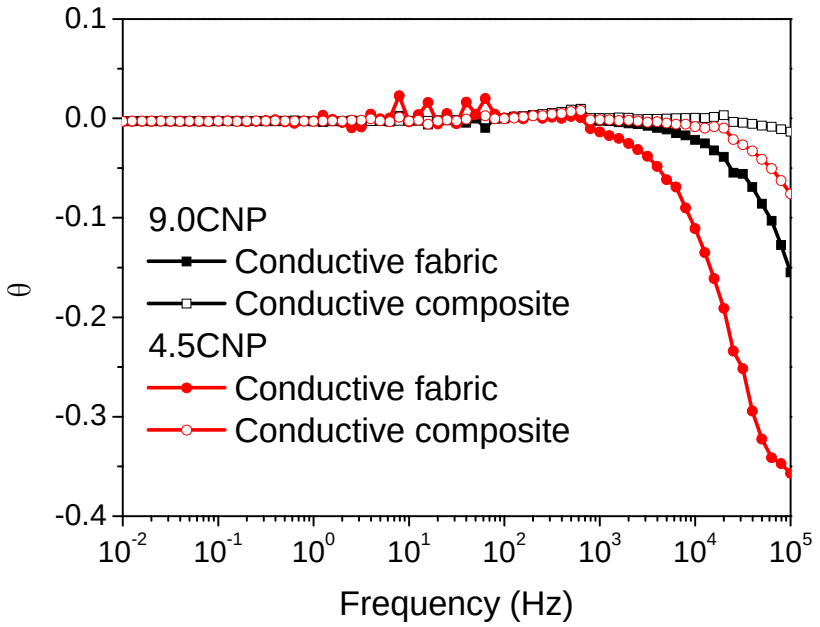

(b)

Figure 4.6 Impedance spectra of conductive fabrics and corresponding conductive composites without extension (a) magnitude and (b) phase angle

Stretching conductive fabric plays a similar role as decreasing CNP concentration of the

conductive composite. As shown in Figure 4.7 and Figure 4.8, the conductive fabrics are more frequency dependent with the increase of tensile strain. For conductive fabric of 4.5CNP, the impedance spectra becomes unstable when the strain is 30% and the frequency is 10^2 Hz, while for conductive fabric of 9.0CNP, the impedance spectra still keeps stable when strain reached to 60% and the frequency reached to 10^3 Hz. Considering the potential applications of the conductive fabric as sensing element of fabric strain sensor, the ones with smaller frequency dependent can support a higher tensile strain without affecting its accuracy.

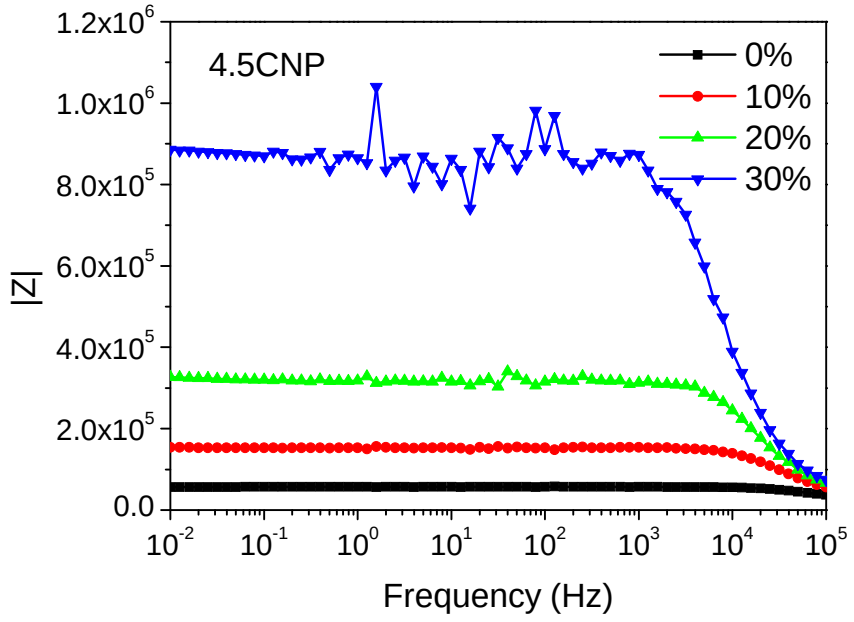

(a)

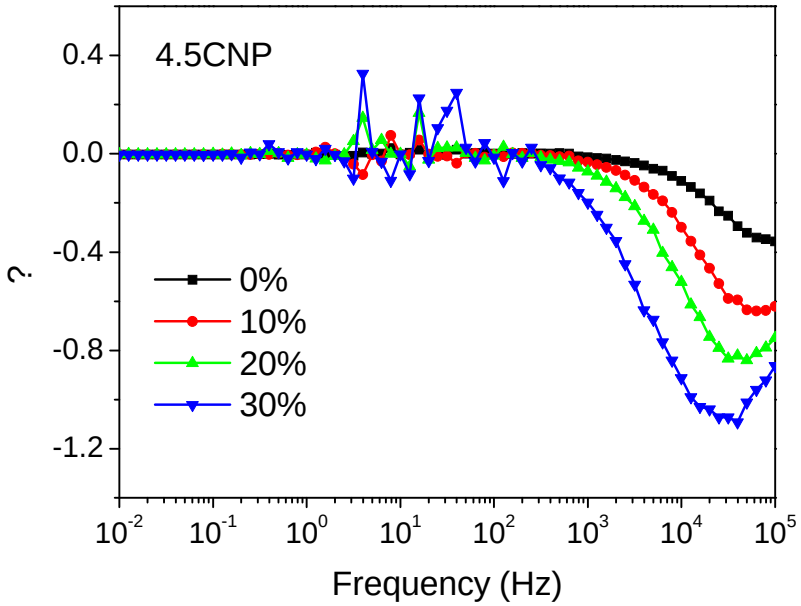

(b)

Figure 4.7 Impedance spectra of conductive fabric 4.5CNP with extension (a) magnitude and (b) phase angle

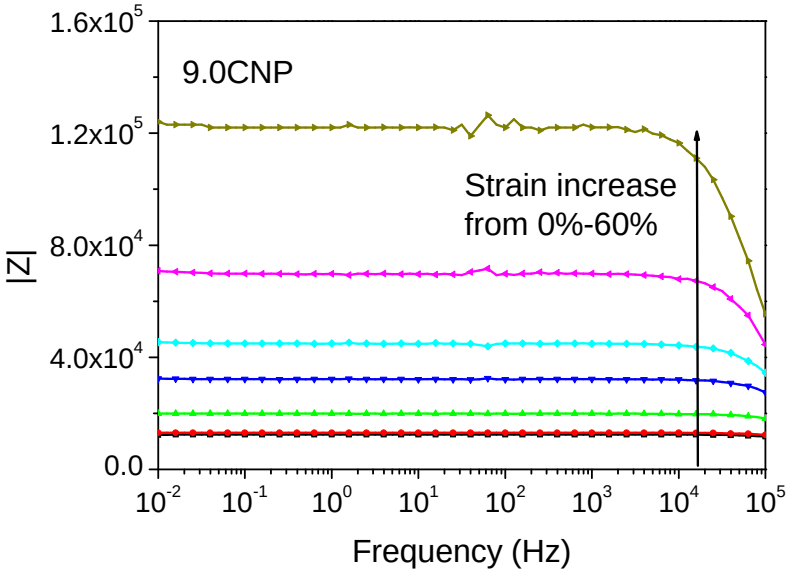

(a)

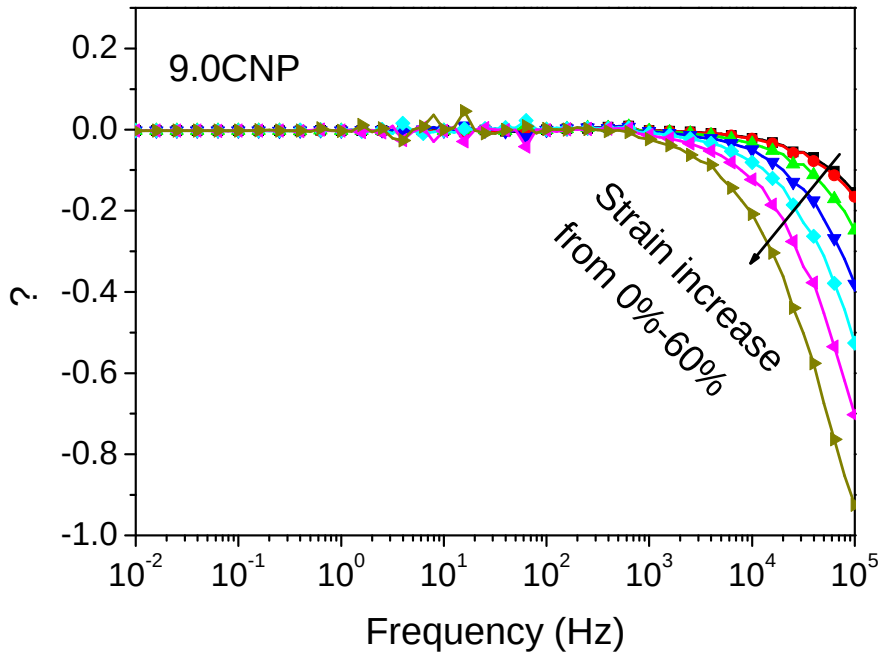

(b)

Figure 4.8 Impedance spectra of conductive fabric 9.0CNP with extension (a) magnitude and (b) phase angle

4.3.3 Responding Time

Fast electrical response to mechanical strain is an important requirement for strain sensors used in smart textiles for health monitoring or impact measurement. Figure 4.9 shows the resistance change of the conductive fabric when the tensile strain increases from 0 to 40% at a speed of 2400mm/min (corresponding to strain rate of 4/s). The peak in resistance and strain occur simultaneously, demonstrating that the conductive fabric has an instantaneous response as a load is applied, though a relative high overshoot of about 27.83% can be observed. The overshoot is due to the instantaneous destruction of the conductive chains in conductive composite [2], resulting from overshoot of mechanical force under high loading speed. The time of the conductive fabric from overshoot to

balance resistance is less than 10s, which is in equal level as the carbon nanotube strain sensor [3], and much quicker than that of CNP filled thermoplastic composite, whose recovery time is more than 100 s with a much lower strain speed [1]. This is because the introduction of knitted fabric accelerated the recovery of conductive composites from transient position to balance position when the tensile strain is in its elastic deformation range.

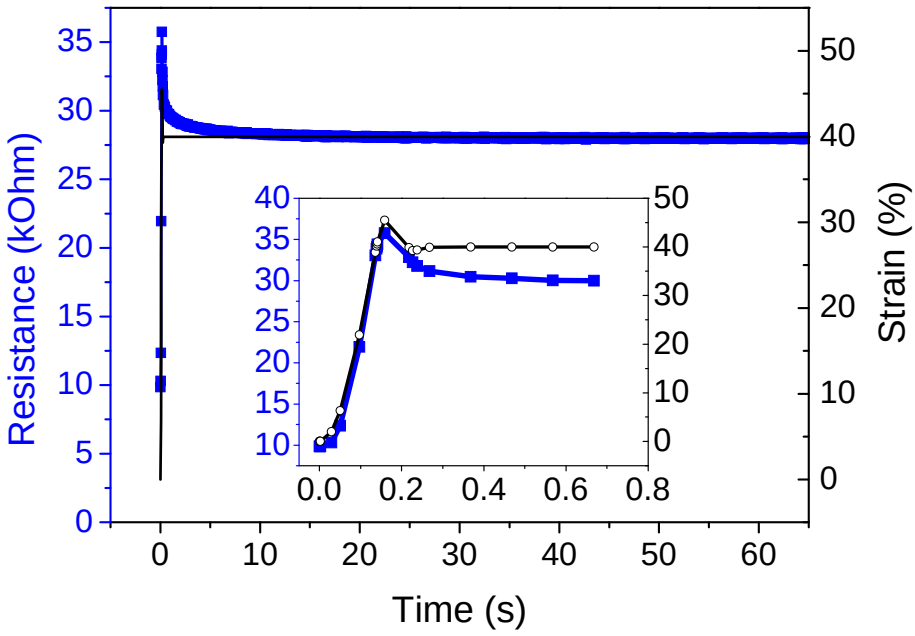

Figure 4.9 Resistance of the conductive fabric against time in response to a mechanical tensile strain up to 40% (Inset is close-up of the overshoot)

Figure 4.10 illustrates that when the applied load is removed, the electrical resistance of the conductive fabric decreases quickly, but the recovery process is much longer than the loading period, which is due to the viscoelastic property for both the conductive coating and the knitted fabric. For most sensor applications, the loading and holding process are more concerned, which means the relative longer recovery time will not affect the usage of the fabric strain sensor in such cases. Under repeated loading-holding-unloading cycles, the sensor shows nearly identical responding behavior and very good repeatability, as

shown in Figure 4.11.

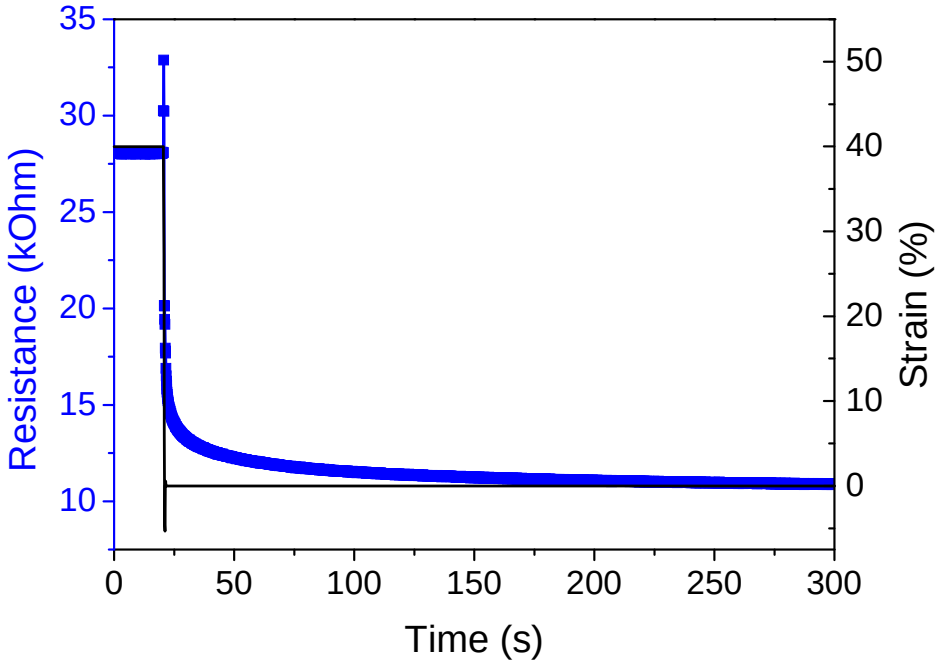

Figure 4.10 Resistance change of the conductive fabric in response to a mechanical tensile strain up to 40% at the recovery phase

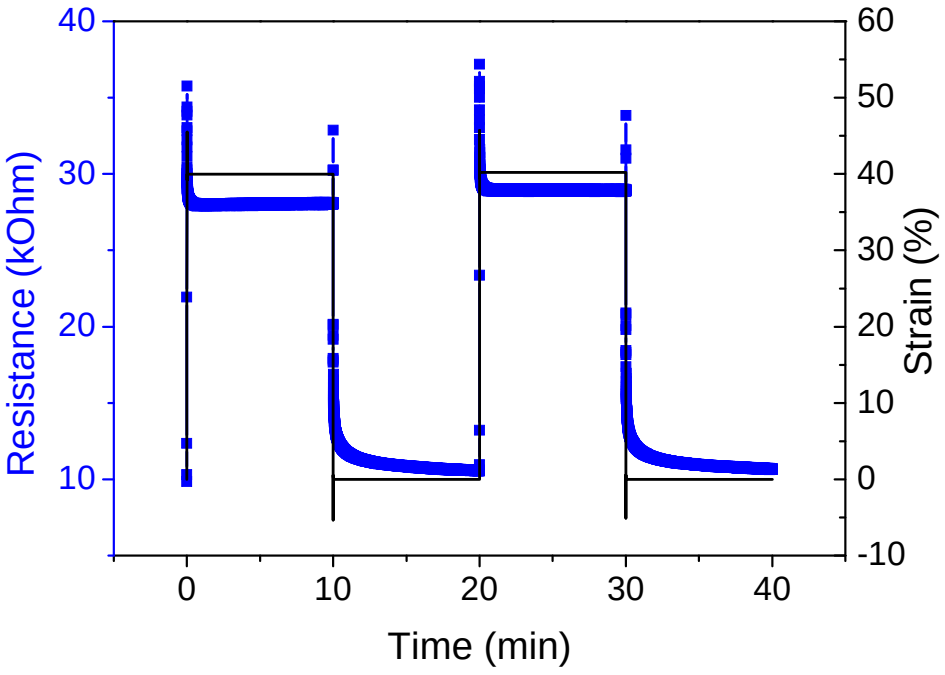

Figure 4.11 Repeated responding behavior of conductive fabric to fixed strain.

4.3.4 Effect of Fabric structure on Sensitivity

For metal based strain gauges, the changes in electrical resistance is mainly contributed to the changes in configuration due to the constant electrical resistivity under deformation, leading to a sensor with a gauge factor of 2 at the most. While for CNP/SE/SO composites, besides the changes in configuration, the changes in electrical resistivity originate from the changes with the amount of conductive pathways and conductive types during extension, and result in a higher sensitivity than metal based sensors. A very high gauge factor can be achieved for conductive composite with CNP concentration in the percolation range. However, to achieve a conductive composite with less capacitive behavior, the CNP concentration should be as high as possible within the permission of fabrication condition, result in a decreased sensitivity. The plain knitted fabric has good elasticity in both wale and course direction as shown in Figure 4.12 and Figure 4.13, respectively. Furthermore, it can resist long-term cyclic extension without changing the original physical properties within its elastic range. After coated with conductive composite, the Young's modulus of the knitted fabric increased. However, the value is still less than 1 MPa, especially for the knitted fabric 9.0CNP, whose value is 0.34 MPa, much smaller than that of human skin (Table 4.), make it possible for the conductive fabric to be used as strain gauge to measure the deformation of human skins without influencing their activities.

Table 4.4 Tensile modulus of the conductive fabric with different CNP concentrations

Sample code	Tensile modulus (MPa)
Knitted fabric	0.16
3.5CNP	0.80
4.5CNP	0.67
9.0CNP	0.34

When stretched, the deformation of the knitted fabric mainly composed of extension in the longitudinal direction and shrinkage in width direction as well as transfer and extension of yarn. In the process, the conductive composite on yarn is little extended, and the resistance change is mainly contributed to the extension of conductive composite between the neighboring yarns if they are continuous. The partially extension of conductive composite on knitted fabric leads to a higher sensitivity for conductive fabric than that of conductive composite if the resistance-strain curve of the conductive composite is nonlinear.

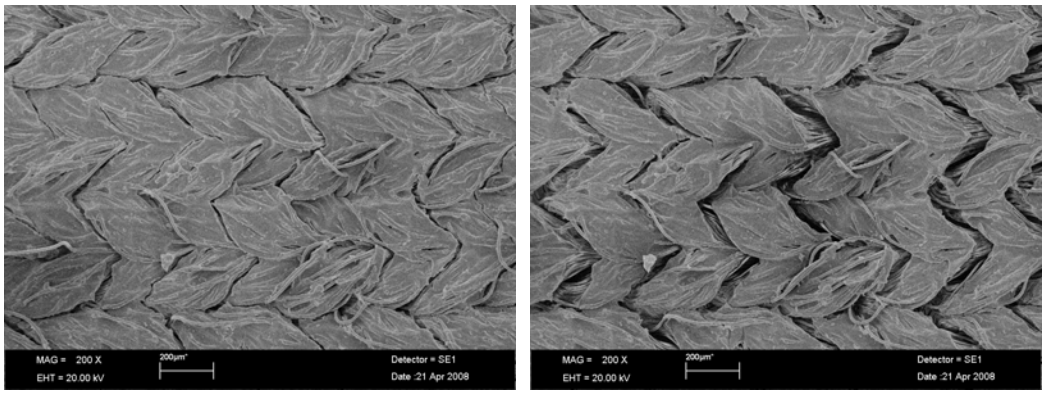

(a) (b)

Figure 4.12 SEM photographs of the knitted fabric before and after extension in the wale direction

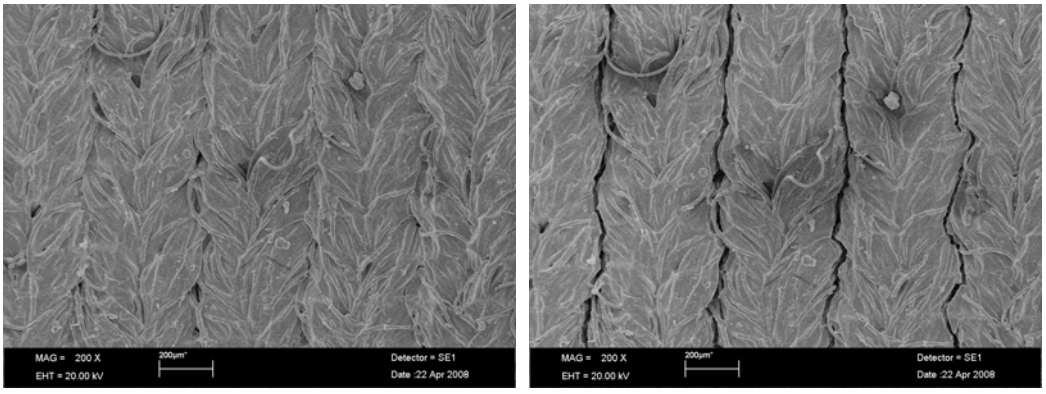

(a) (b)

Figure 4.13 SEM photographs of the knitted fabric (a) before and (b) after extension in the course direction

Due to the good elasticity of plain knitted fabric in both course and wale directions, the piezo-resistive behavior can be observed on both tensile directions after coated with CNP/SE/SO composite. Figure 4.14 depicts the typical stress-stain and electrical resistance-strain curves for the conductive fabric (9.0CNP) in two directions obtained from the electromechanical test. Both stress and resistance of the conductive fabric synchronous changed with tensile strain up to 100% without yield. For resistance-strain curves, the linearity of the conductive fabric at wale direction is much better than that of course direction during extension. Furthermore, the stress and electrical hysteresis at wale direction is much smaller than that of course direction, meaning that the wale direction is more appropriate as the working direction of the conductive fabric.

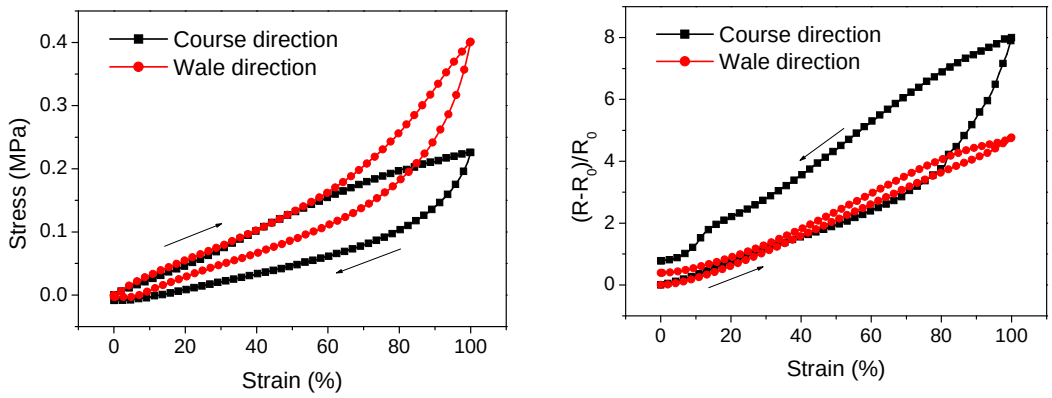

Figure 4.14 Typical (a) stress-strain and (b) resistance-strain curves of CNP/SE/SO coated conductive fabric in course and wale directions

Figure 4.15 shows the dependence of relative electrical resistance on tensile strain for the conductive fabrics of 4.5CNP, 9.0CNP and corresponding conductive composites extended in wale direction. The results show that the 4.5CNP conductive fabric has a higher sensitivity and a quick increase in sensitivity beyond the tensile strain of 40% compared to that of conductive composite with same CNP concentration, as shown in Figure 4.15 (a). For sample with higher CNP concentration, the linearity is much better for samples of 9.0CNP as shown in Figure 4.15 (b). The sensitivity of conductive fabric 9.0CNP is 4.76, which is about 2 times as that of conductive composite of 9.0CNP due to the non-uniform deformation behavior of the knitted fabric. The knitted structure, good linearity, suitable sensitivity and much larger working range of conductive fabric 9.0CNP make it suitable to be flexible strain gauges for smart textiles.

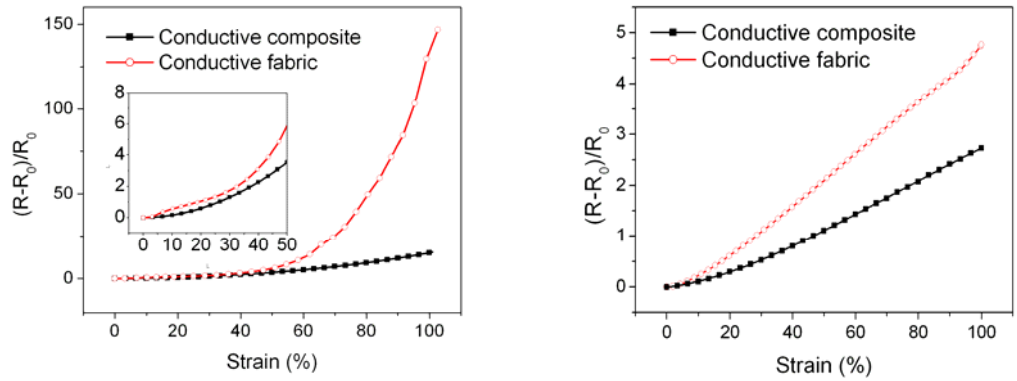

(a) (b)

Figure 4.15 Resistance change of conductive composites and corresponding conductive fabric with tensile strain for sample (a) 4.5CNP and (b) 9.0CNP

4.3.5 Effect of Mechanical Pretreatment on Stability

Figure 4.16 (a) shows the stress-strain and resistance-strain curves of a virgin conductive fabric as it was stretched to various strain levels with increased sequence. Typical irreversible curves for conductive fabrics can be found in Figure 4.16 (b), which cannot accurately reflect the strain level of the objectives. After mechanical treated with extension to 170% of its original length for 1 time, the conductive fabric shows a stable and repeatable mechanical and electrical response as strains lower than the pretreated one, as shown in Figure 4.17. The hysteresis of stress-strain curve and resistance-strain curve significantly decreased from 32.35% to 11.72% and from 17.58% to 5.55%, respectively, meaning that the mechanical pretreatment is effective to increase the stability and accuracy of the conductive fabric.

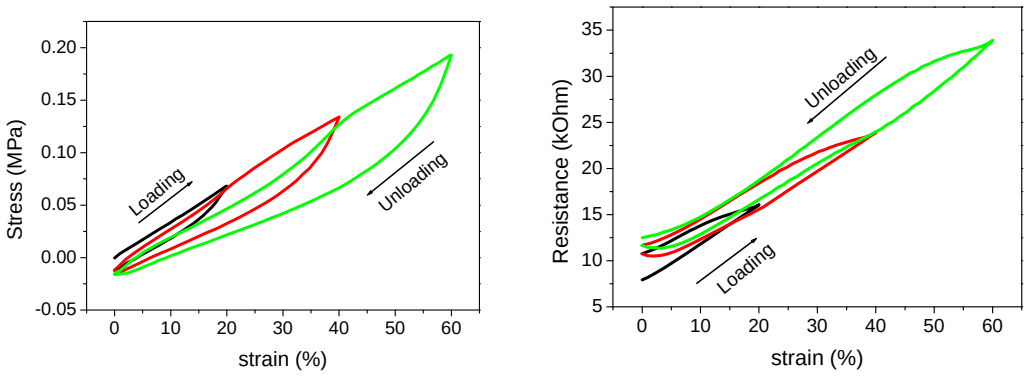

(a) (b)

Figure 4.16 (a) Mechanical and (b) electrical response of conductive fabric without mechanical pretreatment with sequence of increased strain levels. (The black, red and green colors stand for the maximum tensile strain is 20%, 40% and 60%, respectively)

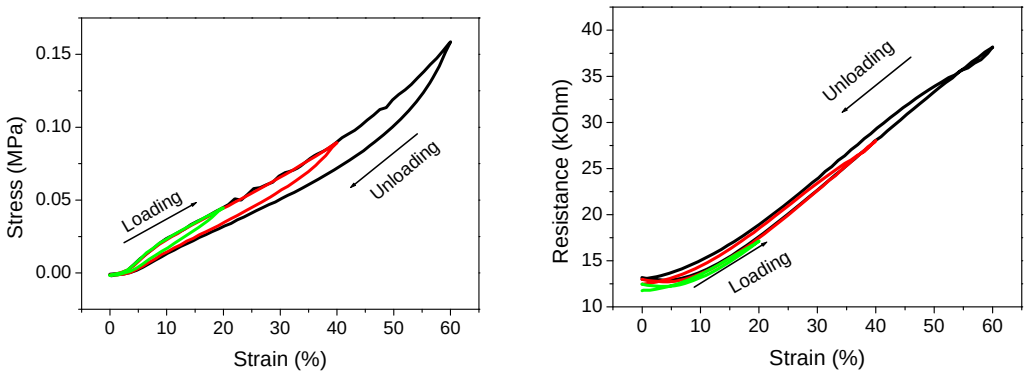

(a) (b)

Figure 4.17 (a) Mechanical and (b) electrical response of conductive fabric to various strains after mechanical pretreatment. (The black, red and green colors stand for the maximum tensile strain is 60%, 40% and 20%, respectively)

Figure 4.18 shows the fatigue resistance of conductive fabric to strain of 30% with and without mechanical pretreatment for 10,000 cycles. For the untreated one, the electrical resistance of conductive fabric slowly increased with repeated cycles, which is due to the irreversible structural change of the continuous conductive composite on knitted fabric.

After the mechanical pretreatment by applied a tensile strain beyond measuring range of the conductive fabric, there will be no more structure changes appeared, and the conductive fabric can resist more loading-unloading cycles. The fatigue properties of conductive fabric is much better than that of conductive composites for the good mechanical properties of knitted fabric that can resist the further destruction of conductive pathways of coated composite layer, while a little defect in conductive composite will result its continuous destruction in cyclic test, as described in Chapter 3.

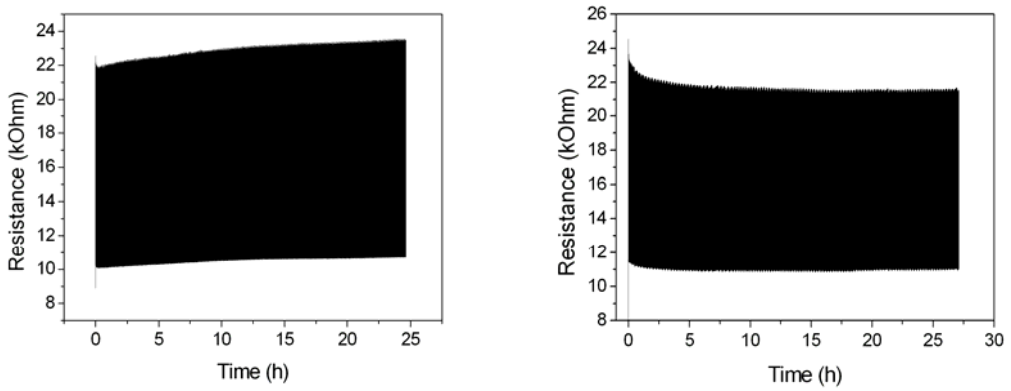

Figure 4.18 Fatigue test results of conductive fabric (a) without and (b) with mechanical pretreatment

4.3.6 Effect of Strain Rate

Figure 4.19 demonstrates a good linearity between strain and resistance within measuring range of 70% for the conductive fabric with a pre-extension of 10%. With the increase of loading speed from 12 mm/min to 2400 mm/min (corresponding to strain rate 0.02 to 4/s), the resistance of the conductive fabric increased, which can be reflected by the change in the slope of resistance-strain curves. The dependence of electrical resistance on strain rate has been observed for CNP filled elastomers [4-7] and PPy coated conductive fabric [8], even at a much smaller strain rate range from 10^{-4} to 10^{-1} /s. The effect of strain rate on resistance is related to the conductive network of composite on knitted fabric. When the

conductive fabric was extended, the continuous conductive pathways in composites will change and result in resistance change. During this process, relaxation of electrical resistance also appeared simultaneously, which compensate part of the disconnection of conductive pathways. The resistance relaxation behavior is time dependent and correspondingly related to strain rate. With the increase of strain rate, there is fewer time for resistance relaxation and the sensor shows a higher resistance. The sensor is viscoelastic material for both CNP filled elastomer and knitted fabric show viscoelasticity. The relationship between the resistance and the strain rate can be fitted with an exponential function (as shown in Figure 4.20):

$$R(x)=1.56-0.62e^{(-x/1.07)} \quad (4\text{-}1)$$

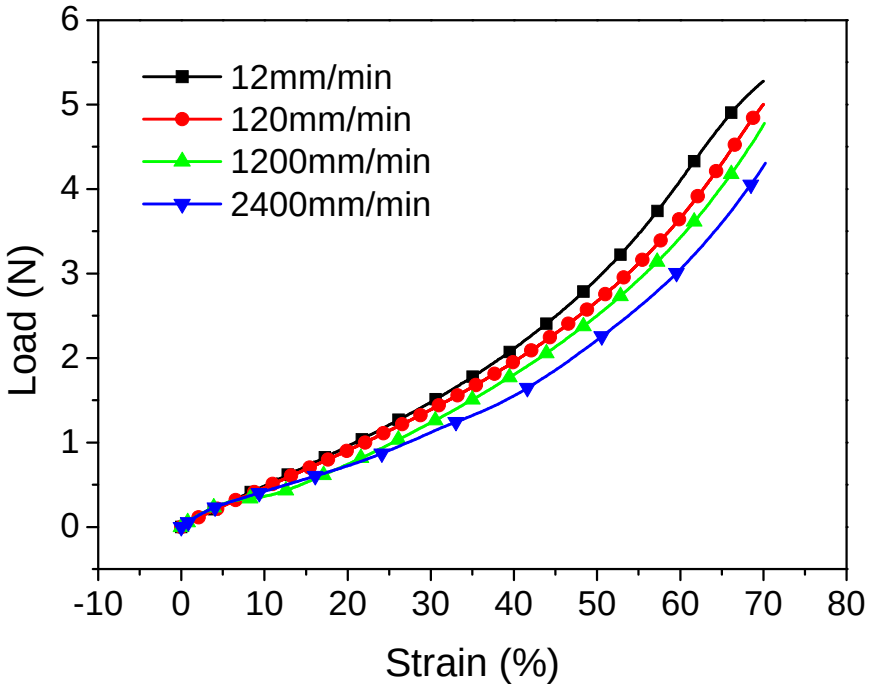

(a)

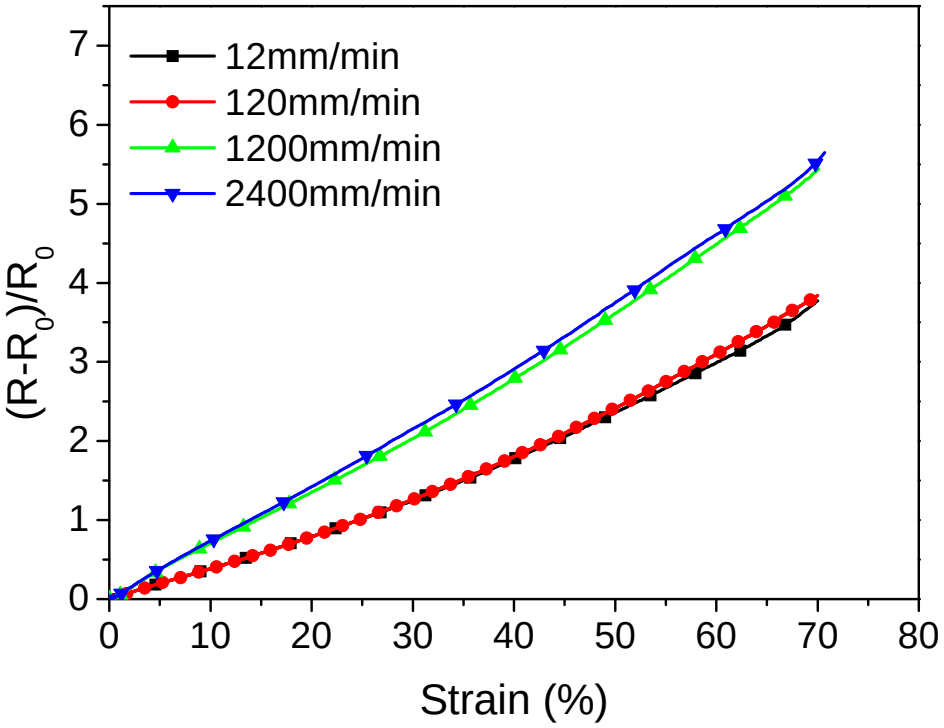

(b)

Figure 4.19 Effect of loading speed on (a) mechanical and (b) electrical behavior of the conductive fabric

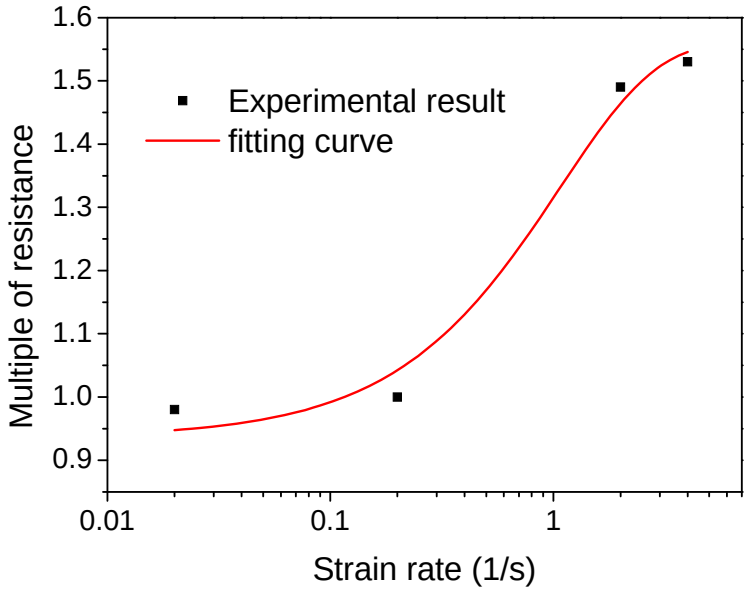

Figure 4.20 Multiple of resistance versus strain rate

4.3.7 Effect of Temperature

Figure 4.21 depicts the variation of relative resistance as a function of temperature for the conductive fabric (9.0CNP) and corresponding conductive composite. The resistance of the conductive fabric decreases as the temperature increases from 0 ^{0}C to 40 ^{0}C (the temperature coefficient of resistance is approximately -1.75 $^0C^{-1}\times10^{-3}$), and then increases from 40 ^{0}C to 60 ^{0}C (the temperature coefficient of resistance is approximately 1.2 $^0C^{-1}\times10^{-3}$). In CNP/SE/SO composite, the dependence of electrical resistance on temperature is due to the variation of conductive pathways, resulted from the competing between excitation/flocculation of electrons in the CNP particles and the different thermal expansion coefficient of SE and CNP. When temperature increases, the former one leads to the decrease of electrical resistance while the latter one leads to the increase of the distances between conductive domains, then increase of electrical resistance. For conductive fabric, the expansion of knitted fabric with the increase of temperature plays a similar role as that of resistance increase, result to the smaller resistance decrease in temperature from 0 ^{0}C to 40 ^{0}C and increase from 40 ^{0}C to 60 ^{0}C. The repeatability of the resistance-temperature curves is relatively good, demonstrates that the temperature effect can be compensated separately between 0-40 ^{0}C and 40-60 ^{0}C.

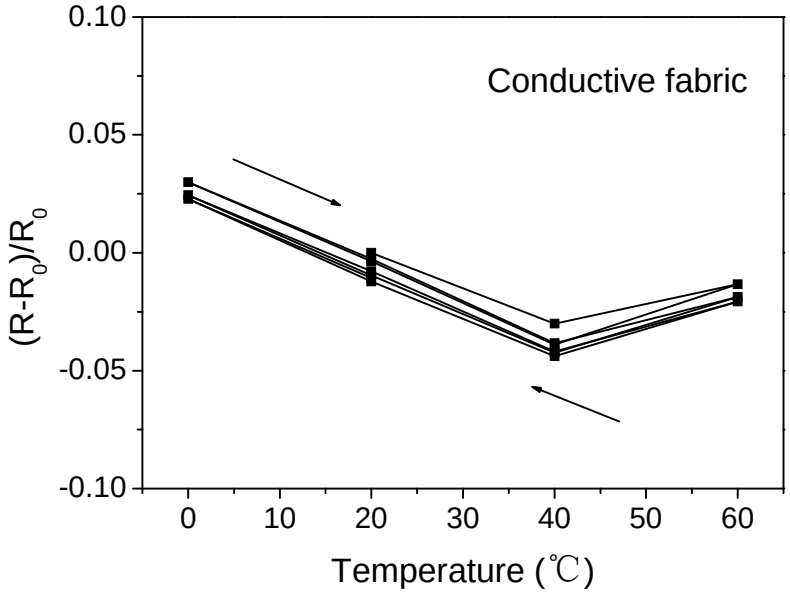

(a)

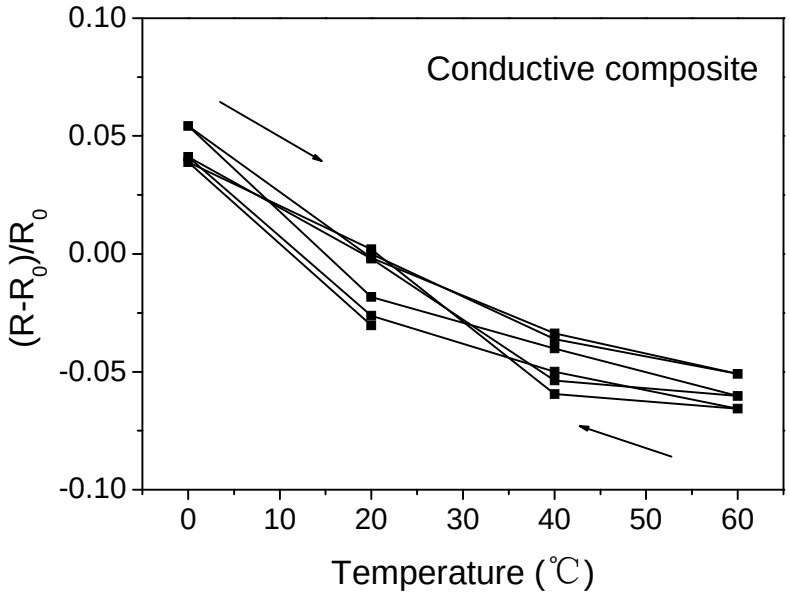

(b)

Figure 4.21 Dependence of relative resistance on temperature for the (a) conductive fabric and (b) conductive composite under cyclic measurement

Considering from the view point of application, the sensing performance of the conductive fabric should be characterized at different temperatures. Figure 4.22 shows a

three dimensional figure based on the variation of electrical resistance with tensile strain and temperature for the conductive fabric in the strain range between 0-30% and temperature range between 0-60 ^{0}C. At any given strain level, the increase of temperature plays a similar role as that of tensile strain for the conductive fabric, the variation of the whole resistance resulted from temperature is about 5%, corresponding to 5% strain.

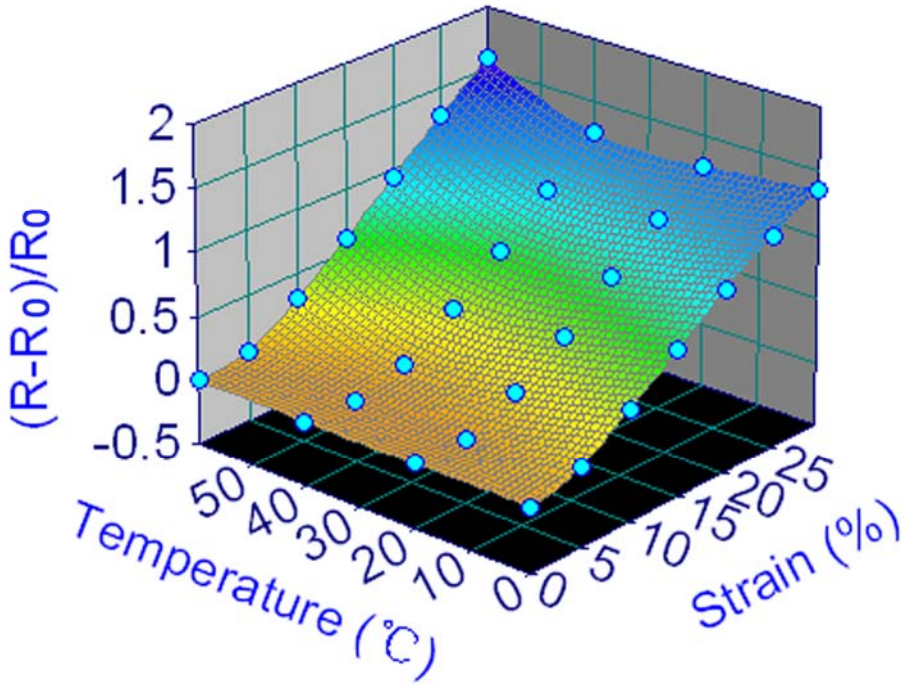

Figure 4.22 Dependence of electrical resistance on tensile strain and temperature for the conductive fabric (9.0CNP)

4.3.8 Effect of Humidity

The electrical resistance of the conductive composite is little affected by humidity, which is demonstrated in chapter 3 due to the water repellent property of SE and SO. Although the porous CNP is benefit for water absorption, most of them are embedded in the SE/SO matrix. For the conductive fabric, the dependence of electrical resistance on relative humidity is shown in Figure 4.23. When temperature is fixed at 20 ^{0}C, the electrical resistance of the conductive fabric first decreases and then increases as the humidity

increases from 20% to 90%. However, the whole resistance change in the humidity range is only 3%, which is little higher than that of conductive composite, but much smaller than that of thermoplastic elastomers (TPE)/CNP composite [9] and PPy coated fibers [8] of about 30%. Compared to the conductive composite, knitted fabric is more sensitive to humidity for the porous structure though water hydrophobic materials are used. However, the relatively small dependence of electrical resistance on humidity can be further reduced by waterproof packaging.

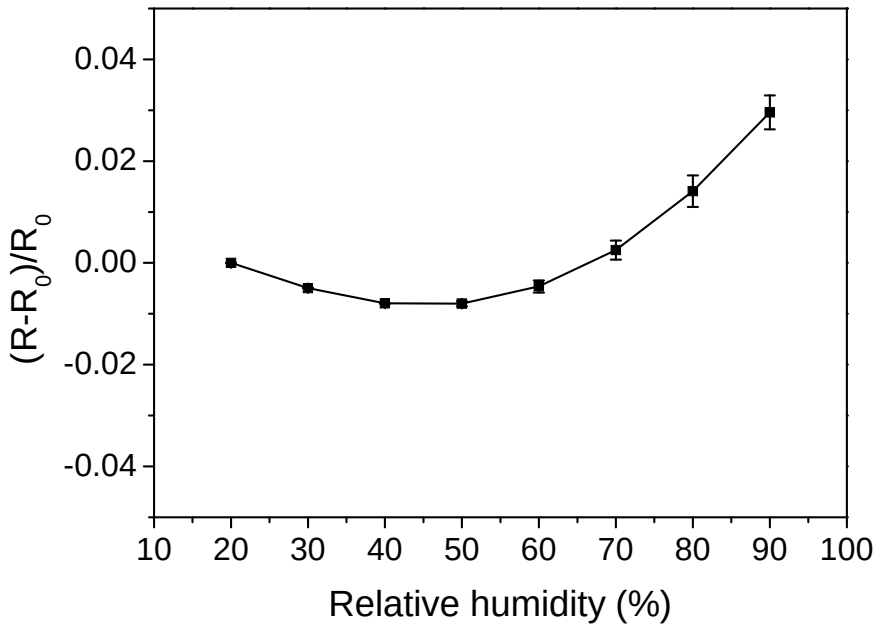

Figure 4.23 Dependence of electrical resistance on relative humidity for the conductive fabric

4.4 Conclusions

In this chapter, the strain sensing conductive fabrics were fabricated based on conductive CNP/SE/SO composites with CNP loading beyond percolation transition range and the fabrication parameters were optimized. I-V curves of the conductive fabrics are linear no matter they are extended or not, when the voltage is the range between ±1.0V/mm. The

frequency dependent impedance spectra demonstrates that the conductive fabric exhibit capacitive behavior under extension, which can be neglected for sample 9.0CNP at frequency lower than 10^3 Hz even with a stain of 60%. Quick loading of the conductive fabric exhibits that it has an instantaneous response as a load is applied. Due to the low modulus of knitted fabric, the modulus of the conductive fabric is still much smaller than that of human skin. Mechanical pretreatment has an obvious effect on the improvement of accuracy and stability of the conductive fabric. A strain rate dependent behavior can be observed for the conductive fabric; however, the dependence of electrical resistance on strain rate is predictable in the range of 0.02-4/s. Study of temperature and humidity effect on resistance of the conductive fabric demonstrate that the electrical resistance is compensable in temperature ranges of 0-60 ^{0}C, and resistance variation resulted from temperature is about 5%, corresponding to 5% strain, while the effect of humidity is only about 2% in humidity range of 20-90% due to the hydrophobic nature of the materials used in conductive fabric. The conductive fabric of 9.0CNP has better performances and will be used as sensing element of flexible strain sensor.

References

1. Mattmann, C., F. Clemens, and G. Troster, *Sensor for measuring strain in textile.* Sensors, 2008. **8**(6): p. 3719-3732.
2. Kost, J., M. Narkis, and A. Foux, *Resistivity Behavior of Carbon-Black-Filled Silicone-Rubber in Cyclic Loading Experiments.* Journal of Applied Polymer Science, 1984. **29**(12): p. 3937-3946.
3. Yamada, T., Y. Hayamizu, Y. Yamamoto, Y. Yomogida, A.I. Najafabadi, D.N. Futaba, et al., *A stretchable carbon nanotube strain sensor for human-motion detection.* Nature Nanotechnology, 2011.
4. Kost, J., M. Narkis, and A. Foux, *Effects of Axial Stretching on the Resistivity of Carbon-Black Filled Silicone-Rubber.* Polymer Engineering and Science, 1983. **23**(10): p. 567-571.
5. Das, N.C., T.K. Chaki, and D. Khastgir, *Effect of axial stretching on electrical resistivity of short carbon fibre and carbon black filled conductive rubber*

composites. Polymer International, 2002. **51**(2): p. 156-163.
6. Mattmann, C., O. Amft, H. Harms, and G. Troster. *Recognizing upper body postures using textile strain sensors*. in *11th International Symposium on Wearable Computers*. 2007. Boston, MA.
7. Cochrane, C., M. Lewandowski, and V. Koncar, *A Flexible Strain Sensor Based on a Conductive Polymer Composite for in situ Measurement of Parachute Canopy Deformation.* Sensors, 2010. **10**(9): p. 8291-8303.
8. Xue, P., X.M. Tao, K.W.Y. Kwok, M.Y. Leung, and T.X. Yu, *Electromechanical behavior of fibers coated with an electrically conductive polymer.* Textile Research Journal, 2004. **74**(10): p. 929-936.
9. Cochrane, C., V. Koncar, M. Lewandowski, and C. Dufour, *Design and development of a flexible strain sensor for textile structures based on a conductive polymer composite.* Sensors, 2007. **7**(4): p. 473-492.

CHAPTER 5
SENSOR PERFORMANCES AND SENSING MECHANISM

5.1 Introduction

Previous chapters investigated the conductive CNP/SE/SO composites and conductive fabrics, which are basic sensing elements of fabric strain sensors. In this chapter, the focus will be on the design and fabrication, performance evaluation and sensing mechanism of the packaged fabric strain sensors. We start from the sensor fabrication and packaging methods as well as characterization methods. Then, the performance characteristics such as strain sensitivity, working range, fatigue life, etc. will be systematically investigated. Finally, based on conductive behavior of CNP filled elastomer and strain distribution of knitted fabric, the sensing mechanism of the sensor will be examined.

5.2 Fabrication and Characterization of Fabric Strain Sensor

5.2.1 Experimental

5.2.1.1 Materials and Processing

Previously developed conductive fabric with sample code of 9.0CNP was used as sensing element for the strain sensor. Silver coated nylon yarn (70D/24F/2, Xiamen Unibest Import and Export Co., Ltd) was used as conductive connecting wire. Plain woven nylon fabric (Kin Hing Hang Textile Ltd., Hong Kong) with density of 3.94×3.54 ends/mm

and thickness of 0.3 mm was used. Thermoplastic polyurethane film with thickness of 0.1 mm was taken to combine the conductive and woven fabric together. Silicone elastomer (ELASTOSIL®LR3070 A and B, Wacker Chemie AG, Germany) was used as packaging material of the sensor. A polyester strain limit belt with width of 5mm was used to protect the fabric strain sensor from large strain beyond working range.

5.2.1.2 Sensor Design and Fabrication

After balanced at ambient temperature (20 ^{0}C and RH 65%) for 24 hours, the conductive fabric was connected with two parallel arranged silver coated nylon yarns using stitching method. To minimize contact resistance and to reduce resistance variation between conductive fabric and conductive yarns, a lab made conductive adhesive consisting of CNP and SE was coated on the conductive yarns, and the woven fabric was combined on backside of non-sensing unit of the sensor with thermoplastic polyurethane film to fix the conductive yarn and to reduce the resistance variation caused by conductive connection. To protect the fabric strain sensor from water and dust, abrasion damage, and increase the reliability of conductive connection and durability, packaging of the sensor is very essential. To address this, both sides of the fabric strain sensing element and conductive yarns were packaged with a thin silicone elastomer layer. To prevent over stretching of the sensing element, a non-stretchable belt was sewed onto the sensing fabric. The size of the sensing element between two conductive yarns is 10 mm×10 mm×0.55 mm. The key steps of fabrication process and the photograph of semi-product without the strain limitation belt are shown in Figure 5.1 and Figure 5.2, respectively.

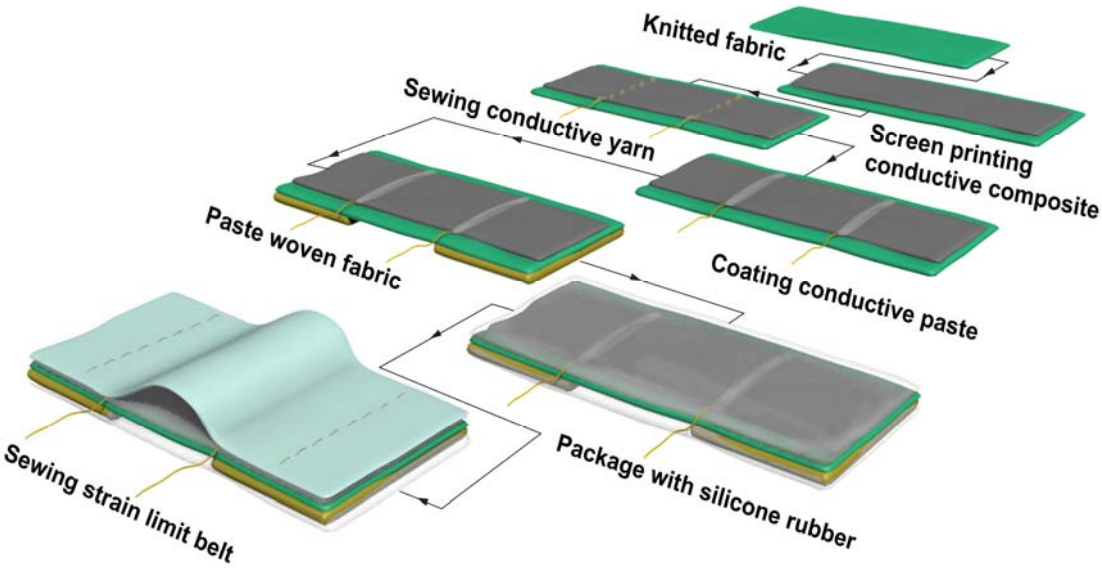

Figure 5.1 Fabrication process of the fabric strain sensor

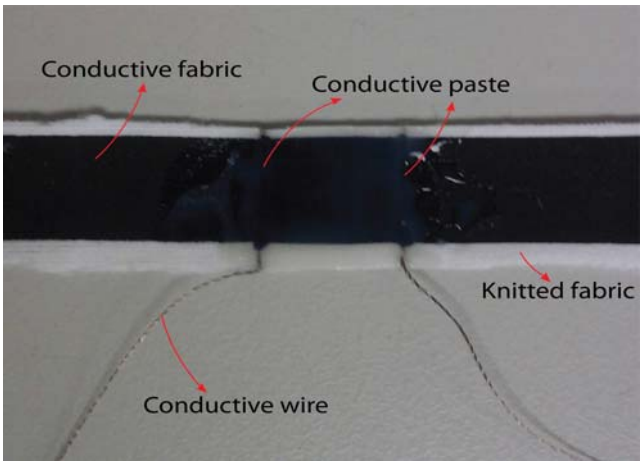

Figure 5.2 Photograph of the fabric strain sensor without strain limit belt

5.2.1.3 Characterization

The experimental setup for characterizing the electromechanical properties of the sensor is shown in Figure 5.3. Non-sensing part of the sensor at two ends was fixed by the clamps and the tensile strain and force were recorded by an Instron. Silver coated nylon yarns were connected to multimeter directly instead of the copper electrodes described in Chapter 4 for electrical resistance measurement. The data were coupled and treated by a computer.

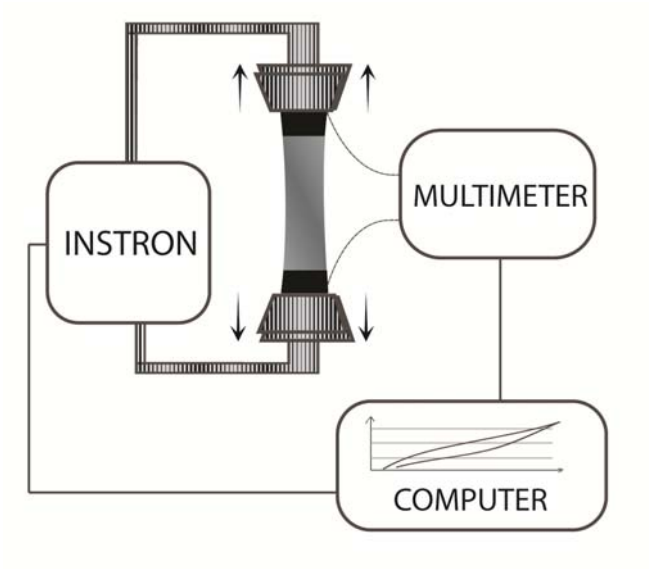

Figure 5.3 Experimental setup for coupled electromechanical measurement of fabric strain sensor

5.2.2 Results and Discussion

5.2.2.1 Modulus

As shown in Figure 5.4, the modulus of the fabric strain sensor increased from 0.51MPa to 0.68 MPa after packaged with SE, which is much higher than that of conductive composite. However, the modulus of the packaged strain sensor is still lower than that of human skin (about 1MPa), which can be used in smart textiles applications.

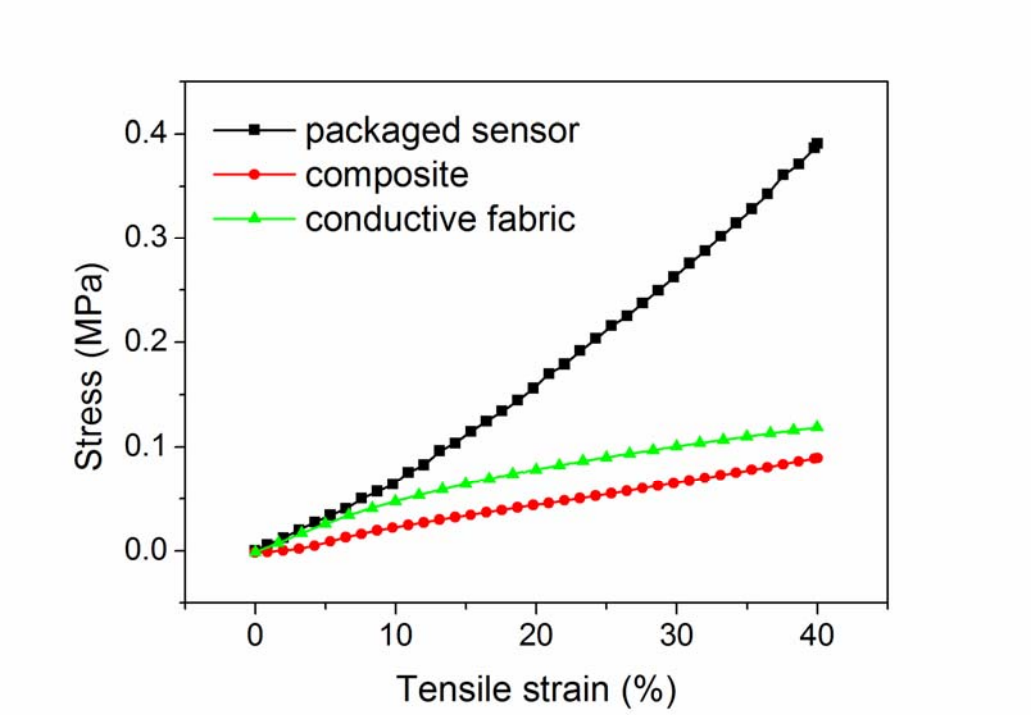

Figure 5.4 Stress-strain curves of the packaged fabric strain sensor, composite and conductive fabric

5.2.2.2 Strain Sensitivity

Figure 5.5 depicts the variation of electrical resistance as a function of tensile strain for the fabric strain sensor obtained from electromechanical test. The data of CNP/SE/SO composite and conductive fabric are also shown in the figure for comparison. The resistance-strain curve of packaged strain sensor coincides with that of conductive fabric within strain of 0-40%, and the slope of the curve in the range is about double compared to that of the conducive composite. With the further increase of tensile strain, the electrical resistance of the packaged strain sensor is higher than that of conductive fabric, which can be attributed to the additional pressure of SE applied on the sensing element of the sensor in the thickness direction, which increased the electrical resistance of the packaged sensor due to the piezoresistive behavior of conductive composite. The gauge factor of the package strain sensor calculated is 4.76 within the strain of 0-40%.

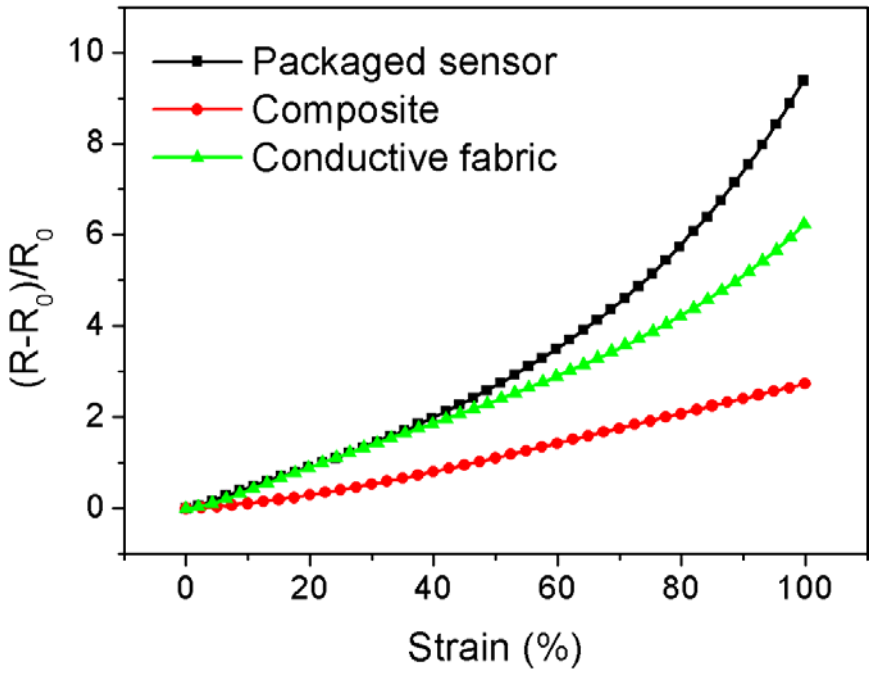

Figure 5.5 Electrical resistance versus tensile strain for packaged fabric strain sensor, conductive composite and conductive fabric.

5.2.2.3 Hysteresis

Figure 5.6 shows electrical resistance plotted as a function of tensile strain for the fabric strain sensor pretreated with 5 loading-unloading cycles to strain of 40%. The results show that with the increase of maximum tensile strain, the resistance exhibits good repeatability at various strain levels. The observed hysteresis of electrical resistance increased with maximum tensile strain and the maximum hysteresis is about 5.5% for the sensor with tensile strain of 40%. The hysteresis might be resulted from the viscosity of both CNP/SE/SO composite and knitted fabric between loading and unloading cycles, where certain time is needed to return from a transient position to balance position. The internal friction also adds to the time-independent component of the hysteresis.

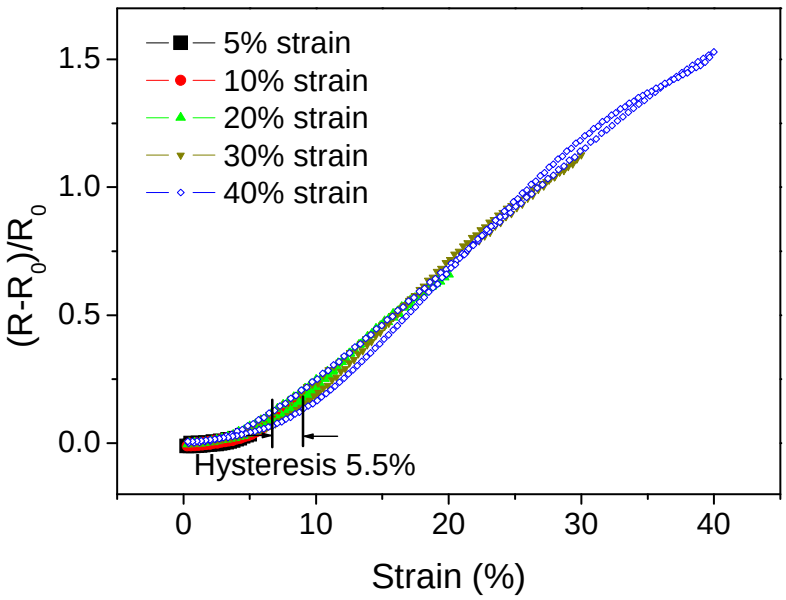

Figure 5.6 Hysteresis of the fabric strain sensor

5.2.2.4 Responding Time and Relaxation Behavior

Figure 5.7 shows the response of electrical resistance of the packaged fabric strain sensor as the applied tensile strain increases from 0 to 40% at a speed of 4/s, and then kept constant. The peak in resistance is lag to that of strain by 0.015s, demonstrating that the fabric strain sensor is able to response in some dynamic sensing applications in smart textiles.

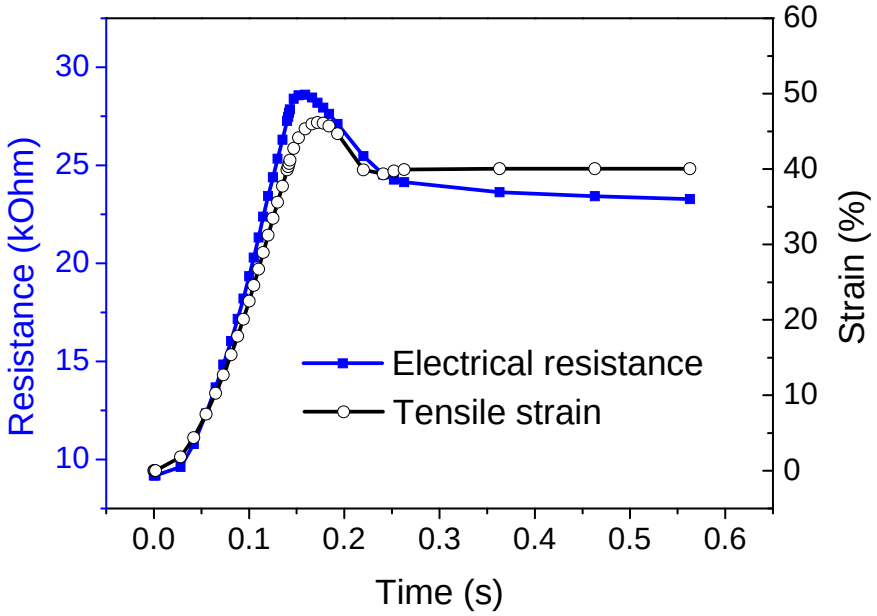

Figure 5.7 Responding time of the fabric strain sensor in response to a function of tensile strain (constant strain up to 40%).

Figure 5.8 shows the variation of electrical resistance with time for the fabric strain sensor subject to tensile strain of 10%, 20%, and 40%, respectively, when the loading speed is 0.1 /s. The resistance has a time-dependent relaxation behavior. The relaxation takes about 11.5 s to reach equilibrium when the tensile strain is 10%, and the relative resistance decrement is 4.46%. With increase of tensile strain, the equilibrium time increases to 13.4 and 24.8 s for strain of 20% and 40%, respectively, and the relative resistance reduction is about 3.57% and 5.56%, respectively.

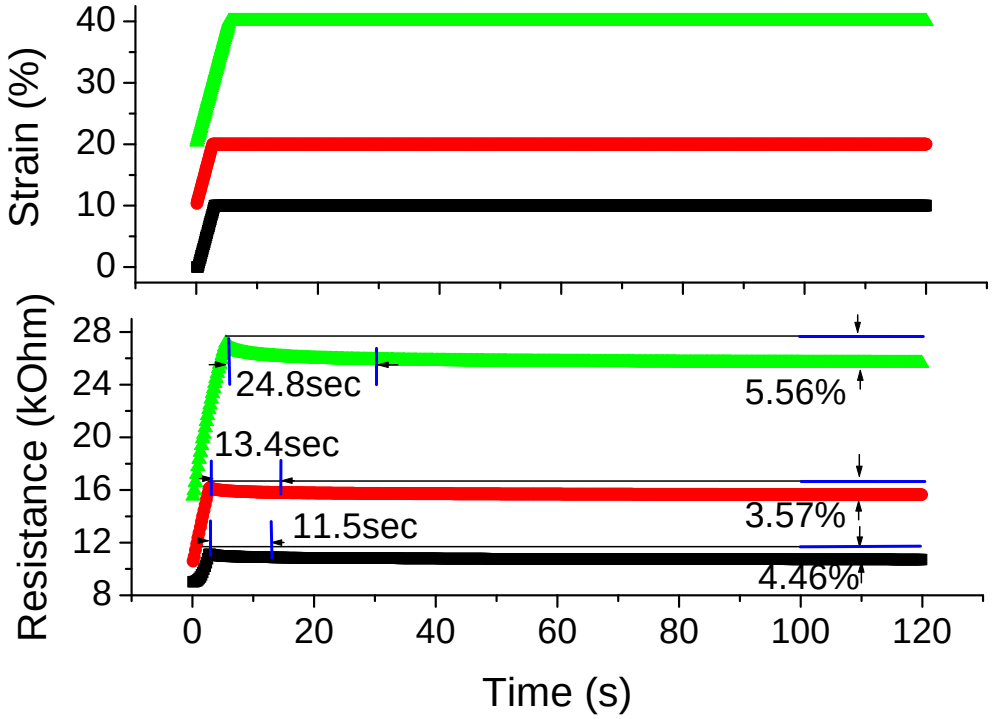

Figure 5.8 Relaxation behavior of the fabric strain sensor subject to various tensile strains

5.2.2.5 Fatigue Life

Cyclic straining at reasonably high strain levels, most strain sensors will reach their fatigue life limit when their electrical resistance irreversibly increase with strain cycles and produce a positive zero shift or completely open-circuit. The highest fatigue life of 10^8 cycles can be achieved for iso-elastic alloy based strain sensor; however, its strain level is only about 0.2%. Comparing to the low strain levels of most metal and foil strain sensors, the fabric strain sensor survives as shown in Figure 5.9 with more than 10^5 times at strain of 30%. The first reported high fatigue life at this strain level means that the sensors can be used for long-term health monitoring. For metal foil strain gauges, with the increase of strain cycles, cracks usually appear at the edges first and then gradually expand across the whole sensor width. These cracks exhibiting on the sensor produce an apparent increase in sensitivity due to the opening and closing of cracks, contributed to irreversible resistance changes. However, the strain sensor based on CNP/SE/SO

composite coated knitted fabric has excellent elasticity, which can endure large repeated strain cycles without cracks if the tensile strain is limited in its elastic range. Furthermore, even cracks appear at very high strain levels, the structure of knitted fabric can prevent further expansion of the cracks, which means in cyclic measurement, the fabric strain sensor can work stably after a pretreatment with strain beyond the working strain level.

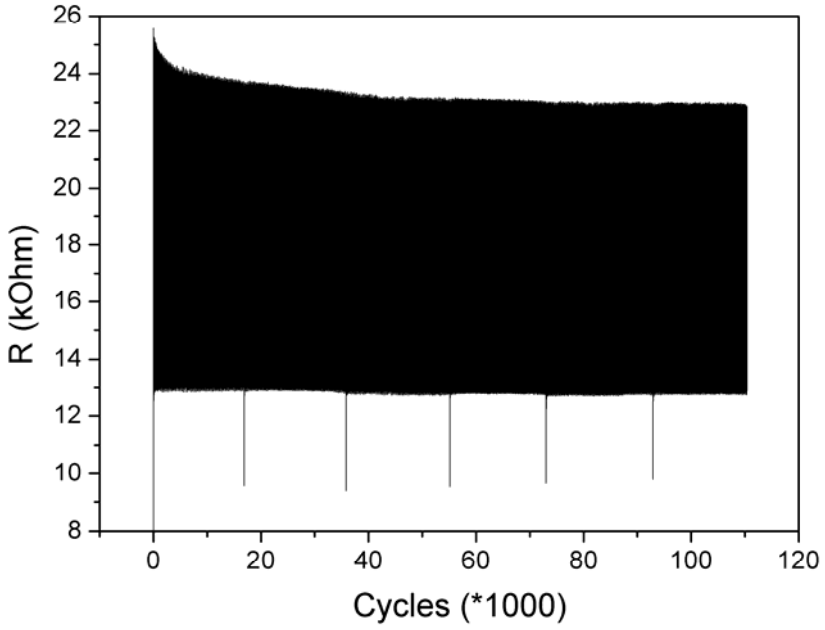

Figure 5.9 Fatigue life of the fabric strain sensor

5.3 Sensing Mechanism of the Fabric Strain Sensor

The sensing unit of the fabric strain sensor is the conductive fabric, consisting of a knitted fabric as the supporting layer and the conductive composite as the conductive layer. The electrical resistance of the conductive fabric increases when it is stretched due to the extension of the conductive composite. Different from the pure conductive composite, the deformation behavior of the supporting knitted fabric influences the strain distribution of the conductive layer obviously. To study the sensing mechanism of fabric strain sensor, the strain distribution in the knitted fabric and conductive fabric under tensile extension

as well as the conductive mechanism of CNP/SE/SO composite are considered.

5.3.1 Deformation Behavior of Knitted Fabric under Unidirectional Extension

Viewing from the face side, the knitted fabric consists of loop stems. Two loop stems in a knitted loop can be simplified to be a unit cell and many of them are connected in serial and parallel to form a network as shown in Figure 5.10.

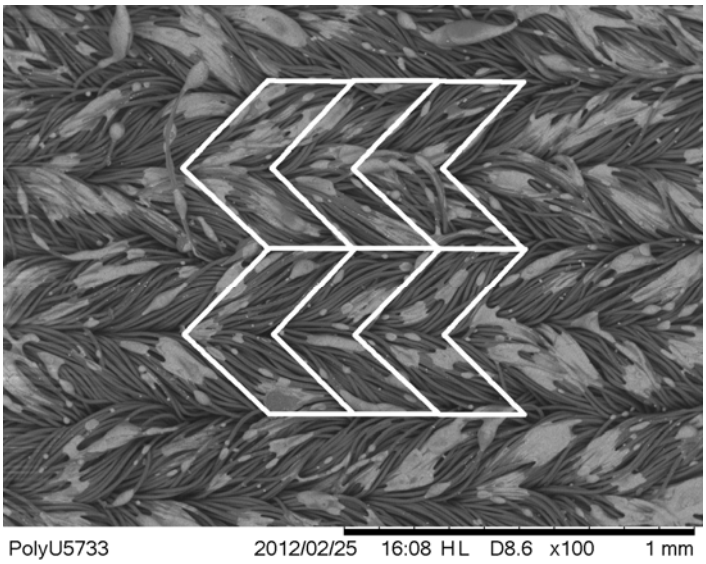

Figure 5.10 Structure of knitted fabric and simplified unit cell network

To examine the strain distribution of the knitted fabric under extension, digital image correlation analysis (DIC) method [1-5] was used. Black particles were spray onto the knitted fabric to form marking speckles; images of knitted fabric under different levels of strains were taken by digital camera on an optical microscopy. The contour maps of strain distribution in specimen surface subject to various tensile strains along wale (X) direction (exx in the figure stands for the strain along the X axis) were obtained and calculated through Lagrangian finite strain tensor (it is a finite strain measure which includes higher order displacement terms and was commonly used for materials undergoing large strains) by the Vic-2D software (Correlated Solutions, Inc.) and shown in Figure 5.11. The

corresponding strain distribution curves along the extension direction at two positions of the loops are shown in Figure 5.12. The knitted fabric does not uniformly deform under unidirectional extension along the wale direction, but many repeated unit cells with similar strain distribution behavior can be observed. In each unit cell, gradient strain distribution with the lowest strain in the middle part of the unit cell and highest at the edge of the unit cell can be observed. With the increase of effective tensile strain, the difference in strain level between middle and edge part of the unit cell is more obvious, and the local strain between two adjacent unit cells is much larger than the effective fabric strain, which is due to the domination of yarn transfer from loops to stems when the knitted fabric deforms in its elastic range.

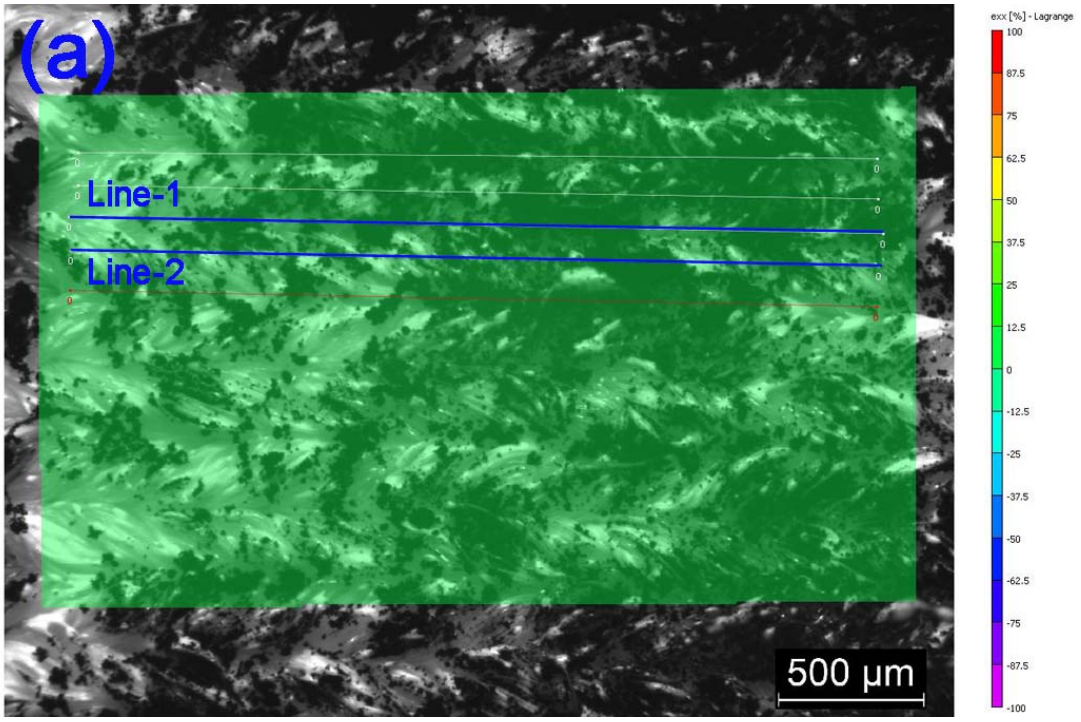
(a)
Line-1
Line-2
500 µm
exx [%] - Lagrange
100
87.5
75
62.5
50
37.5
25
12.5
0
-12.5
-25
-37.5
-50
-62.5
-75
-87.5
-100

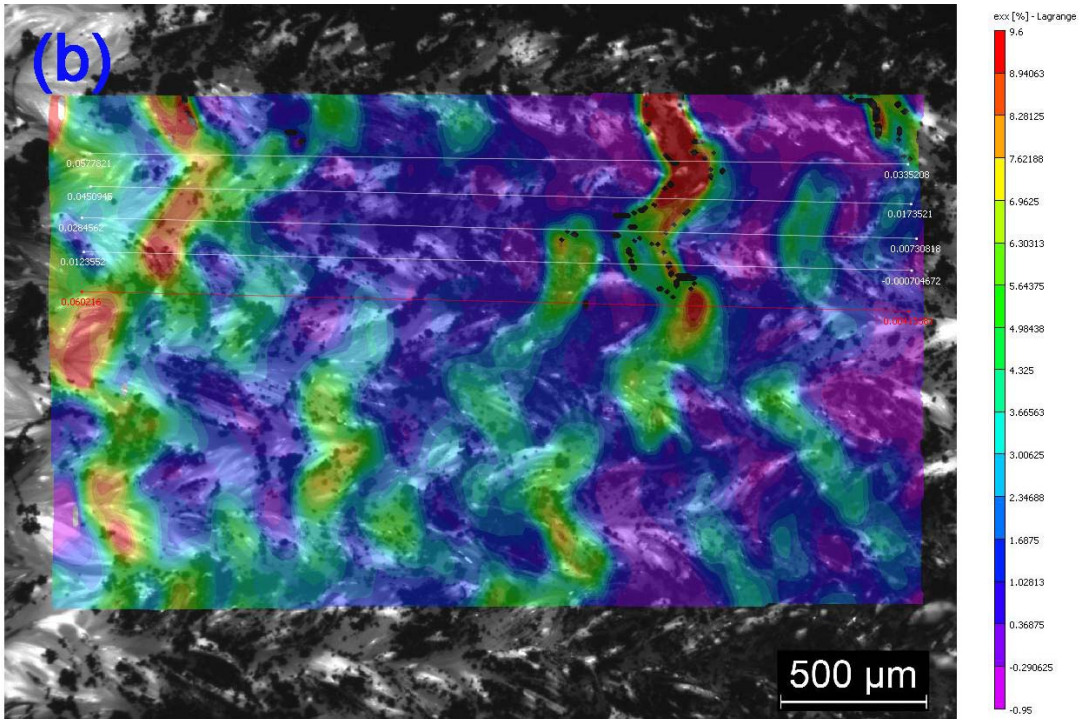
(b)
0.0577621
0.0450945
0.0284562
0.0123552
0.050216
0.0335208
0.0173521
0.00730818
-0.000704672
500 µm
exx [%] - Lagrange
9.6
8.94063
8.28125
7.62188
6.9625
6.30313
5.64375
4.98438
4.325
3.66563
3.00625
2.34688
1.6875
1.02813
0.36875
-0.290625
-0.95

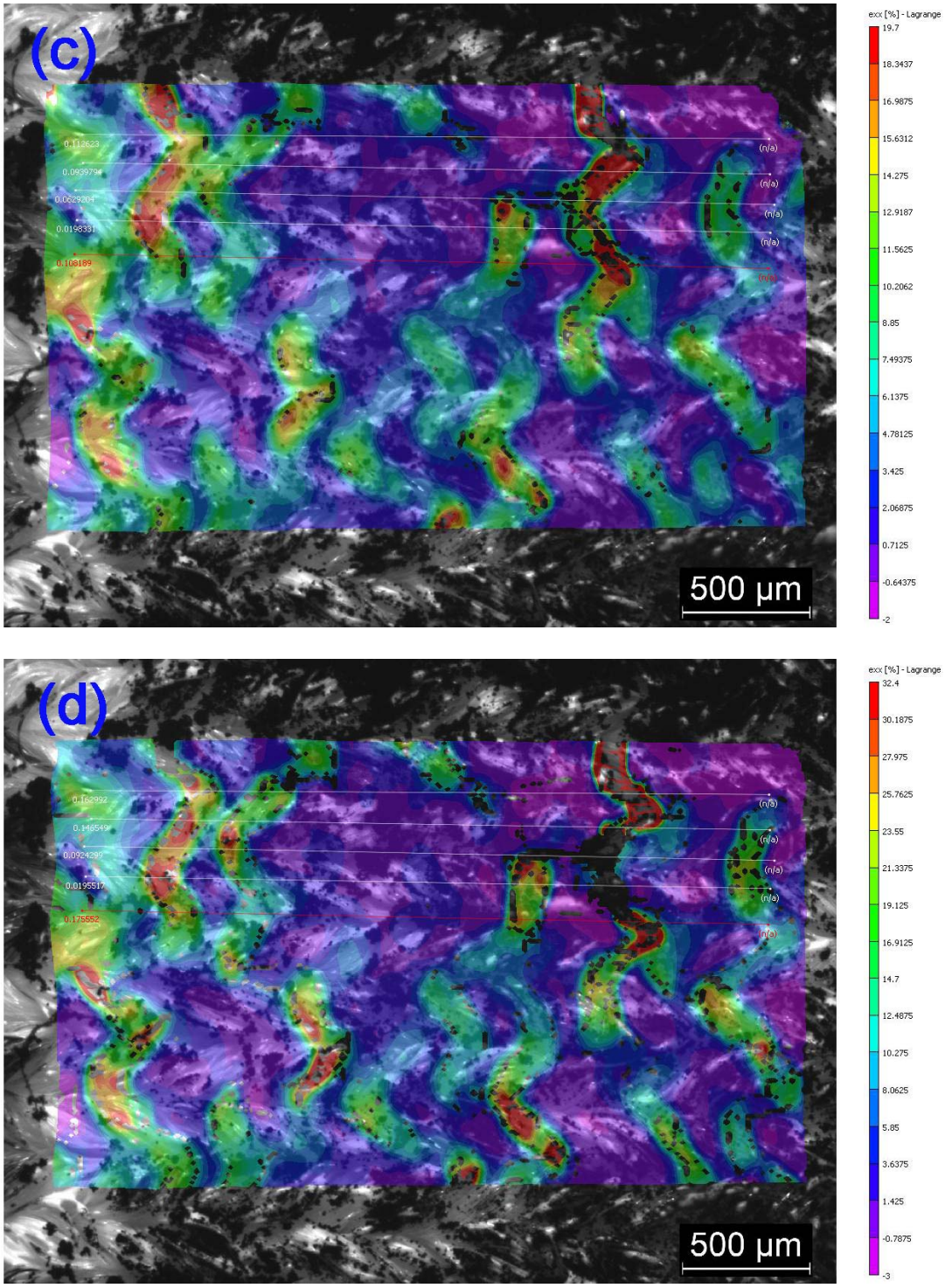

Figure 5.11 Contour strain maps of knitted fabric extended in wale direction with effective fabric strain of (a) 0%, (b) 3.125%, (c) 6.25% and (d) 9.375%, respectively.

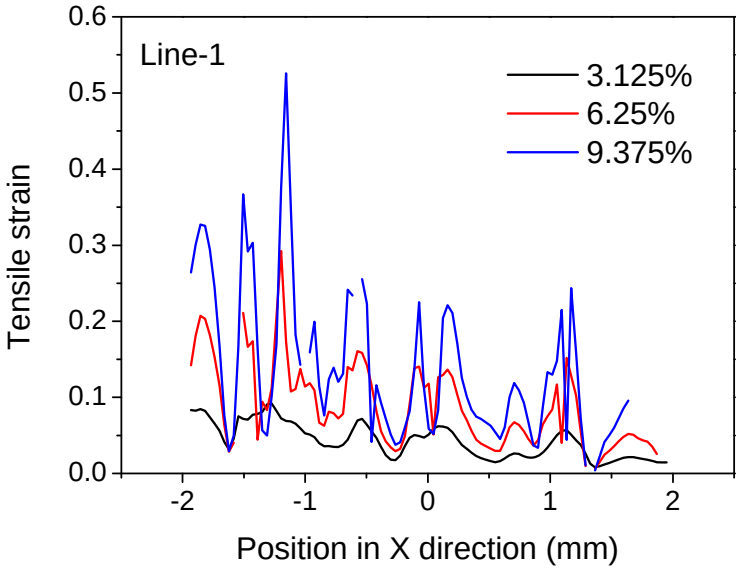

(a)

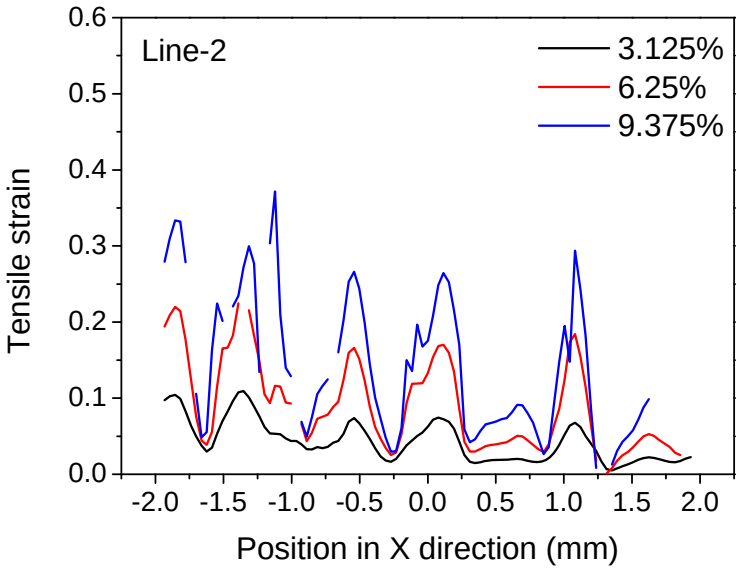

(b)

Figure 5.12 Spatial strain distribution of knitted fabric extended in wale direction at various effective fabric strain levels. (a) line 1 and (b) line 2. (The position of the two lines is shown in Figure 5.11)

5.3.2 Conductive Mechanism of CNP/SE/SO Composites under Extension

The experimental results shown in Chapter 3 have demonstrated that the bonds between SE matrix and conductive CNPs are much stronger than that between CNPs at extension, which contributed to the good reversibility of the composites in terms of both mechanical and electrical properties. The equivalent electrical resistance of the conductive composites is the function of resistance of CNPs, SE matrix and volume fraction of CNPs. Compared to conductive CNPs, the electrical resistance of the SE is so large that the equivalent resistance of the composites mainly composes of the tunnel resistance between conductive domains if the distance between them is short enough for current to flow through.

According to the model derived in reference [6], the equivalent electrical resistance R of the conductive composite based on tunneling current [7] is calculated as:

$$R = \left(\frac{L}{N}\right)\left[\frac{8\pi hs}{3a^2\gamma e^2}\exp(\gamma s)\right] \tag{5-1}$$

Where R is the equivalent resistance of the composite; L is the number of conductive particles forming a single conductive path parallel to the conductive direction; N is the number of conductive pathways; h is the Plank's constant; s is the least distance between conductive particles or domains; a^2 is the effective cross-sectional area in which the tunneling current passes through; e is the electron charge, and γ is calculated as:

$$\gamma = \frac{4\pi}{h}\sqrt{2m\varphi} \tag{5-2}$$

where m is the electron mass and φ is the height of potential barrier between adjacent conductive particles.

If the conductive composite is stretched, the electrical resistance will be changed due to the change in distances between conductive particles or domains. Assuming the distance between conductive particles or domains changes from s_0 to s, then the relative electrical resistance ($(R - R_0)/R_0$) is given by:

$$\frac{R - R_0}{R_0} = \left(\frac{s}{s_0}\right)\exp\left[\gamma\left(s - s_0\right)\right] - 1 \tag{5-3}$$

where R_0 is the initial resistance and s_0 the initial distance between particles, respectively. As the modulus of CNP is much higher than that of SE, and the distance change under extension is mainly from the deformation of SE, then the distance s can be calculated as:

$$s = s_0\left(1 + \varepsilon\right) \tag{5-4}$$

where ε is the tensile strain of the conductive composite. Substitute Eq. 5-4 into Eq. 5-3 yields:

$$\frac{R - R_0}{R_0} = \left(1 + \varepsilon\right)\exp\left(A_0\varepsilon\right) - 1 \tag{5-5}$$

where $A_0 = \gamma s_0$. The fitting of the experimental data for 9.0CNP conductive composite to Eq. 5-5 is shown in Figure 5.13. It can be seen that the fitting curve based on the model agrees well with the experimental data at A_0=0.6568 with coefficient of correlation of 0.996.

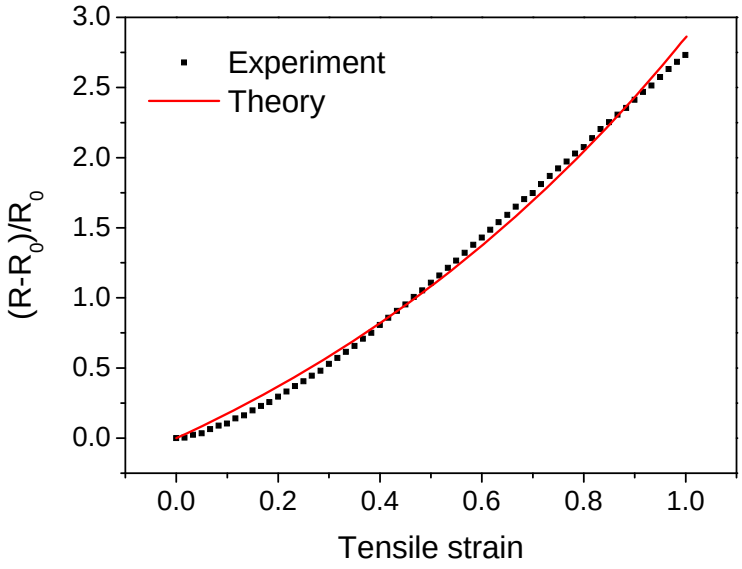

Figure 5.13 Fit of relative resistance-strain curve for 9.0CNP conductive composite based on the theoretical model.

5.3.3 Deformation Behavior of Conductive Fabric under Extension

The non-uniform deformation of knitted fabric affects strain distribution of the conductive composite when it was coated on the knitted fabric. The contour strain maps of conductive fabric with various tensile strains are shown in Figure 5.14. The strain distributions of the conductive fabric along tensile direction at five locations are demonstrated in Figure 5.15. Due to the good adhesion between knitted fabric and conductive composite, the obvious non-uniform strain distribution of knitted fabric in one unit cell at various effective tensile strains is partly compensated. However, the conductive fabric still shows similar strain distribution as that of the knitted fabric.

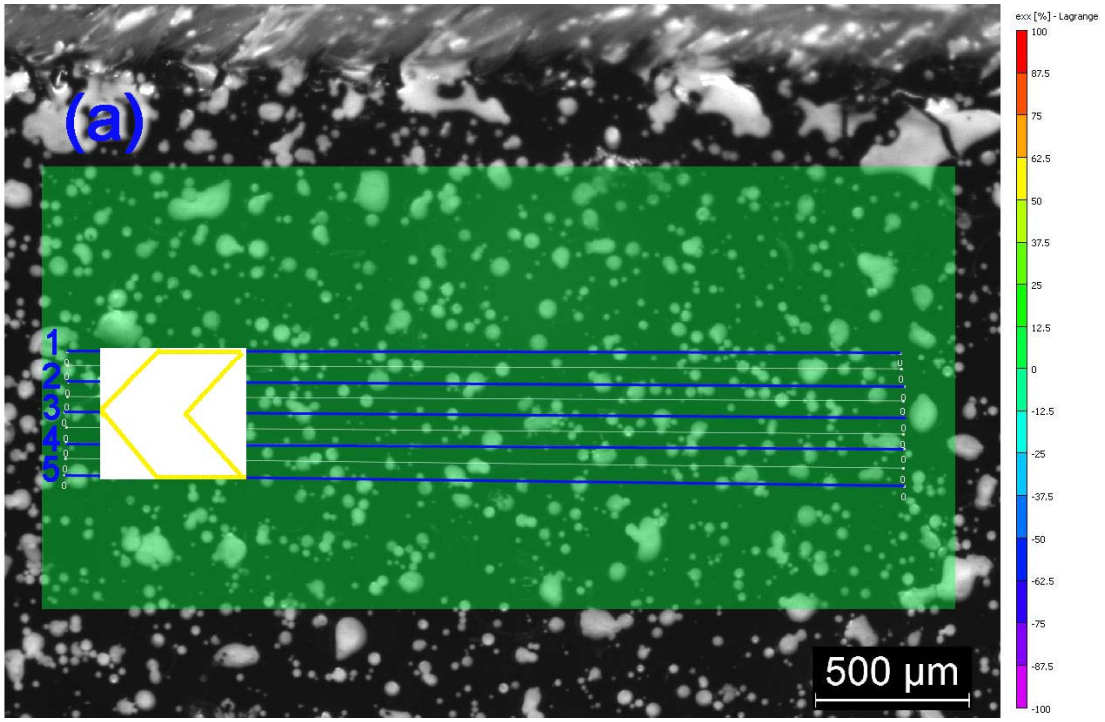
(a)
1
2
3
4
5
500 µm
exx [%] - Lagrange
100
87.5
75
62.5
50
37.5
25
12.5
0
-12.5
-25
-37.5
-50
-62.5
-75
-87.5
-100

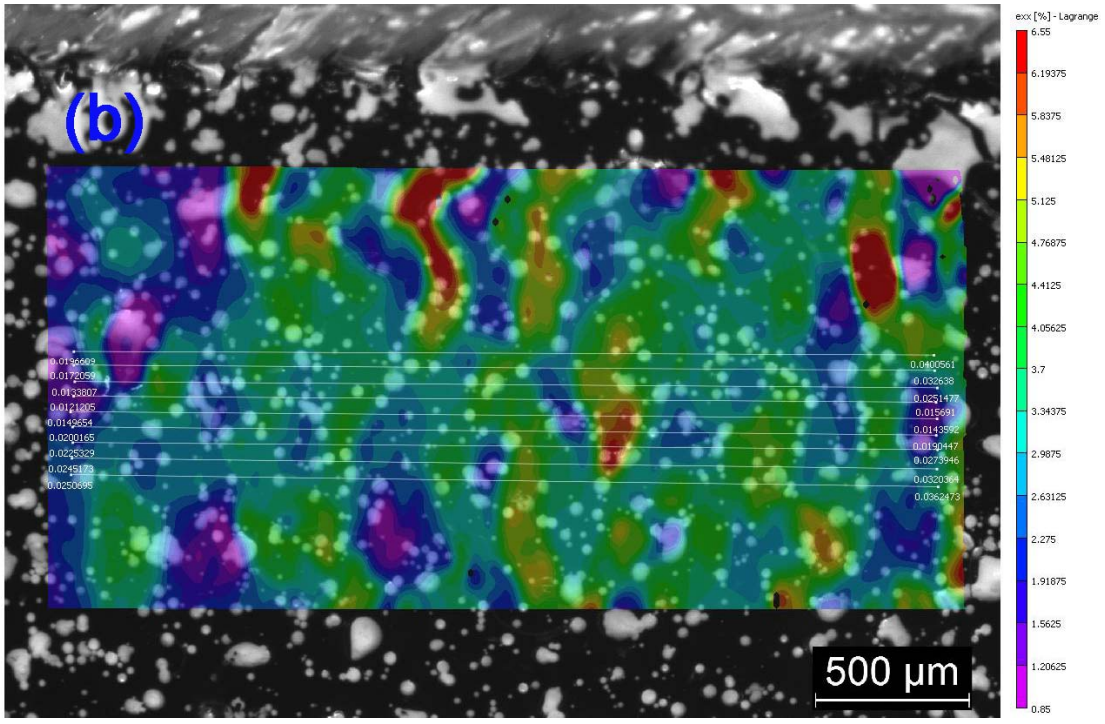
(b)
500 µm
exx [%] - Lagrange
6.55
6.19375
5.8375
5.48125
5.125
4.76875
4.4125
4.05625
3.7
3.34375
2.9875
2.63125
2.275
1.91875
1.5625
1.20625
0.85

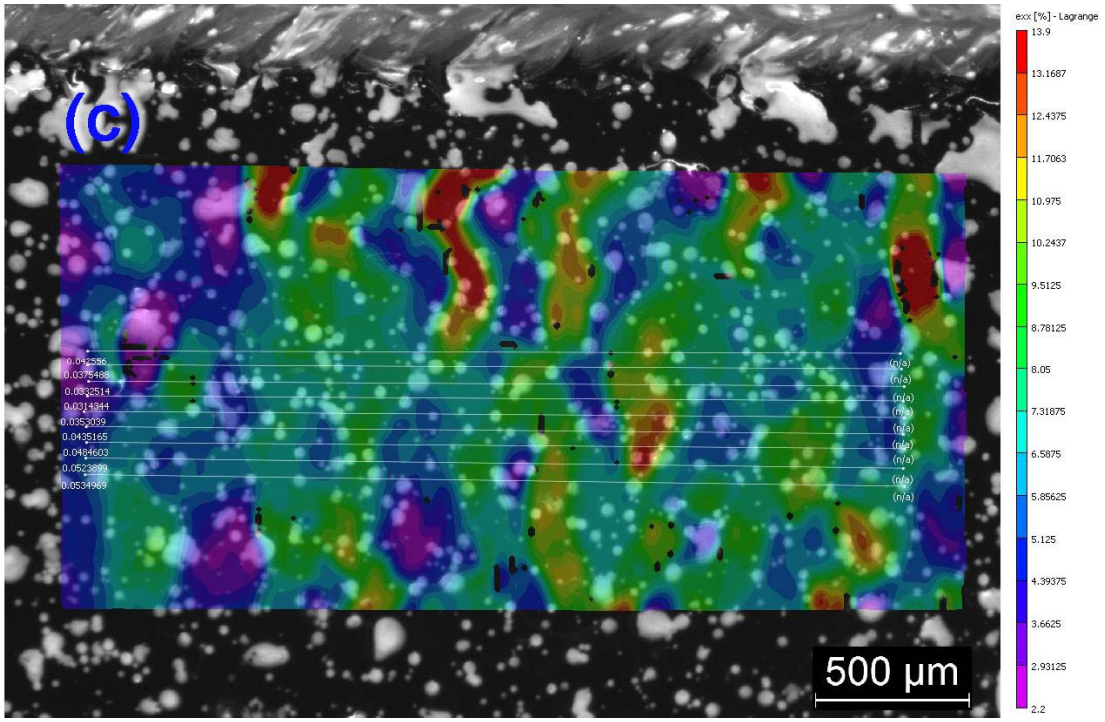
(c)
exx [%] - Lagrange
13.9
13.1687
12.4375
11.7063
10.975
10.2437
9.5125
8.78125
8.05
7.31875
6.5875
5.85625
5.125
4.39375
3.6625
2.93125
2.2
0.042556
0.0375488
0.0325514
0.0314344
0.0353039
0.0435165
0.0484603
0.0523899
0.0534969
(n/a)
500 µm

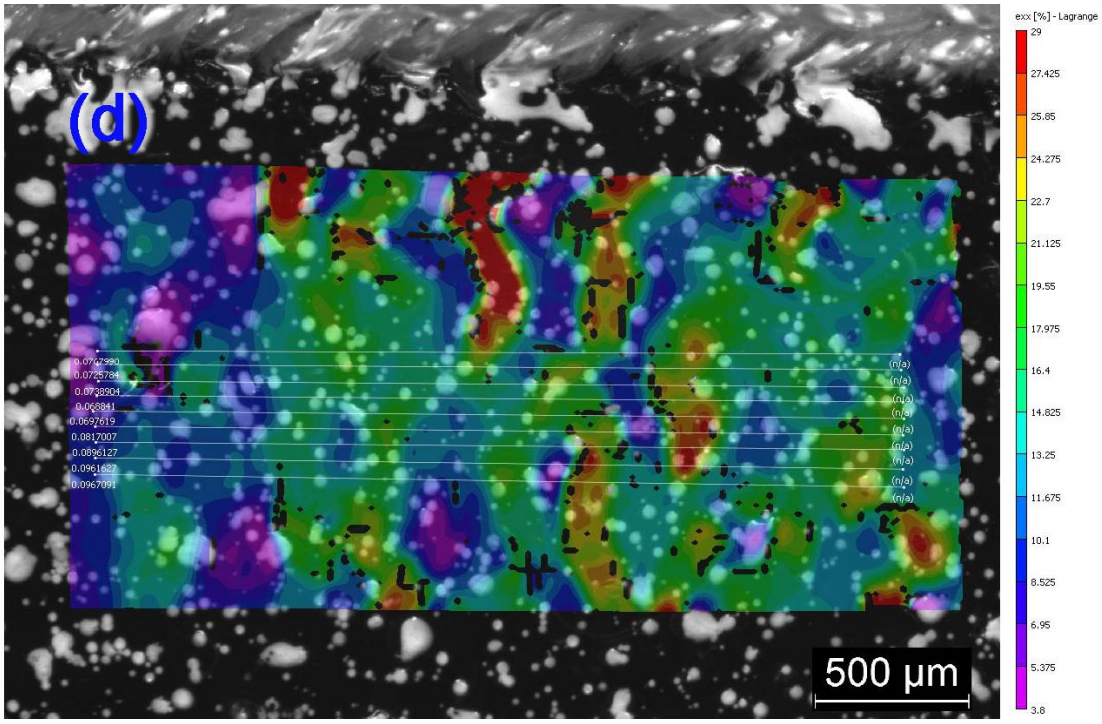
(d)
exx [%] - Lagrange
29
27.425
25.85
24.275
22.7
21.125
19.55
17.975
16.4
14.825
13.25
11.675
10.1
8.525
6.95
5.375
3.8
0.0717990
0.0725784
0.0738904
0.0638841
0.0697619
0.0817007
0.0896127
0.0961627
0.0967091
(n/a)
500 µm

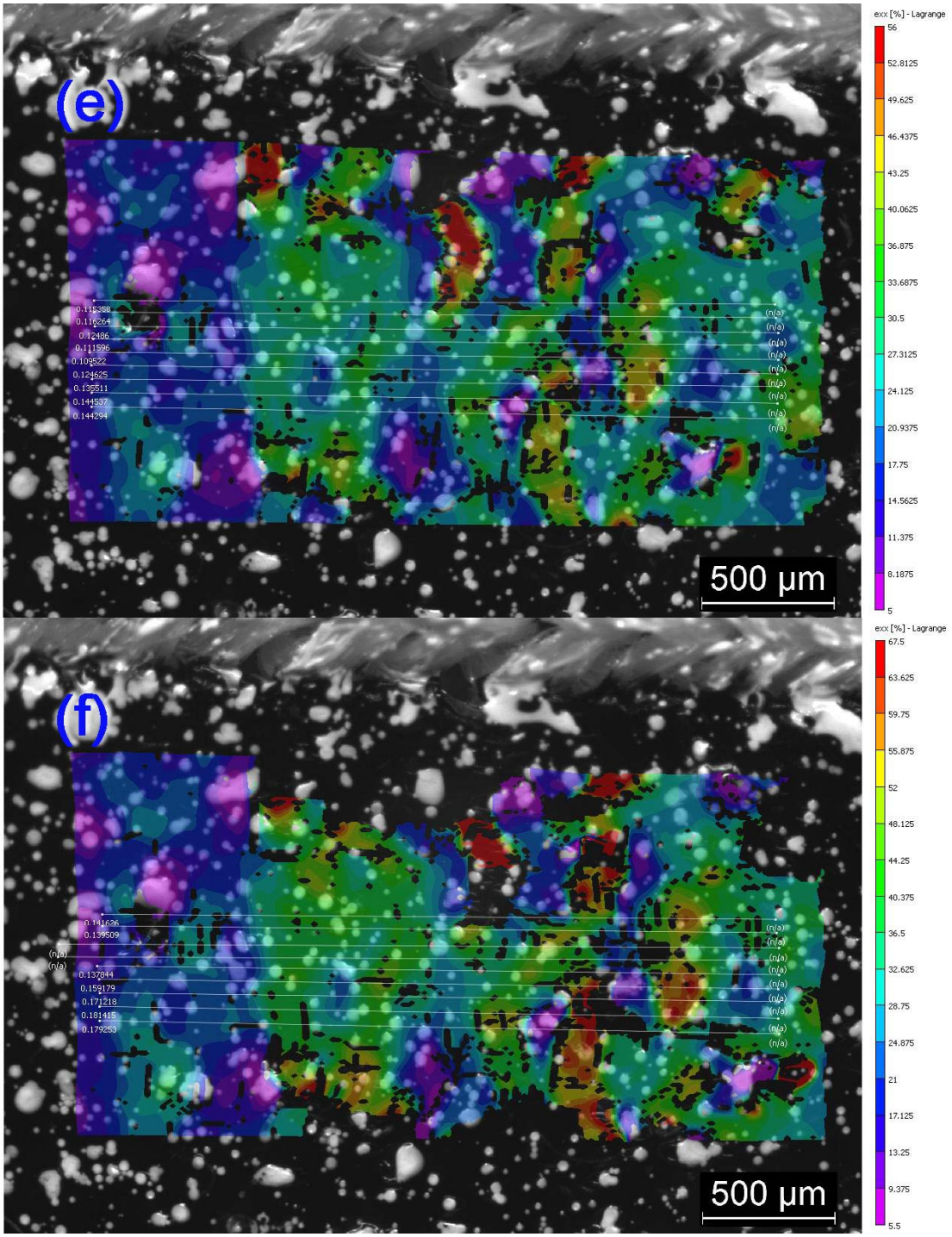

Figure 5.14 Contour strain maps of conductive fabric extended in wale direction with effective tensile strain of (a) 0%, (b) 5%, (c) 10%, (d) 20%, (e) 32.5% and (f) 42.5%, respectively.

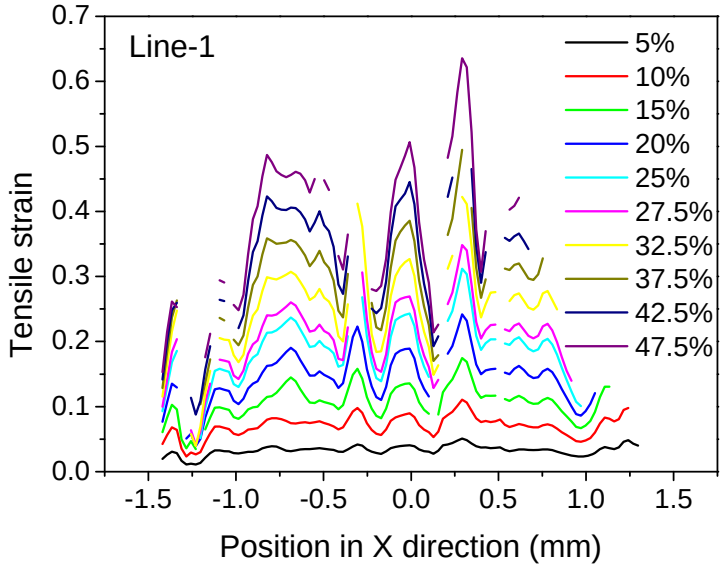
Line-1
Tensile strain
Position in X direction (mm)
5%
10%
15%
20%
25%
27.5%
32.5%
37.5%
42.5%
47.5%
0.0
0.1
0.2
0.3
0.4
0.5
0.6
0.7
-1.5
-1.0
-0.5
0.0
0.5
1.0
1.5

(a)

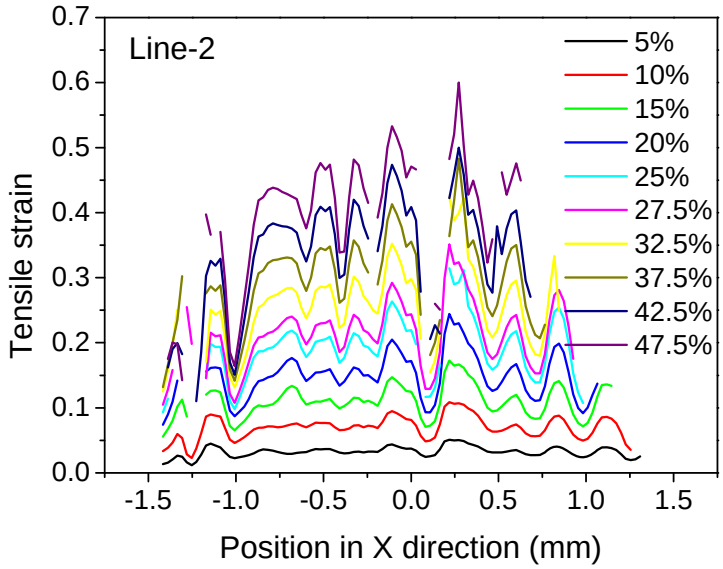
Line-2
Tensile strain
Position in X direction (mm)
5%
10%
15%
20%
25%
27.5%
32.5%
37.5%
42.5%
47.5%
0.0
0.1
0.2
0.3
0.4
0.5
0.6
0.7
-1.5
-1.0
-0.5
0.0
0.5
1.0
1.5

(b)

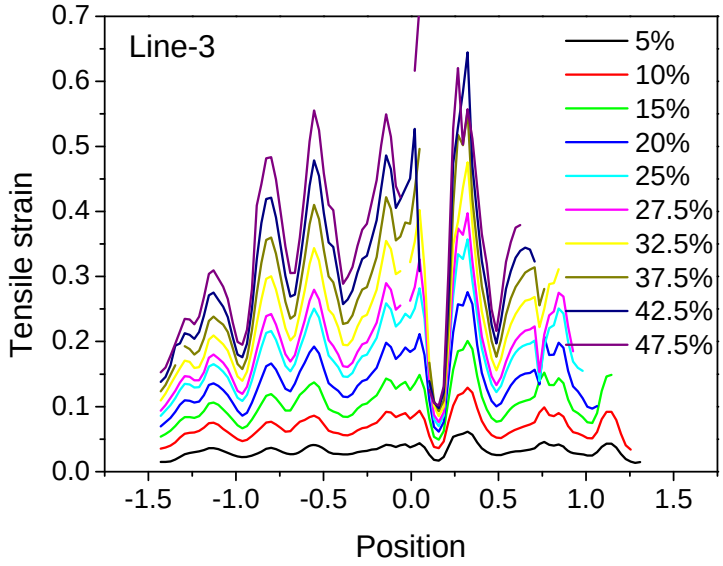
Line-3
Tensile strain
Position
5%
10%
15%
20%
25%
27.5%
32.5%
37.5%
42.5%
47.5%
0.0
0.1
0.2
0.3
0.4
0.5
0.6
0.7
-1.5
-1.0
-0.5
0.0
0.5
1.0
1.5

(c)

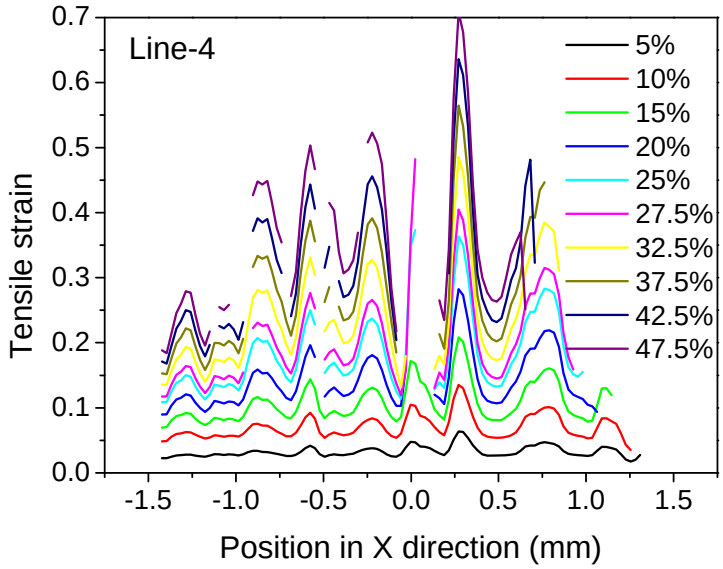
Line-4
Tensile strain
Position in X direction (mm)
5%
10%
15%
20%
25%
27.5%
32.5%
37.5%
42.5%
47.5%
0.0
0.1
0.2
0.3
0.4
0.5
0.6
0.7
-1.5
-1.0
-0.5
0.0
0.5
1.0
1.5

(d)

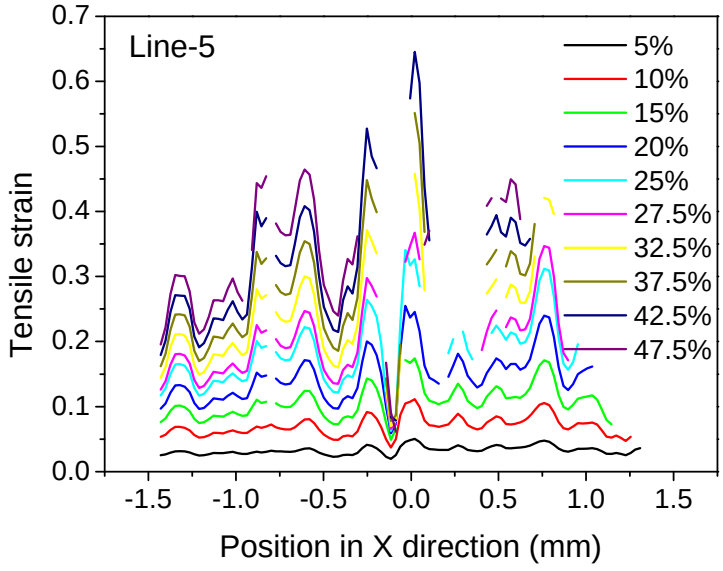

(e)

Figure 5.15 Strain distribution of conductive fabric extended in wale direction at various effective fabric strain levels. (a) line 1, (b) line 2, (c) line 3, (d) line 4 and (e) line 5.

5.3.4 Electrical Resistance of Conductive Fabric under Extension

For the conductive composite,

$$\frac{R-R_0}{R_0} = f(\varepsilon) \tag{5-6}$$

Then,

$$R = R_0(f(\varepsilon)+1) \tag{5-7}$$

In each conductive fabric unit cell, the electrical resistance can be expressed with a circuit of resistors in series as demonstrated in Figure 5.16. For each tensile strain, the electrical resistance is,

$$R_i = R_{0i}(f(\varepsilon)+1) \tag{5-8}$$

The equivalent electrical resistance of the unit cell is

$$R_U = \int_0^L R_{0i}(f(\varepsilon)+1)dl = \frac{R_{0U}}{L}\int_0^L (f(\varepsilon)+1)dl \tag{5-9}$$

where L is the length of the unit cell. In each unit cell, the tensile strain is the function of position in X direction, which obey the Gaussian distribution,

$$\varepsilon = g(l) \tag{5-10}$$

Substitute Eq. 5-10 into Eq. 5-9 yields,

$$R_U = \frac{R_{0U}}{L}\int_0^L (f(g(l))+1)dl \tag{5-11}$$

Where R_U is electrical resistance of the unit cell.

Figure 5.16 Equivalent resistance of the unit cell

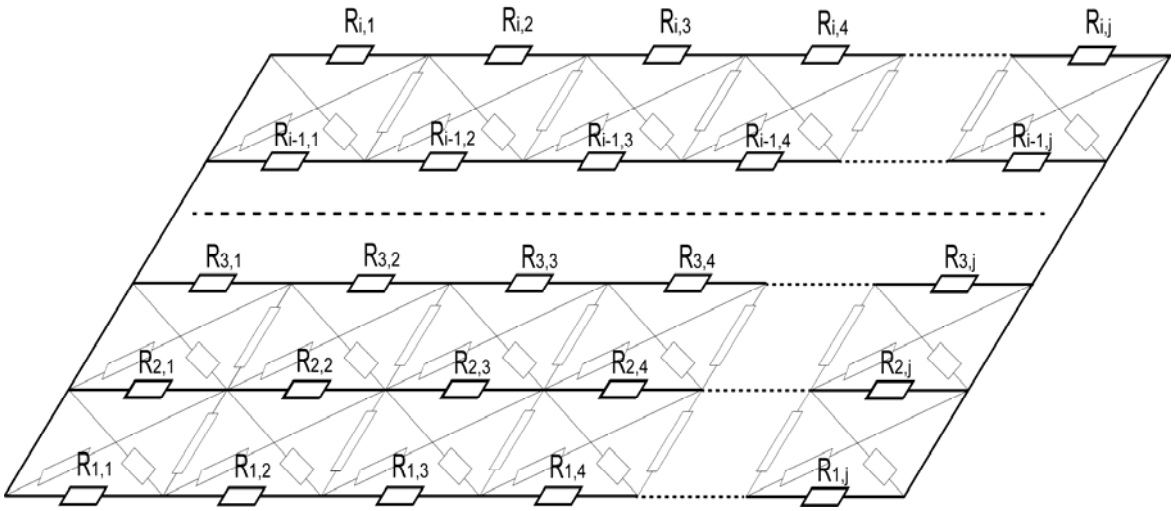

Figure 5.17 Equivalent circuit of the conductive fabric

In the conductive fabric, the unit cells are connect in both serial and parallel directions and form a continuous conductive network as demonstrated in Figure 5.17, in which the R_{ij} represents the electrical resistance of each unit cell, i.e. the equivalent resistance, which is a function of effective fabric tensile strain. For simplification, assuming the conductive fabric is even, the deformation of each conductive fabric unit cell is the same

and the amount of conductive pathways has not changed, then the equivalent conductive network can be simplified by eliminating the parallel connections between unit cells, and the whole electrical resistance of the conductive fabric is equal to that of one unit cell. Select a typical strain distribution curve as shown in Figure 5.18 for calculation, then the total electrical resistance change of the conductive fabric is,

$$\frac{\Delta R_F}{R_{0F}} = \frac{\Delta R_U}{R_{0U}} = \frac{1}{L}\int_0^L (f(g(l))+1)dl - 1 \tag{5-12}$$

Substitute Eq. 5-5 into Eq. 5-12, yields:

$$\frac{\Delta R_F}{R_{0F}} = \frac{1}{L}\int_0^L \left[1 + g(l)\exp\left(A_0 g(l)\right)\right]dl - 1 \tag{5-13}$$

Figure 5.18 shows the strain distribution of conductive fabric in one unit cell as it extended in wale direction at various effective fabric strain levels. The data was fitted using the Gaussian function and defined as $g(l)$, and then the electrical resistance of the conductive fabric can be deduced, the results are shown in Figure 5.19. The theoretical results for the conductive fabrics are close to the experimental values of composites but smaller than that of the conductive fabrics. The results can be partially attributed to the neglect of sensor deformation in the perpendicular direction to the extension direction and shear deformation.

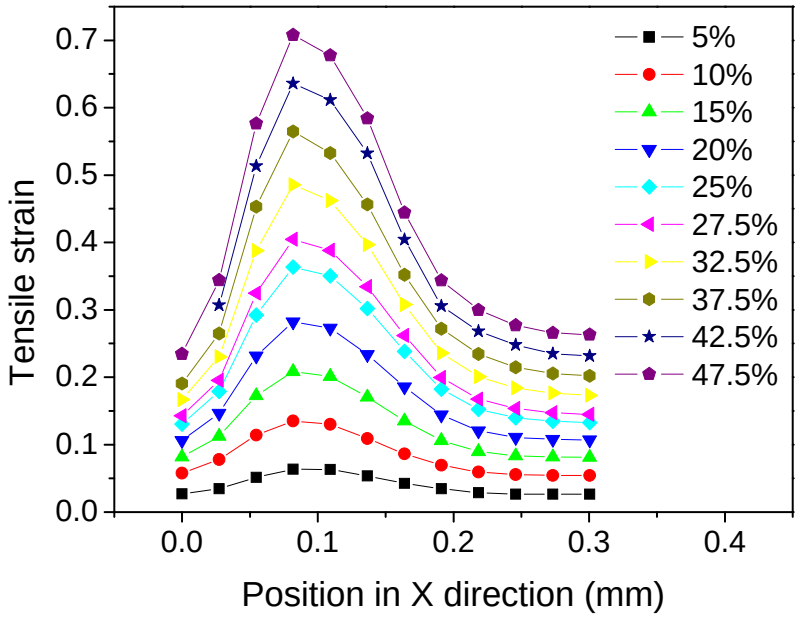

(a)

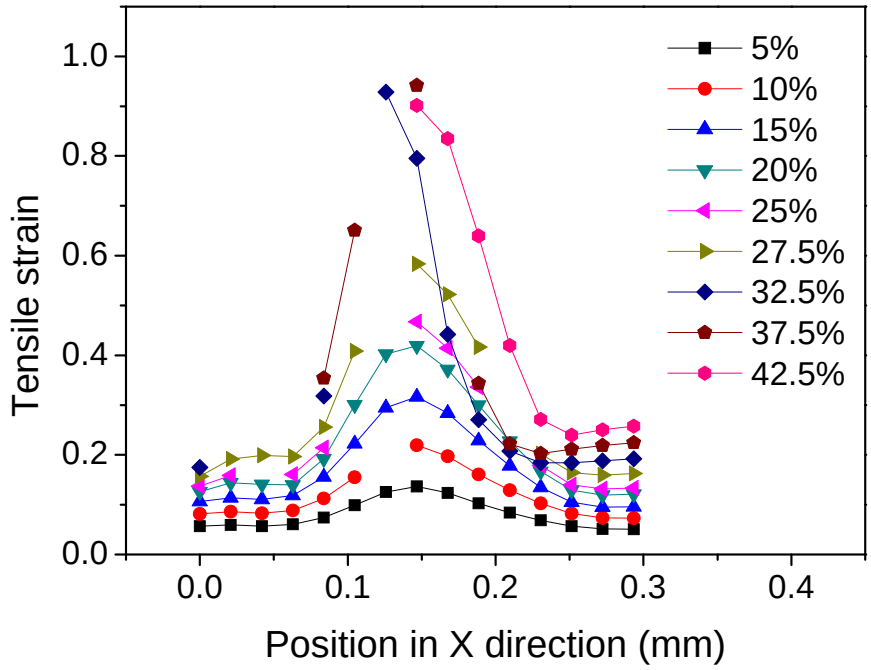

(b)

Figure 5.18 Strain distribution of conductive fabric in one unit cell as it extended in wale direction at various effective fabric strain levels. (a) sample 1 and (b) sample 2

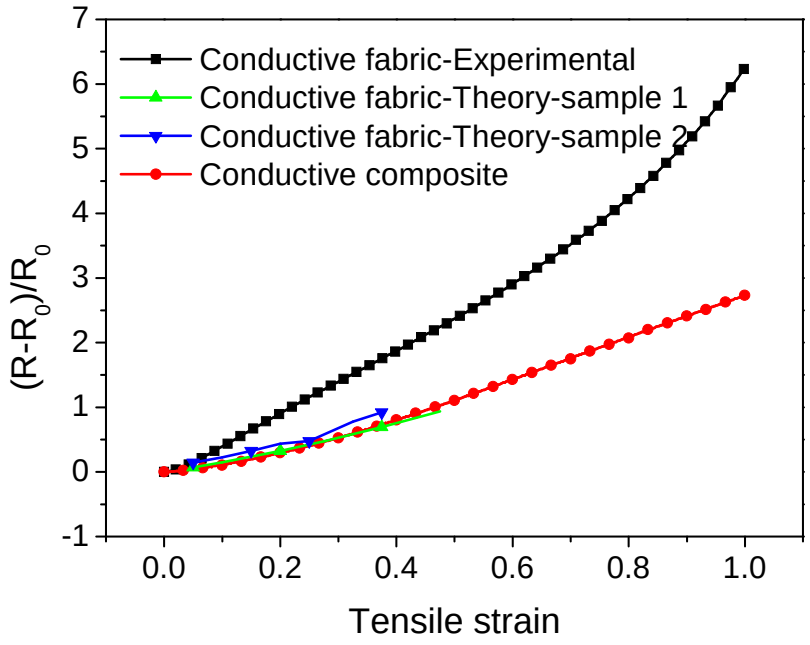

Figure 5.19 Dependence of electrical resistance on tensile strain for experimental results of CNP/SE/SO composite, conductive fabric and calculated value of conductive fabric based on tunneling conductive mechanism and gradient tensile strain distribution of conductive fabric under extension.

5.4. Conclusions

The fabric strain sensor was designed and fabricated based on the conductive fabric described in Chapter 4. Sewing method was used to connect the fabric strain sensor with conductive wire. The performances of the sensor were characterized and the results show that the sensor can meet the requirement of wearable applications with modulus less than 1 MPa, fatigue life more than 100,000 time at working strain range of 30%. Based on the tunneling conductive mechanism of conductive composite and gradient strain distribution of knitted fabric in one unit cells, the sensing mechanism of the fabric strain sensor was studied. The proposed model agrees well with experimental results for composite. However, the discrepancies exist between the theoretical and experimental results of the

sensors, which need to be improved in the future.

References

1. Hufenbach, W., A. Hornig, B. Zhou, A. Langkamp, and M. Gude, *Determination of strain rate dependent through-thickness tensile properties of textile reinforced thermoplastic composites using L-shaped beam specimens.* Composites Science and Technology, 2011. **71**(8): p. 1110-1116.
2. Lomov, S.V., P. Boisse, E. Deluycker, F. Morestin, K. Vanclooster, D. Vandepitte, et al., *Full-field strain measurements in textile deformability studies.* Composites Part A: Applied Science and Manufacturing, 2008. **39**(8): p. 1232-1244.
3. Ridruejo, A., C. González, and J. Llorca, *Micromechanisms of deformation and fracture of polypropylene nonwoven fabrics.* International Journal of Solids and Structures, 2011. **48**(1): p. 153-162.
4. Takano, N., M. Zako, R. Fujitsu, and K. Nishiyabu, *Study on large deformation characteristics of knitted fabric reinforced thermoplastic composites at forming temperature by digital image-based strain measurement technique.* Composites Science and Technology, 2004. **64**(13-14): p. 2153-2163.
5. Zhu, B., T.X. Yu, and X.M. Tao, *Large deformation and slippage mechanism of plain woven composite in bias extension.* Composites Part A: Applied Science and Manufacturing, 2007. **38**(8): p. 1821-1828.
6. Zhang, X.W., Y. Pan, Q. Zheng, and X.S. Yi, *Time dependence of piezoresistance for the conductor-filled polymer composites.* Journal of Polymer Science Part B-Polymer Physics, 2000. **38**(21): p. 2739-2749.
7. Simmons, J.G., *Electric Tunnel Effect between Dissimilar Electrodes Separated by a Thin Insulating Film.* Journal of Applied Physics, 1963. **34**(9): p. 2581-2591.

CHAPTER 6
CONCLUSIONS AND FUTURE WORK

6.1 Conclusions

CNP filled elastomers were prepared via solution aided mixing method. Based on the study on piezo-resistive behavior of the composites, fabric strain sensor by screening printing CNP/SE/SO composite on knitted fabrics were fabricated and characterized. The sensor exhibits a low Young's modulus similar to human skin, large strain measurement range beyond 30% and fatigue life of more than 100,000 loading-unloading cycles at strain level of 30%. In the course of the research, several conclusions that contribute to relevant scientific areas have been drawn. The major findings obtained from the experiments and the conclusions are summarized as the following.

1. Fabrication of the CNP/SE/SO composites based on high porous but low structured CNP and liquid SE using solution aided mixing and cast molding method. The introduction of SO decreases the processing difficulty during mixing period and the modulus of the composites to less than 1 MPa without affecting their elongation property. After volatilization of the excessive SO with heat treatment, the composites show good stability, which is confirmed by thermal gravimetric analysis. Study on the percolation phenomena of the composites demonstrates that the insulating range, percolation range and post-percolation range can be divided at the CNP loadings of 0.5 wt% and 2.5 wt%. The conductive behavior of the composites was explained by an equivalent circuit consisting resistors and capacitors. I-V curves and impedance spectra confirm the domination of electron hopping conductive mechanism for

composites with CNP loading in percolation range, and they are affected by applied voltage and frequency, respectively. In this range, the sensitivity of the composite is high, but the working range is lower and electromechanical behavior is obvious nonlinear, which limited their applications as strain sensors in smart textiles where a large working range is essential necessary. With CNP loading well beyond percolation range, the sensitivity of the composites decreases. However, the sensing working range increases and linearity improved simultaneously. Due to the existence of SO, the modulus of the composites still less than 1 MPa. When CNP loading is increased to 9.0 wt%, the composite shows good repeatability in strain up to 50% in several strain cycles, marginal strain rate dependent, small humidity effect and better linearity, illustrating a strong promise as flexible strain sensors for application in smart textiles if the temperature effect was compensated and fatigue resistance was improved.

2. Conductive fabrics have been fabricated by screen printing CNP/SE/SO composite on knitted fabric. The influence of processing parameters, such as printing times, CNP concentrations, on the variation of electrical resistance was systematically studied. The electrical behavior of the conductive fabrics has been studied at both DC and AC electrical field. Under DC electrical field, the conductive fabrics show linear I-V curves no matter they are extended or not at applied voltage between -1V/mm and 1V/mm, which is the same level as in real application. The impedance spectra under AC electrical field demonstrates that the conductive fabric with higher CNP concentration is less frequency dependent, and the capacitive behavior can be neglected at 10^3Hz even with stain of 60% for the sample of 9.0CNP. Study on electromechanical behavior of the conductive fabric demonstrates that the response of electrical resistance to loading is instantaneous. Compared to CNP/SE/SO composites,

the sensitivity of the conductive fabric was increased while modulus without increased due to the introduction of knitted fabric. The effect of mechanical pretreatment on stability of the conductive fabric has been examined, and the results show that the mechanical pretreatment can obviously increase the stability of the conductive fabric. Strain rate dependent behavior of the conductive fabric can be observed; however, it is predictable in the range of 0.02-4 /s. The effect of temperature and humidity on resistance of the conductive fabric was also studied experimentally. The results demonstrate that the electrical resistance is compensable in temperature ranges of 0-60 ^{0}C, and resistance variation resulted from temperature is about 5%, corresponding to 5% strain. For the hydrophobic nature of the materials used in conductive fabric, the effect of humidity is only about 2% in humidity range of 20-90%.

3. Based on CNP/SE/SO composite coated conductive fabric, the fabric strain sensor was designed and fabricated. The performance of the fabric strain sensor, such as modulus, sensitivity, working range, hysteresis, responding time, relaxation and fatigue life were systematically investigated. The results show that the modulus of the packaged fabric strain sensor is less than 1 MPa; the gauge factor is about 4.76 within the strain range of 0-40% and the hysteresis is about 5.5%; the responding time of the sensor is quick enough to meet the mid or high speed dynamic strain sensing applications; the resistance relaxation of the sensor is 5.56% at a constant strain of 40%; the fatigue resistance of the sensor is more than 100,000 cycles.

4. The conductive mechanism of CNP/SE/SO composites and strain distribution of knitted fabric under uniaxial tensile strain was studied. It was found that the resistance-strain curve of the composite in accordance with the results calculated from

tunneling conduction. The strain distribution in the knitted fabric is uneven, and in one unit cell, shows gradient distribution with highest between two neighboring stiches. Based on the results, the sensing mechanism of fabric strain sensor was discussed. The model of composites has a good agreement with experimental results but the model for conductive fabrics yields lower effective fabric resistance than experimental values.

6.2 Limitations and Recommendations for Future Work

Because of the limitations about performance characterization and sensing mechanism of the CNP/SE/SO composites and fabric strain sensors, the following aspects are suggested to be studied in the future.

1. Improvement of sensor accuracy

   The developed fabric strain sensor has low modulus, high working range and good fatigue resistance that can be widely used in many applications where the traditional strain gauges do not work. However, the accuracy of the sensor is not as good as the metal alloy based strain sensors. Further study should be made to increase the accuracy of the sensor from the view point of materials, fabrication and data processing.

2. Sensing mechanism

   The sensing mechanism of the fabric strain sensor has been studied by considering the conductive behavior of composites and deforming behavior of knitted fabric. However, in the study, there are some limitations and simplifications that affect the accuracy of the simulation results. In the equivalent electrical conductive circuit, there

are many horizontal conductive pathways besides the longitudinal ones, due to the non-uniform strain distributions between unit cells. With the increase of tensile strain, some of conductive pathways will be destroyed and the amount of conductive pathways would decrease. However, both of them are not considered in the study for simplified calculation. Furthermore, when the fabric strain sensor was extended, the effect of strain in Y direction and shear strain on electrical resistance was also ignored. All the simplifications will result in the deviation of calculated results with measured resistance-strain curves. Hence, more future studies are required by including the un-even strain distribution between unit cells and deformations of the sensor in all directions.

3. Miniaturization of the fabric strain sensor

   The size of the developed fabric strain sensor makes it possible to find many applications in smart textiles. However, to measure the strain or pressure distribution in curvature, the smaller sensor size means more information can be achieved in a sensing matrix. Hence, further development of the miniaturized fabric strain sensor should be considered.